University Of Salamanca

Faculty Of Medicine

Department Of Surgery

THESIS DOCTORAL

Evaluating Regenerative Potential: Dental Pulp Stem Cells (DPSCs) and OsteoBiol Gen-Os® Scaffold for Enhanced Bone Repair in Rat Mandibular Defects

Student Name

Haifa Hamad A Alrashid

SALAMANCA 2024

ACKNOWLEDGMENT

********* **********

DEDICATION

إلى من علموني الحب والقوة, إلى من منحوني الحرية والاحترام,

إلى من قدموا لي كل مايملكون دون سبب وبلا شروط, إلى من

زرعوا في روحي الطموح والتفاؤل .. إلى أمي وأبي

INDEX

LIST OF FIGURES

Figure 1. The developmental anatomy of early tooth morphogenesis and the formation of different tooth types: low-crowned molar, continuously growing molar with a complex cusp pattern, and continuously growing incisor lacking a complex cusp pattern.

Figure 2. Shows a cross section along the transverse and sagittal planes of a hypothetical diaphyseal segment of bone. (a) The axis from right to left shows periosteum followed by compact cortical bone in the middle and spongy bone to the left. An osteon, haversian canal, resident blood and lymphatic vessels are surrounded by concentric rings of lamellae. Spaces between lamellae are either lacunae (osteocyte sites) or emanating canaliculi, indicated in the magnified representation on the upper right-hand side are trabecular rods that lamellae are arranged into. (b & c) Magnified views of the cross section of a trabecula indicating the irregular arrangement of lamellae. Fig. 2 c also depicts osteoblastic and osteoclastic activity on the periphery. (Figure taken with permission from Tortora and Derrickson 2009, (1)).

Figure 3. Macroscopic structure of a long bone image shows a long bone (humerus, arm) with structural segments highlighted along a descending vertical axis on the left hand side of image; and sub-cortical structures of a transverse section on the right hand side (Figure taken with permission from Tortora & Derrickson 2009).

Figure 4. Schematic diagram of intramembranous ossification. (1-2) Mesenchymal cells condense to produce osteoblasts, which deposit osteoid matrix. These osteoblasts become arrayed along the calcified region of the matrix. Osteoblasts that are trapped within the bone matrix become osteocytes (3) The extracellular matrix develops into trabeculae that fuse one to another to form spongy bone. (4) The mesenchyme condenses at the periphery of the bone and develops into the periosteom, a thin layer of compact bone will then replace the surface layers of the spongy bone, but spongy bone remains in the centre. (Taken with permission from Tortora and Derrickson, 2009, (1)).

Figure 5. Schematic diagram of endochondral ossification. (1-2) Mesenchymal cells condense and differentiate into chondrocytes to form the cartilaginous model of the bone. (3) Chondrocytes in the centre of the shaft undergo hypertrophy and apoptosis while they change and mineralise their extracellular matrix. Their deaths allow blood vessels to enter. (4) Blood vessels bring in osteoblasts, which bind to the degenerating cartilaginous matrix and deposit

bone matrix. (5-6) Bone formation and growth consist of ordered arrays of proliferating, hypertrophic, and mineralising chondrocytes. Secondary ossification centres also form as blood vessels enter near the tips of the bone. (Taken with permission from Tortora and Derrickson, 2009, (1)).

Figure 6. (a) Exposure of rat mandibuar molar teeth for extraction; (b) Extraction of the rat mandibular molar; (c) & (d) Extracted molar teeth; (e) Dental pulp fragments from the molar teeth.

Figure 7. Surgical procedure: (a) Surgical approach to the right angle of mandible in the rat; (b) Circular bone defect (4.8 mm in diameter) marked in the angle of the mandible; (c) Completed circular bone defect ready for placement of biomaterials; (d) & (e) Closure of the surgical wound in layers (muscle and skin) with resorbable suture materials.

Figure 8. Biomaterial filling within the defect in G+M Group: (a) & (b) Filling the defect with bone substitute (OsteoBiol® Gen-Os®); (c) Covering the filled defect with membrane (OsteoBiol Evolution®)

Figure 9. Bimaterial filling witin the defect in G+M+S Group: (a) Filling the defect with bone substitute (OsteoBiol® Gen-Os®); (b) Administration of dental pulp stem cells to the bone substitute in the defect; (c) Covering the filled defect with membrane (OsteoBiol Evolution®)

Figure 10. Radiological evaluation of the bone defect: (a) Multimodal SPECT/CT Albira II ARS scanner; (b) The study animals placed in prone position during scanning.

Figure 11. Confluence of mesenchymal stem cells derived from dental pulp.

Figure 12. Dot plots of mesenchymal stem cells derived from dental pulp.

Figure 13. Mono-parametric histograms of mesenchymal stem cells derived from dental pulp.

Figure 14. Cell morphology of the differentiated dental pulp stem cells: (a) Osteogenic differentiation with Osteodiff medium (Miltenyi Biotec) showing alkaline phosphatase staining; (b) Adipogenic differentiation, showing the presence of intracellular lipid vacuoles stained with Oil Red; (c) Control sample.

LIST OF TABLES

LIST OF ABBREVIATIONS

ALP: Alkaline Phosphatase

ALS: Amyotrophic Lateral Sclerosis

AMP: Aminomethyl Propanol

APC: Flowchart Of The Study Design

APL: Consort Flowchart Of The Study

ASC: Ibuprofen Mg

BMPs: Bone Morphogenic Proteins

Bsp: Bone Sialoprotein

CA: Calcium

Ca^{2+}: Calcium Ions

CT: Calcitonin

CT: Computed Tomography

CFX: Cresolphthalein Complexone

DFSCs: Dental Follicle Stem Cells

DPSCs: Dental Pulp Stem Cells

DSCs: Dental Stem Cell

ECM: Extracellular Matrix

ERM: Epithelial Cell Rests of Malassez

ENG: Endoglin

FGF: Fibroblast Growth Factor 2

FBS: Fetal Bovine Serum

GBR: Guided Bone Regeneration

GenOs: Collagenated Xenograft Bone

GMSCs: Gingival Tissue Stem Cells

GMP: Good Manufacturing Practices

HA: Hydroxyapatite

HA/TCP: Hydroxyapatite Tricalcium Phosphate

HERS: Hertwig's Epithelial Root Sheath

HFIP: HexaFluoro-2-Propanol

ICM: Inner Cell Mass

Mg: Magnesium

MSCs: Mesenchymal Stem Cells

NF: Collagen Nanofibers

P: Phosphorus

PDL: Periodontal Ligament

PDLSCs: Periodontal Ligament Stem Cells

PLG: Poly-D L-lactide and Glycolide

PLLA: Poly-L-Lactic Acid

PTH: Parathyroid Hormone

Runx2: Runt-related Transcription Factor 2

SCAPs: Apical Papilla Stem Cells

SHED: Human Exfoliated Deciduous Teeth

TGF: Transforming Growth Factor

TGFβ1: Transforming Growth Factor Beta 1

TRF: Temporal Resolution of Fluorescence

1. INTRODUCTION

Alveolar bone defect regeneration is a clinical challenge faced in the field of dentistry and its sub-specialties. Some of the commonest causes of bone loss which require subsequent regeneration and healing include, extraction sockets, alveolar ridge augmentation for implant placement, periodontal and peri-implant bone defects, and pathological conditions such as cysts and tumors (2, 3). Although the response of alveolar bone to injury is similar to that of bone in other parts of the body, the chances for bone defects and factors acting against adequate spontaneous bone

healing are abundant in the oral cavity (3). A simple case in point is the presence of the odontogenic apparatus including the periodontium, which is susceptible to multiple factors affecting bone turnover such as occlusal trauma, periapical pathosis due to dental caries, gingivitis and periodontal infections. This has led to a constant pursuit for better bone regenerative biomaterials and adjunctive strategies to enhance the same (2).

Traditionally, autologous bone grafts were the material of choice for treating alveolar bone defects (4). However, they are fast being replaced by alternatives such as allografts, xenografts and alloplastic biomaterials, owing to the paucity, donor site morbidity and additional surgical procedures associated with autografts (4-6). The performance of these alternative bone graft materials have further been enhanced by the role of adjuncts such as bone morphogenic proteins (BMP), growth factors and mesenchymal stem cells (7-9). Moreover, the field of alveolar bone regeneration has further witnessed effective and clinically relevant bone defect healing through the use of guided bone regeneration (GBR). The technique of GBR employs dual benefits of bone graft placement and isolating the defect site using barrier membranes, for unhindered defect site healing (10). It has been reported that collagen barrier membranes used in GBR, in addition to providing the barrier effect, also plays a role in chemotaxis of osteogenic progenitors and early neovascularization (2, 10). Although the technique of GBR has been reportedly used for healing both non-segmental and segmental critical size defects in animal studies and clinical alveolar bone defect regeneration (6, 8, 10-13), the search for improvised regenerative strategies still persists. Researchers have attempted the same by utilizing novel bone grafts or substitutes along with adjunct cells, proteins or growth factors, with the ultimate aim of replicating bone healing results achieved with autografts (14).

Similar to deproteinized allograft derived from cadaveric bone, xenograft bone obtained from varied sources such as bovine, porcine and equine origins have also been proven to demonstrate osteoconductivity and osteoinductivity when placed in bone defects (4, 6, 15). While collagen used as a barrier membrane in GBR facilitates early bone formation and angiogenesis, it would be intriguing to understand its role when incorporated as a part of the osteoconductive scaffold. Based on an in vitro and in vivo study using a composite graft comprising porcine xenograft bone and collagen, Salamanca et al. (4), reported greater osteoblastic cell differentiation and better bone regenerative ability, than with alloplastic materials such as hydroxyapatite and tricalcium phosphate. Similar results were reported by Pagliani et al. (16), based on a one year follow up post implant placement and alveolar bone augmentation with collagenated porcine xenograft and collage barrier membrane. Falacho et al. (17), compared five different commercially available collagenated porcine bone grafts in differing physical forms Apatos, Gen-Os, mp3, Putty, and Gel 40 within a rabbit model of GBR. They reported similarly enhanced bone formation with all the five substitutes, irrespective of their physical characteristics (17).

The use of mesenchymal stem cells (MSCs) as adjunct to bone regeneration have gained prominence over the last decade (7, 18). Stem cells when placed in an osseous defect site along with osteoconductive graft material during GBR, results in differentiation into osteogenic progenitors and fibroblasts, which enable early matrix formation and collagen deposition respectively (8, 18). While bone marrow has been the most favored source for harvesting MSCs used in bone regenerative strategies, other sources such as adipose tissue, dental pulp, and dental follicle have also been reported (18-20). Based on a systematic review and meta-analysis, Gaubys et al. (21), reported a significant regenerative impact with stem cell therapy for not only alveolar bone, but also the periodontal tissue complex. Furthermore, calcium phosphate based

osteoconductive scaffolds have specifically been shown to induce osteogenic differentiation in MSCs (22). Similar results were reported by Trivedi et al. (23), wherein use of a composite hydroxyapatite-collagen scaffold resulted in osteogenic differentiation of MSCs. Interestingly, in both the above-mentioned studies (22, 23), the MSCs used were from dental pulpal origin (Dental pulp stem cells [DPSCs]). In short, utilizing the innate ability of bone to heal spontaneously and accentuating it through bone regenerative strategies holds great promise for healing of bone defects which would not otherwise heal completely. The use of GBR with adjuncts has been proven to heal even segmental bone defects based on studies in a rat femoral defect model (6, 11, 24). Moreover, there has been significant progress towards the development of vascularized, tissue engineered, bone regenerative constructs, which in the future have the potential to replace vascularized autologous tissue transfer (25).

In view of the above evidences reported in the literature, it would be interesting to surmise that a combination of composite scaffold comprising osteoconductive graft with collagen and DPSCs would be an optimum choice for bone tissue engineering and regeneration. While in vitro studies have been reported about the same, to the best of our knowledge, there are no translational or clinical studies in the literature. As an evidence base, translational animal models using rat bone defects have been reported widely for studying GBR (5-8, 11, 17, 21, 22). Rat bone defects, provided they are of critical size in dimension, are amongst the best to evaluate bone regeneration of membranous and chondrogenic bone defects (26). Therefore, the present study was devised with an objective of evaluating the role of a combination of DPSCs and collagenated xenograft bone (GenOs) for GBR of rat mandibular bone defects. The study further envisages isolation, characterization and differentiation of allogenous DPSCs, harvested from rats, as a possible bone tissue engineering adjunct.

1.1. DENTAL TISSUES

1.1.1. DEVELOPMENT OF DENTAL TISSUES

Tooth development or odontogenesis is the complex process by which dental mineralized tissues form embryonic cells that differentiate into ameloblasts that secrete enamel, odontoblasts that produce dentin, and cementoblasts that make cementum. Enamel is of epithelial origin and covers the crown of each tooth. In contrast, dentin and cementum are of mesenchymal origin. Dentin forms the bulk of the tooth and extends within both the crown and root. It has a yellow color, in contrast to the much whiter and harder enamel. Cementum is deposited only in the root area on the recently mineralized dentin matrix. The tooth is anchored onto its socket (alveolar bone) by the periodontal ligament (PDL), a connective tissue structure that surrounds the tooth root and connects each tooth to the alveolar bone through a specialized set of collagen fibers. The most defining characteristic of tooth development is its origin from a combination of embryogenic neuroectoderm and ectomesenchyme, thereby bestowing a pluripotential property to developmental tooth tissue.

1.1.2 MORPHOGENESIS AND CELL DIFFERENTIATION DURING TOOTH DEVELOPMENT

Teeth are formed as epithelial appendages and their morphogenesis is regulated by interactions between the epithelium and the underlying neural crest derived mesenchyme. The mammalian dentition consists of groups of highly specialized teeth; incisors, canines, and molars, which arise from different regions of oral epithelium. While teeth can be formed from both endoderm and

ectoderm (27), in mammals teeth seem to be derived only from the ectoderm. The earliest morphological sign of tooth formation is the appearance of the primary dental laminae (odontogenic bands), which are stripes of thickened epithelium marking the future tooth rows (27). Within the primary dental lamina placodes form which resemble morphologically, as well as in their molecular regulation, the placodes found during the development of other ectodermal organs (28, 29). The placodes consist of thickened epithelium and underlying neural crest derived mesenchyme, and they function as the first signaling centers of the tooth **(Figures 1 and 2)**. One particular hypothesis suggests that each dental placode gives rise to an entire tooth family (incisor, canine, molar). In this scenario only the first tooth of the family buds directly from the placode while the other teeth form successionally from the primed odontogenic epithelium and mesenchyme.

During the bud stage the dental epithelium segregates into two histologically distinct cell lineages, the peripheral basal cells contacting the basement membrane, and centrally located loosely arranged cells, called the stellate reticulum, which are derived from the suprabasal cell layers of the surface ectoderm. These two tissue layers will form the epithelial components of the stem cell niche in the continuously growing teeth. The dental mesenchyme condenses around the bud and segregates into two cell lineages, the dental papilla which later becomes surrounded by dental epithelium and gives rise to the tooth pulp and dentin producing odontoblasts, and the peripheral dental follicle giving rise to the cementoblasts and periodontal tissues. The size and shape of the tooth crown become apparent during the cap and bell stages and they are regulated by the enamel knots. Signals from the enamel knots regulate growth and determine the sites of epithelial folds which correspond directly the cusp pattern of the mature tooth (30). The crown shape becomes

fixed as the cells at the epithelial-mesenchymal interface differentiate into ameloblasts and odontoblasts, and secrete the mineralizing matrices of enamel and dentin, respectively.

During the cap and bell stages the lateral sides of the epithelial bud start enveloping the underlying dental mesenchyme, and from this point onwards the leading edge of the epithelium is called the cervical loop. The basal epithelial cell layer of the loop bordering the dental papilla is known as the inner enamel epithelium and the part facing the dental follicle is known as the outer enamel epithelium. The core of the loop is populated by loosely arranged stellate reticulum cells and a thin layer of stratum intermedium cells facing the inner enamel epithelium This cervical loop structure is maintained in continuously growing teeth and constitutes the epithelial part of the adult stem cell niche (31, 32). In non-continuously growing teeth (including all human teeth) the cervical loop will actively undergo a structural modification when root formation is initiated. The central core of epithelium disappears leaving only a double layer of basal epithelium known as Hertwig's epithelial root sheath (HERS). It directs root growth and gives rise to a fenestrated network of epithelial cells overing the root and is known as epithelial cell rests of Malassez (ERM). Both the HERS and the ERM are thought to have a limited growth capacity. Nevertheless, remnants of the above two epithelial tooth developmental appendages are postulated to give rise to neoplastic odontogenic tumors and cysts, thereby indicating their innate growth potential long after tooth development is complete. The same tendency of odontogenesis, later in life, leading to cyst and tumor and formation is also seen with remnants of the dental lamina and the basal layer of the oral epithelium. While more detailed descriptions of the developmental anatomy and histology of teeth can be found in textbooks (33), the entire tooth developmental process is graphically described in **Figure 1**.

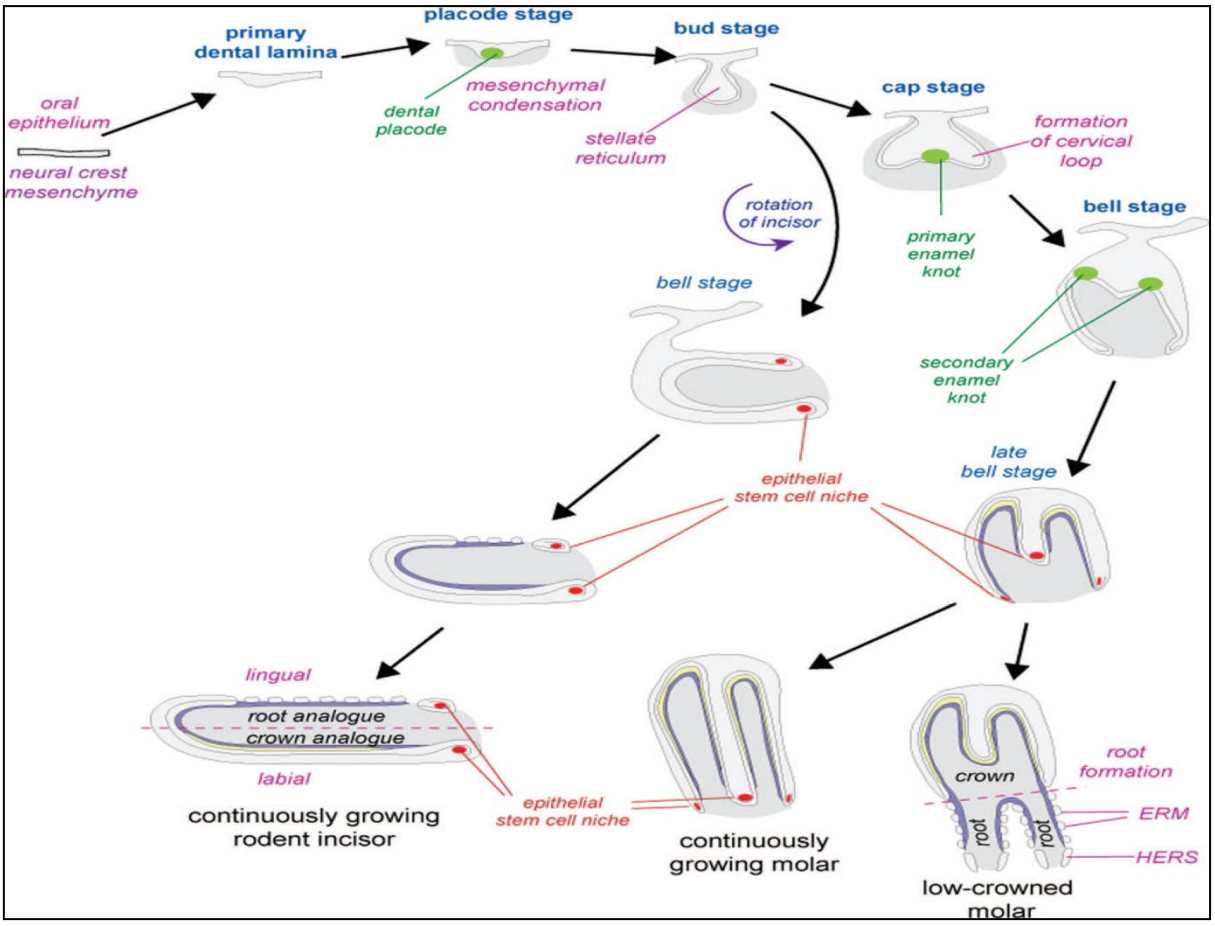

Figure 1. The developmental anatomy of early tooth morphogenesis and the formation of different tooth types: low-crowned molar, continuously growing molar with a complex cusp pattern, and continuously growing incisor lacking a complex cusp pattern.

The primary dental lamina forms as a thickening of the oral epithelium at the site of the future tooth row. Tooth morphogenesis starts from the dental placodes where neural crest derived mesenchymal cells condense under the epithelial placode. The epithelium first buds into the mesenchyme and then grows to encompass the mesenchymal dental papilla during the cap stage. The epithelial cervical loop is formed during the cap stage on the lateral sides of the bud. Different developmental choices are made at this point leading to the formation of different tooth types. The epithelial stem cell niche in the cervical loop is maintained in continuously growing teeth, but

disappears in teeth which develop roots such as all human teeth. Signaling centers are present at various stages of tooth development (placode, primary and secondary enamel knots). The enamel knots regulate tooth crown morphogenesis characterized by folding of the enamel epithelium. The locations of secondary enamel knots correspond to the future sites of tooth cusps. ERM, epithelial cell rests of Malassez; HERS, Hertwig's epithelial root sheath.

1.2. OSTEOGENESIS

1.2.1. BONE

Bone is a strong anatomical structure that has the ability to provide protective covering of vulnerable structures in the body such as brain, rigid internal support for the body and the articulation and attachments of muscles. It provides a site of storage of minerals and lipids in addition to blood cell production (34). Bone can be divided into two types; compact and spongy bone. These are depicted in **Figures 2 and 3**. Based on the microscopic features, osseous tissue is a collagen and calcified mineral based extracellular matrix (ECM). It is divided into two distinct types based on the architecture of the connective tissue ECM; cortical and cancellous **(Figure 2)**. The former is a relatively dense, compact type of osseous forming the outer part of a bone. The cancellous type occurs as spongy with a 'honey comb' of branching bars, plates and rods called 'trabeculae. This architecture accommodates a higher level of vascular tissue compared to cortical bone that nourishes bone marrow and its embedded populations of various stem cells (35). Cortical and cancellous bones constitute 80% and 20% of the adult skeleton, respectively. The predominant mineral salt is a combination of calcium phosphate and calcium hydroxide called hydroxyapatite (35).

Macroscopically, skeletal bones are divided into four types; long, short, flat and irregular. A prototypic long bone is composed of seven structural entities: diaphysis, epiphyses, metaphysis, articular cartilage, periosteum, medullary cavity and endosteum. The initial three constitute the larger bone structure; with the articular cartilage and periosteum forming on the outside, and medullar cavity and endosteum within it. Other bones are composed of different combinations of these structural elements. The various macro structural attributes of a prototypic long bone are described in **Figure 3** (35). The vertebrate skeleton is the outcome of cells from three distinct embryonic lineages. Cranial neural crest cells are responsible for the formation of craniofacial skeleton, whereas the axial skeleton is derived from paraxial mesoderm (somites), and the limb skeleton is the product of the lateral plate mesodermal cells.

There are three major bone cell types, and all of them arise from osteopreogenitor cells, which are a lineage from the bone marrow mesenchymal stromal or stem cells. Among these three cell types, osteoblasts are responsible for building up bone in a process called osteogenesis. They secrete the collagenous and non-collagenous proteins of bone matrix. As the osteoblasts lay down the bone matrix, they get entrapped within the matrix and further contribute to the processes of matrix mineralization and physiological bone turnover. These trapped osteoblasts are termed as osteocytes, and are mature bone cells that are contained in a lacunar space filled with bone fluid, mineralised collagen fibrils and proteoglycans. The osteocytes are anatomically and physiologically interconnected to one another through and intricate system of Haversian and Volkmann canals, called as the Haversian system. The third type of bone cell, is the osteoclast which performs a scavenging function, as it contributes to bone resorption by degrading old mineral matrix to facilitate new bone deposition by osteoblasts. All these three bone cells play a networked role for maintaining bone physiology and bone healing.

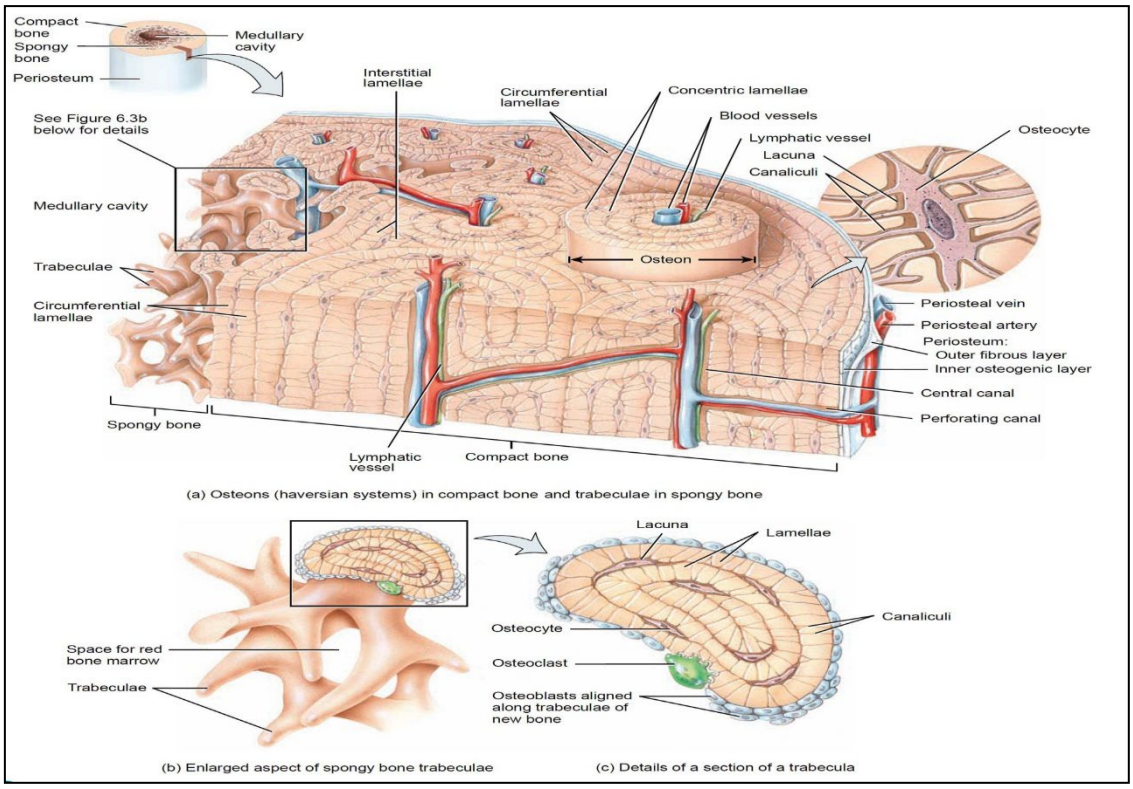

Figure 2. Shows a cross section along the transverse and sagittal planes of a hypothetical diaphyseal segment of bone. (a) The axis from right to left shows periosteum followed by compact cortical bone in the middle and spongy bone to the left. An osteon, haversian canal, resident blood and lymphatic vessels are surrounded by concentric rings of lamellae. Spaces between lamellae are either lacunae (osteocyte sites) or emanating canaliculi, indicated in the magnified representation on the upper right-hand side are trabecular rods that lamellae are arranged into. (b & c) Magnified views of the cross section of a trabecula indicating the irregular arrangement of lamellae. Fig. 2 c also depicts osteoblastic and osteoclastic activity on the periphery. (Figure taken with permission from Tortora and Derrickson 2009, (1)).

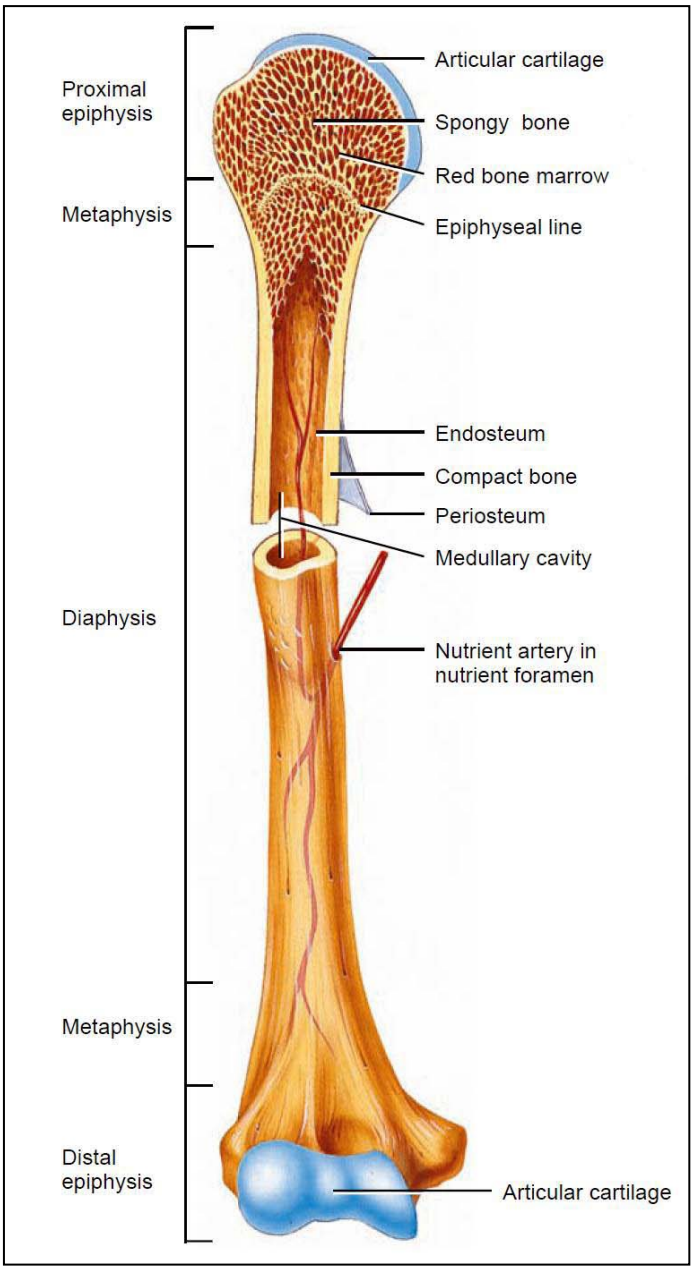

Figure 3. Macroscopic structure of a long bone image shows a long bone (humerus, arm) with structural segments highlighted along a descending vertical axis on the left-hand side of image; and sub-cortical structures of a transverse section on the right-hand side (Figure taken with permission from Tortora & Derrickson 2009).

The bone cells perform their physiological and bone healing function through an interplay between several biologically active molecules leading to the formation of bone. The main ones of

high significance include bone morphogenic proteins (BMPs), Runx2, alkaline phosphatase (Alp) and bone sialoprotein (Bsp). Several bone morphogenic proteins (BMPs) are capable of acting as potent bone inducer factors, including BMP-2, -4, and -7 (36-39). BMP-7 is considered a weaker bone inducer than BMP-2 and -4 (38). The BMPs initiate their signalling pathway by binding to BMP receptors that activate the expression of target genes (38). Runx2 is also involved in this signalling cascade mediating the osteogenic differentiation initiated by BMPs (38). Other proteins and hormones involved in osteogenic regulation and differentiation include Parathyroid hormone (PTH), vitamin D and TGF-β1.

Runt-related transcription factor 2 (Runx2) (a member of a small transcription factor family that shares DNA-binding domains of homology with *Drosophila Runt*) is a key regulator of osteoblast differentiation and function (40-43). It also interacts with and controls the expression levels of several osteogenic genes, including osteocalcin (an osteoblast-specific marker), Bsp, Alp, and type I collagen (40). Alkaline phosphatase (Alp) is a commonly used osteogenic marker; mature Alp is glycolyzed and anchored to the cell plasma membrane. Alp is expressed at high levels in mineralised tissues and its importance for osteogenic differentiation is well established as an inorganic phosphate donor to growing calcium phosphate crystals. Alp is essential for expression of necessary genes to produce osteogenic extracellular matrix (ECM) (44). Bone Sialoprotein (Bsp) is first expressed at the onset of bone, cementum, and dentin formation. Its expression is restricted to mineralised connective tissues (45, 46). Bsp is believed to initiate calcium deposition by binding calcium ions. It is also involved in the regulation of cell attachment to bone matrix (47).

1.2.2. OSSIFICATION

Osteogenesis, or bone development takes place through two ways; these are intramembranous and endochondral ossification. Intramembranous ossification occurs in craniofacial region, in which cranial neural crest cells migrate to the location where the skeletal elements will develop and differentiate into osteoblast cells that start bone formation by replacement of sheet-like connective tissue membrane with bony tissue (48). The endochondral ossification, leading to development of limbs and trunk, involves the formation of cartilage tissue from aggregated mesenchymal cells, and subsequent replacement of cartilage tissue by bone (48). A depiction of this process is illustrated in **Figures 4 and 5**. The mechanism of intramembranous ossification involves bone morphogenetic proteins and the activation of Runx2. Bone morphogenetic proteins from the head epidermis are thought to instruct the neural crest-derived mesenchymal cells to become bone cells directly (49). The BMPs activate the Runx2 gene in the mesenchymal cells. The Runx2 transcription factor appears to be able to transform mesenchyme cells into osteoblasts.

The process of endochondral ossification starts by the commitment of the mesenchymal cells to become cartilage cells (chondrocytes), which proliferate rapidly to form a model for the bone. The chondrocytes then stop dividing and increase their volume (hypertrophic chondrocytes); they alter the matrix they produce to enable it to become mineralised. Finally, the blood vessels invade the cartilage model formed. The hypertrophic chondrocytes die by apoptosis. This space will become bone marrow. As the cartilage cells die, a group of cells that have surrounded the cartilage model differentiate into osteoblasts. The osteoblasts begin forming bone matrix on the partially degraded cartilage (50, 51). Eventually, all the cartilage is replaced by bone. Thus, the cartilage tissue serves as a model for the bone that follows. The skeletal components of the vertebral column, the pelvis,

and the limbs are first formed of cartilage and later become bone. This process is depicted in **Figure 5**.

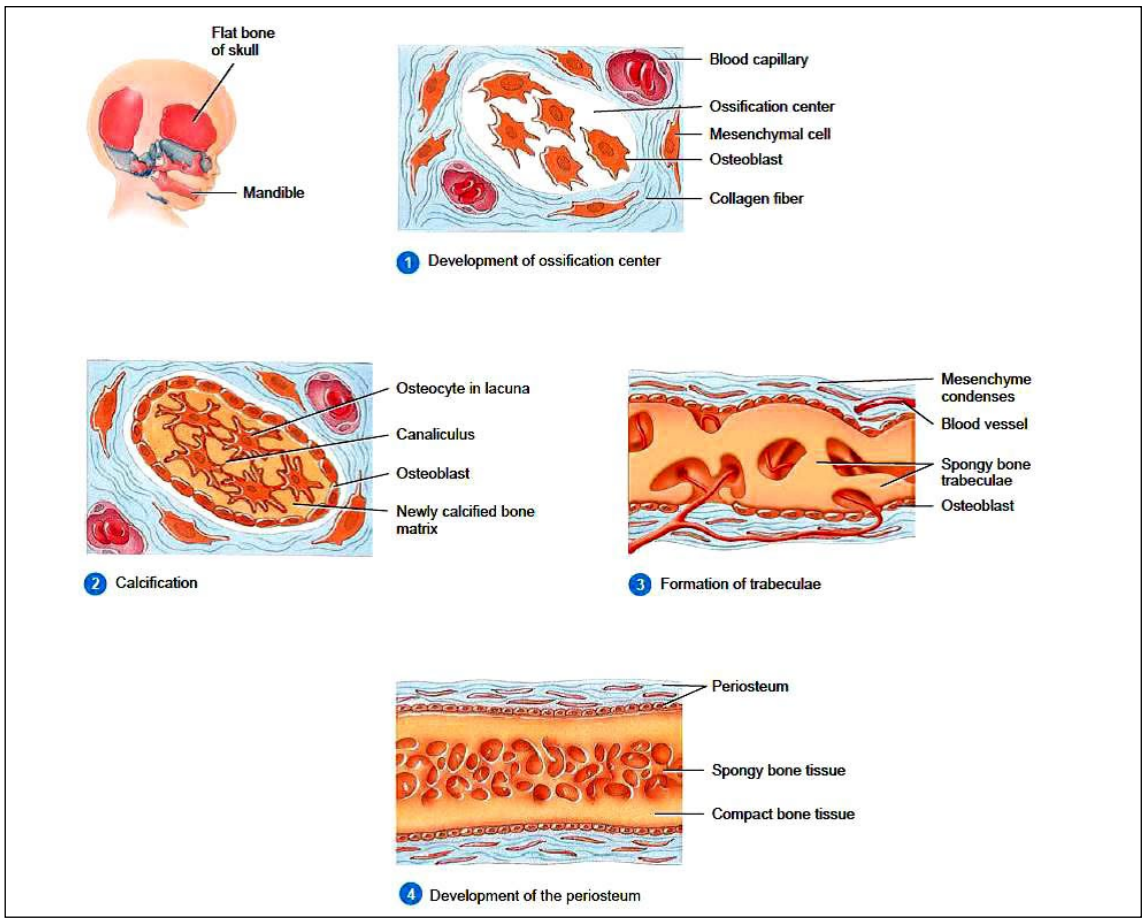

Figure 4. Schematic diagram of intramembranous ossification. (1-2) Mesenchymal cells condense to produce osteoblasts, which deposit osteoid matrix. These osteoblasts become arrayed along the calcified region of the matrix. Osteoblasts that are trapped within the bone matrix become osteocytes (3) The extracellular matrix develops into trabeculae that fuse one to another to form spongy bone. (4) The mesenchyme condenses at the periphery of the bone and develops into the periosteum, a thin layer of compact bone will then replace the surface layers of the spongy bone, but spongy bone remains in the centre. (Taken with permission from Tortora and Derrickson, 2009, (1)).

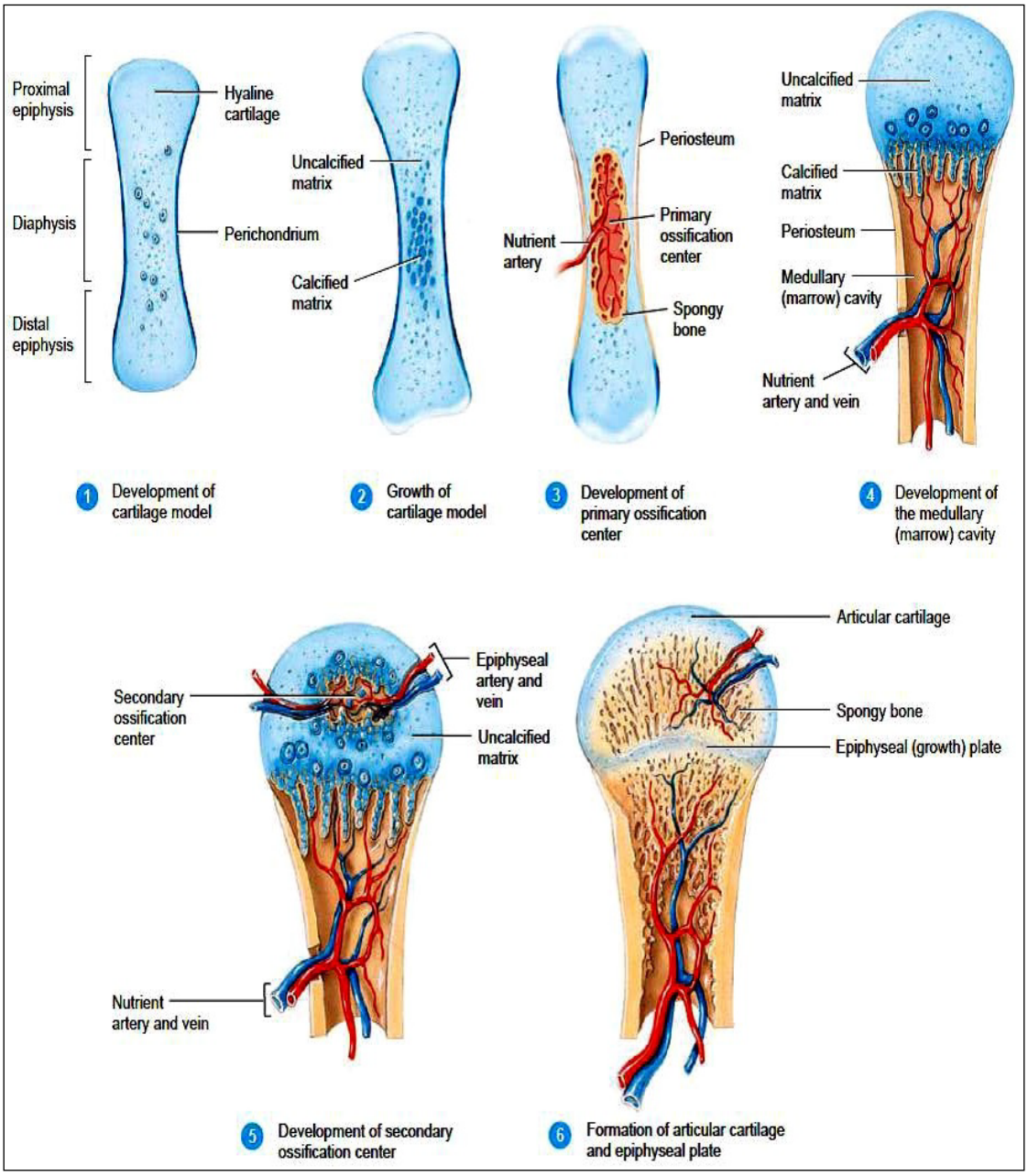

Figure 5. Schematic diagram of endochondral ossification. (1-2) Mesenchymal cells condense and differentiate into chondrocytes to form the cartilaginous model of the bone. (3) Chondrocytes in the centre of the shaft undergo hypertrophy and apoptosis while they change and mineralise their extracellular matrix. Their deaths allow blood vessels to enter. (4) Blood vessels bring in osteoblasts, which bind to the degenerating cartilaginous matrix and deposit bone matrix. (5-6) Bone formation and growth consist of ordered arrays of proliferating, hypertrophic, and mineralising chondrocytes. Secondary ossification centres

also form as blood vessels enter near the tips of the bone. (Taken with permission from Tortora and Derrickson, 2009, (1)).

1.2.3. OSTEOGENIC POTENTIALS OF DENTAL PULP STEM CELLS

Despite the fact that mesenchymal stem cells are being widely recognised as a primary source of osteoprogenitor cells, non-bone-marrow sources are important to pursue as an alternative to bone marrow when patients do not wish to have a bone marrow aspirate or when the bone marrow is compromised, as can occur in the elderly or in those with bone marrow disease. Non-bone-marrow-derived cells might also be more easily obtained when tissues are accessible during a surgical procedure. There are several potential sources of stem cells which have been reported in the literature including blood, bone marrow, adipose tissue, muscle and foetal umbilical cord. Dental pulp stem cells have gained significance in recently reported literature with the possibility of even commercially banking stem cells of dental pulp origin from exfoliated and extracted healthy teeth, similar to what is being done for the umbilical cord blood-based stem cells. Irrespective of their origin, all stem cells have been shown to be pluripotential in character, when cultured in vitro with the right biological molecules, to form desired tissue types.

1.3. STEM CELLS

Stem cells are non-specialised cells which have two distinct properties; (1) the ability for long term self-renewal and, (2) the capability to differentiate into one or more specialised cells. The differentiation ability or so-called plasticity decreases with maturity. Cells taken from the early divisions of the zygote are totipotent, that is they are able to form any cell type in the embryo and

the cells of the placenta (52). A few days later, the inner cell mass (ICM), a group of cells within the blastocyst, from which embryonic stem cells (ES) are derived, and they are capable of producing any cell product of the three germ layers but not the placenta. Hence, these cells are called pluripotent (52). Postnatally and during adult life tissue specific stem cells, adult stem cells, reside in most organs of the developing animal. The role of these cells is to act as a source of new cells for postnatal growth and repair or as a mechanism for tissue maintenance, growth and repair in later life (53). Stem cells are present in various niches throughout the body, such as bone marrow, brain, liver and skin, as a mechanism for tissue maintenance, growth and repair in later life (54, 55). In addition to the above-mentioned tissues adult stem cells were also reported to be present in craniofacial skin, palate, oral mucosa, periodontal ligaments surrounding the tooth and dental pulp, etc (56-59).

In theory, adult stem cells could be harvested from a patient, differentiated in the laboratory and transplanted back into the same individual for tissue repair, thus bypassing the need for immunosuppression. However, for some stem cell types, low frequency, difficulties in accessing the niche and isolating the cells, restricted lineage potential and poor growth in cell culture may render their use impractical for tissue engineering purposes. In these cases, embryonic stem cells are likely to provide a more appropriate cell source (60). Wherein, embryonic stem cells are the ones sourced from embryonic tissue including amniotic fluid, umbilical cord and blood. They are regarded as the most pluripotent of all stem cell niches, owing to their immaturity, differentiation ability and plasticity. Nevertheless, the sourcing of embryonic stem cells is associated with its procedural and logistical difficulties, and more importantly has raised ethical concerns.

Until recently, adult stem cells were thought to be committed to regeneration of specific lineages associated with their niche, however a growing amount of data suggests these stem cells may be pluripotent (52). Plasticity of the adult stem cell was originally investigated by studies on stem cells derived from bone marrow (mesenchymal stem cell (MSC)). These studies found, experimentally, that MSCs have the ability to differentiate into other cell types including muscle, fat, liver, etc. (61-63). Human embryonic and adult stem cells each have advantages and disadvantages regarding potential use for cell-based regenerative therapies. One major difference between adult and embryonic stem cells is their different differentiation potentials compared to adult stem cells. Embryonic stem cells can become all cell types of the body while adult stem cells are thought to be limited to differentiating into different cell types of their tissue of origin (64).

Finding an easy reproducible method for isolating and expanding adult stem cells is still subject to investigation. Embryonic stem cells, on the other hands, can also be relatively easily grown in culture. This is an important distinction as large numbers of cells are needed for stem cell replacement therapies. Other main difference would be the immune rejection after transplantation. Adult stem cells, and tissues derived from them, are currently believed less likely to initiate immune rejection after transplantation. This is because a patient's own cells could be expanded in culture, properly treated by necessary agents, and then reintroduced into the patient. This represents a significant advantage, as immune rejection can be avoided only by continuous administration of immunosuppressive drugs (64). Biological difficulty is also a challenge for using bone marrow stem cells as patients may have compromised bone marrow or simply do not want to have bone marrow aspirate (65). Therefore, work has focused on finding other sources of stem cells that may have the same abilities of the MSCs and might also be more easily obtained when tissues are exposed as part of surgical procedure. These include skeletal muscle which is

considered being a promising source of stem-like cells as it is relatively easier to access especially craniofacial muscle (masseter), which can be accessed intra-orally under local anaesthesia with no scar formation.

Due to their properties, stem cells have the potency to become an important tool of tissue engineering and regenerative medicine. Tissue engineering is merging the principles of engineering and bioscience aiming to develop biological substances for the restoration, conservation and/or improvement of the tissue function (66). Tissue engineering is aiming to provide the stimulus to the organism to regenerate the tissue from the inside or to develop the tissue externally which could be transplanted as natural tissue. The applications are based on the ability of the cells to proliferate and differentiate as well as on the construction of structures through cell and bio-scaffold interactions (67, 68). The most frequently reported tissue engineering regenerative strategy utilizing stem cells has been that for bone regeneration using in vitro cultures and in vivo animal models. Mesenchymal stem cells from a variety of sources have been reportedly used to accentuate the processes of bone healing and osseous defect regeneration, either with or without osteoconductive graft materials. Going a step further studies have also reported utilizing tissue engineered osteoconductive scaffold constructs, on which are cultured the stem cells in vitro, until they differentiate to osteogenic lineage, and then are transplanted to a bone defect site in vivo for osseous regeneration.

The loss or the absence of a tooth is a situation that could occur due to various conditions such as dental caries, periodontitis, traumatic injury or various pathological syndromes. The replacement of the lost tooth is very important not only for aesthetic reasons but also for functional purposes. Recent efforts in the field of biomaterials have led to the creation of osseointegrated implants from

biocompatible materials which invade the jawbone to replace the missing tooth or to provide support. However, the successful outcome of this application depends on many parameters. Although the success rate of the technique is relatively high it is not always adequate as the implant is of different consistency to the recipient substrate. To overcome this shortcoming, novel approaches are suggested, deriving from the field of stem cells and tissue engineering. Recently, tooth tissue engineering is providing the scientific ground for novel therapeutic applications regarding the tooth loss, compensating the existing prosthetic methodology. Dental tissue engineering is focusing on three main parameters: the type of cells that should be used, the scaffolds where the cells should be seeded on and the growth factor/molecular signals that should be applied.

1.3.1. DENTAL STEM CELLS

1.3.1.1. Types of dental stem cells

Teeth develop due to interactions between the oral ectodermal epithelial cells and the ectomesenchymal tissue. The ectomesenchymal tissue is rich in mesenchymal stem cells (MSCs), and upon being influenced by the oral ectodermal tissue, it helps form the enamel first and secondly forming the dental papilla and dental follicle. MSCs give rise to other components of the tooth, such as dentin, pulp, cementum, and the periodontal ligament. The presence of different types of MSC populations in teeth has been described, which depending on the harvest site are called dental pulp stem cells (DPSCs), periodontal ligament stem cells (PDLSCs), apical papilla stem cells (SCAPs), dental follicle stem cells (DFSCs), and gingival tissue stem cells (GMSCs), although they are generically referred to as dental stem cell (DSCs). This set of stem cells is particularly interesting because teeth, despite their small size, are a source of abundant cells for

therapeutic procedures, and their preparation can be linked to routine tooth extraction, which does not place an additional burden on the patient. However, some authors suggested that this broad heterogeneity of DSCs could be a drawback for clinical applications if the cellular origin is not identifiable because different subpopulations of DSCs may have different potentials for proliferation and differentiation that could prevent obtaining perfectly predictable and reproducible results.

DPSCs, also known as postnatal dental pulp stem cells, were first isolated by Gronthos et al. from third molars and were characterized as cells with a high level of clonogenicity and proliferation and the ability to generate densely calcified colonies and occasional nodules. The identity of the DPSCs as MSCs has been confirmed by their ability to differentiate into neural ectodermal cells and adipocytes, odontoblasts, osteoblasts, chondrocytes, and myoblast cells of mesodermal origin, confirming their plasticity. These cells are located within the dental crown, in a “niche sealing” or “pulp chamber” that houses the connective tissue known as pulp. The resident tissue cells are a heterogeneous population represented by stromal fibroblasts also known as pulpoblasts and accompanied by odonto/osteoprogenitor populations, neural, vascular cells and inflammatory immune cells such as granulocytes and macrophage cells.

During embryonic development, the dental pulp is a tissue that some authors have described as “ectomesenchyme” because it is derived from ectodermal cells that grow at the periphery of the neural tube, migrate to the oral region, and then differentiate into cells of the mesenchymal phenotype. The epithelial cells give rise to enamel forming ameloblasts, and the MSCs form odontoblasts, pulp, and periodontal ligament. Functionally, the dental pulp is responsible for the maintenance and repair of the periodontal tissue and its associated immune system, has a high

regenerative capacity, and responds to various types of damage. For example, in cases of severe irritation caused by deep caries or restorative procedures leading to the destruction of the layer of odontoblasts or pulp progenitors (DPSCs), dental pulp cells proliferate and migrate into the damaged tissue to differentiate into odontoblast and form reparative dentin which has been proposed to be the main mechanism leading to reparative dentinogenesis.

DPSCs are stem cells derived from human exfoliated deciduous teeth (SHED), from permanent secondary dentition systems (properly known as DPSCs), from teeth extracted by orthodontists due to impaction or irreversible periodontitis, or from inflamed pulp tissue. SHED cells were isolated by Miura et al. from primary dentition systems and were characterized as cells with a high proliferation rate and the ability to differentiate into osteoblasts, neural cells, adipocytes, and odontoblasts (70). As in the case of DPSCs obtained from permanent teeth, SHED cells can generate tissue pulp/dentin and bone cell type, with different levels of odontoblast-like cells and dentin mineralized when transplanted into immunodeficient mice in a hydroxyapatite tricalcium phosphate (HA/TCP) scaffold. It has been suggested that SHED cells have a proliferative ability greater than that of DPSCs isolated from third molars, incisors, or supernumerary teeth or that of bone marrow derived MSCs, because they represent a more immature stem cell population. Thus, as bone marrow-derived MSCs and umbilical cord-derived MSCs have been show to differ, in the case of dental pulp-derived MSCs, it has been shown that the age of the teeth that served as the source of the dental pulp tissues imparted different characteristics and propensities toward differentiating along a specific lineage.

1.3.1.2. Dental pulp stem cells

DPSCs are mesenchymal type of stem cells inside dental pulp. DPSCs have osteogenic and chondrogenic potential *in vitro* and can differentiate into dentin, *in vivo* and also differentiate into dentin-pulp-like complex. Recently, immature dental pulp stem cells were identified which are a pluripotent sub-population of DPSC generated using dental pulp organ culture.

DPSCs are putative candidates for dental tissue engineering due to:

i. Easy surgical access to the collection site and very low morbidity after extraction of the dental pulp.
ii. DPSCs can generate much more typical dentin tissues within a short period than nondental stem cells.
iii. Can be safely cryopreserved and recombined with many scaffolds.
iv. Possess immuno-privilege and anti-inflammatory abilities favorable for the allotransplantation experiments.

1.3.2.3. Identification of dental pulp stem cells

There are four commonly reported stem cell identification techniques, which can be used for the identification of DPSCs. These are:

i. Fluorescent antibody cell sorting: Stem cells can be identified and isolated from mixed cell populations by staining the cells with specific antibody markers and using a flow cytometer.
ii. Immunomagnetic bead selection.

iii. Immunohistochemical staining.

iv. Physiological and histological criteria, including phenotype, proliferation, chemotaxis, mineralizing activity and differentiation.

1.3.2.4 Isolation approaches of dental pulp stem cells

Similar to the stem cell identification techniques, isolation of conventional MSCs techniques can be applied for isolation of DPSCs from the dental pulp tissue. These are described as follows:

i. **Size-sieved isolation:** Enzymatic digestion of whole dental pulp tissue in solution of 3% collagenase Type I for 1 h at 37°C is done. Through process of filtering and seeding, cells with diameter between 3 and 20 μm are obtained for further culture and amplification. Based on this approach, small-sized cell populations containing a high percent of stem cells can be isolated.

ii. **Stem cell colony cultivation:** Enzymatic digestion of the dental pulp tissue is done to prepare single cell suspension cells of which are used for colony formation containing 50 or more cells that is further amplified for experiments.

iii. **Magnetic activated cell sorting (MACS):** Is an immune-magnetic method used for separation of stem cell populations based on their surface antigens (CD271, STRO-1, CD34, CD45, and c-Kit). MACS is technically simple, inexpensive and capable of handling large number of cells, but the degree of stem cell purity is low.

iv. **Fluorescence activated cell sorting (FACS):** Is a convenient and efficient method that can effectively isolate stem cells from cell suspension based on cell size and fluorescence. Demerits of this technique are a requirement of expensive equipment, highly skilled

personnel, decreased viability of FACS-sorted cells and this method is not appropriate for processing bulk quantities of cells.

As mentioned earlier, DPSCs are stem cells derived from either exfoliated primary dentition (SHED teeth) or extracted healthy permanent teeth for orthodontic or therapeutic reasons. The studies of Suchánek et al. showed that SHED cells have a higher doubling time than DPSCs which is consistent with their cell cycle distribution, wherein 69.8% of the SHED cells were in S and G2 stage, but only 56% of the DPSCs were in that phase. Furthermore, the surface antigen profile of SHED cells has been shown to differ from those of DPSC and bone marrow-derived MSC. Because proliferation-related and extracellular matrix formation genes, such as those encoding transforming growth factor (TGF) and fibroblast growth factor 2 (FGF), were expressed, genes encoding molecules such as collagens I and III and pluripotency markers, such as POU5F1 (OCT3/4), SOX2, and NANOG were expressed higher than DPSC (69). Further, SHED cells exhibited a reduced ability to form neurospheres which was related to the expression of nestin, a marker of neuroepithelial stem cells, which is poorly expressed in SHED cells compared with DPSCs. Furthermore, some authors have shown that subpopulations of SHED cells and some stromal elements of the bone marrow were c-kit/CD34+, though these antigens are considered specific markers of hematopoietic lineages, which suggest that stem cells can share characteristics despite having different odontogenic origins. The DPSCs of permanent teeth, impacted third molars, and supernumerary teeth, which today are considered medical waste [50–52], are particularly interesting stem cells. DPSCs recently isolated as the CD90+, CD146+, CD105+, and CD45− cells of supernumerary teeth were found to be capable of multilineage differentiation and were also OCT4+ and NANOG+.

Until recently it was believed that SHED cells, compared with the DPSCs isolated from adult teeth, had advantages for tissue engineering, including their increased proliferation rate, which could allow the rapid expansion of these cells in vitro before their reimplantation, and the painless nature of collecting these stem cells from tissues regarded as "disposable" and easily accessible, which were ideal for young patients who had suffered invasion pulp necrosis in their immature permanent incisors following a trauma. Considering these aspects, Akpinar et al. analyzed the degree of heterogeneity of natal DPSCs, SHEDs. Cells and DPSC derived from impacted third molars were found that, regardless of the origin (female baby born with a tooth, a girl who lost a deciduous tooth at the age of six years and one impacted third molar belonging to a 27-year-old man, resp.), these DSCs had similar characteristics in terms of their morphology, rates of proliferation, expression of cell surface markers, and differentiation potentials (100)

Interestingly, flow cytometric analysis indicated that all three types of DSCs were positive for CD13, CD29, CD44, CD73, CD90, CD146, CD166, and HLA-ABC. The results also showed that SHED cells and DPSCs had a similar cell cycle distribution, with most of the cells (78%) in the G1 phase of the cell cycle, which indicate that the cells were growing in size and synthesizing mRNAs and proteins, whereas cells in S- and G2-phases were present in lower proportions (12% and 10%); and the number of cells that were undergoing mitosis was less than that of the actively growing cells. These recently obtained results showed that DPSCs and SHED cells were more similar to each other than originally supposed. Thus, the implementation of these two cell types at the clinical level should provide the same opportunities and the same level of ease of access to autologous stem cells, which is a competitive advantage over that of stem cells derived from other niches, such as bone marrow-derived MSCs. Although more human transplantation assays have

been performed using DPSCs compared with those performed using SHED cells, the results obtained were similar **(Table 2 and Figure 1)**.

1.3.2.5. DPSC isolation

Two basic methods for the isolation of DPSCs have been described: (a) the explant method (DPSC-OG) and (b) the enzymatic digestion of pulp tissue method (DPSC-ED). Using the first method, the pulp tissue is surgically removed, and the cells are grown from tissue fragments whereas, using the second technique, the dental pulp is digested using collagenase and dispase, after which the cells are seeded, when cell proliferation is observed, and the MSCs are characterized using flow cytometry based on staining with specific markers. Alternatively, some authors have proposed that the isolation of more immature stem cells requires a tissue explant multistage process in which the progenitor cells are first grown in culture; subsequently, enzymatic digestion is performed, and the isolated cells are expanded. To date, an isolation technique that is superior to the others in terms of proliferative capacity, karyotypic stability, or clinical use of DPSCs has not been found; however, most protocols involve enzymatic digestion rather than systemic explantation and generally the cells obtain a sufficient number of cells to at least one round of in vitro expansion for biomedical use. In this regard, different groups have designed and evaluated increasingly efficient methods for the isolation, expansion, and maintenance of clinically safe human DPSCs in sufficient numbers for various protocols; for example, 1 × 106 cells are needed for xenotransplantation into immunodeficient mice, to retain their capacity for regeneration and differentiation with a minimum of any potential risk. Unfortunately, much about the physiology of DPSCs and how these protocols could be optimized is unknown (6).

1.3.2.6. DPSC culture

The initial growth period of MSCs on a plastic surface is characterized by the formation of colonies derived from a single cell. The colonies generated in primary culture can be subcultured, typically through multiple passages, because these cells have a strong tendency to expand in culture. Interestingly, studies have shown that DPSCs can be grown for long periods without compromising their plasticity and ability to form bone nodules in vitro. Suchánek et al. showed that DPSCs achieved 60 population doublings in culture medium designed for bone marrow (102) whereas Laino et al. accomplished 80 passages by maintaining the DPSCs-substrate interaction and cell-cell communication in the central region of the secreted extracellular matrix. Interestingly, it has been reported that after reaching the maximum number of passages before entering senescence (the Hayflick limit), DPSCs still had a normal karyotype and doubling period at up to 40 doublings, which was between 12 and 50 hours but which increased to 60 to 90 hours after 50 replications. However, it is generally accepted that a prolonged expansion period may induce senescence and that after 20 to 40 population doublings, MSCs may lose some biological activities (potency).

Therefore, one of the most important issues regarding DPSCs, and in general for all cells with potential clinical use, is the number of in vitro passages that is most favorable to allowing an in vivo therapeutic effect. The information available for DPSCs is limited, but it has been shown, at least for the treatment of GVHD using MSCs, that the number of cells in fresh tissue (bone marrow or adipose tissue) was not sufficient for therapy. The vast majority of clinical trials exploring the ex-vivo expansion of MSCs found that the smallest number of passages, employed for MSC expansion, correlated with a better patient response and a better survival. Thus, von Bahr et al.

showed that 75% of patients with GVHD who received MSCs from first and second passage had a one-year survival; however, only 21% of those who received MSCs from third to fourth passages survived (106). These results agree with those of Choi et al. who compared the therapeutic effect of bone marrow-derived MSCs that had undergone 3, 5, 7, and 9 passages in the treatment of amyotrophic lateral sclerosis (ALS) and found that MSCs of early passages were best suited for therapy because of their stability, their anti-inflammatory properties, and their more powerful neuroprotective effect, compared with those of MSCs with the highest number of passages [80]. Therefore, although the DPSCs of early passages might be more suitable for human therapy, comparative studies of the biological behavior of human DPSCs, obtained from different numbers of passages, are essential to ensure that one type is superior to the others in terms of clinical efficacy (107).

It is accepted that the proliferation rate of MSCs is highly variable depending on the formulation of the medium (basal media and supplements), the substrate area, the density of cell seeding, and the physical-chemical environment (oxygen and dissolved CO_2 concentrations, temperature, pH, osmolality, and buffer system). Thus, whereas the cells in a mature tooth pulp are not exposed to a hypertoxic environment, the ambient oxygen tension in conventional cell-cultures ranges from 18% to 21% O2 (69); in contrast, the physiological levels of O_2 in a tooth range from 3% to 6%. Recently El Alami et al. compared the proliferation rate of human DPSCs cultured under these contrasting atmospheric pressures (21% and 3% O_2) and found that, under the conventional culture conditions, there was a low rate of proliferation, with oxidative stress and the activation of antioxidants-defense genes such as that of NRF-2, which can interact with proteins related to the cell cycle that play important roles in regulating cell proliferation, thus suggesting that cultivating DPSCs under normal cell-culture oxygen concentrations may not allow obtaining high yields of

viable stem cells. Furthermore, protocols for growing human DPSCs involve the use of fetal bovine serum (FBS), the composition of which is unknown, and which varies between batches, thus hampering the reproducibility of experiments; however, although the use of FBS is considered to be relatively safe for human therapeutic applications, the use of supplements of nonhuman origin is still a matter of substantial debate. In this sense, there is a risk that nonhuman growth supplements may be contaminated with human pathogens such as viruses, mycoplasmas, prions, or other toxic or immunogenic agents. (105)

Although these quality-control and biosecurity concerns are more theoretical than real because no such problems have been reported for transplants of DPSCs obtained from cultures that were expanded in serum-containing medium, in response to this risk, various methods of serum-free culture, using chemically defined materials as supplements, have been proposed. Thus, Takeda-Kawaguchi et al. recently used a chemically defined medium (MSCGM-CD) to grow isolated human DPSCs that did not have a reduced colony forming ability as compared with that of cells grown in medium supplemented with FBS and had the ability to differentiate into odontoblasts in vitro and to form dentin-like structures when transplanted into immunodeficient mice. In contrast, some authors have proposed that, pending the availability of completely serum-free defined medium of GMP (“Good Manufacturing Practices”) grade, products derived from secure human blood, such as platelet lysates, might be considered a viable alternative to FBS. Therefore, the conditions for serum-free cell expansion comparable to that obtained using serum-containing medium must be defined in the future, and it is necessary to analyze whether to employ rigorous expansion protocols (104).

1.3.2.7. DPSC applications

It has been suggested that dental pulp is a potential source of stem cells for orthopedic, oral, and maxillofacial reconstruction. For example, Yamada et al. demonstrated in canines that MSCs derived from the pulp of the deciduous teeth of puppies and that of adult teeth have the ability to form bone when grafted into the jaw. Although there is a possibility that such cells have applications beyond the scope of the stomatognathic system, to date, most of the studies in which human DPSCs, isolated from third molars, or incisors and SHED cells had been transplanted reported the ability of these cells to generate mineralized tissue, extracellular matrix type structures dentin, periodontal ligament, or dental pulp **(Table 2)**. Interestingly, the general procedure for human DPSC administration is to implement them in scaffold or porous biomaterial to reinforce the graft site and induce tissue regeneration (103)

Various materials have been used to produce scaffolds, including the following: collagen nanofibers (NF) poly-L-lactic acid (PLLA), chitosan, PEGylated fibrin HA/TCP, or a combination of these materials; for example, Ravindran et al. applied DPSCs, PDLSCs, and bone marrow-derived MSCs to collagen/chitosan scaffolds at a density of 2 × 106 cells/scaffold and observed the odontogenic differentiation of DPSC and bone marrow-derived MSCs, without the need to add exogenous growth and differentiation factors (70). Zhang et al. seeded 2 × 106 DPSCs/per silk fiber/collagen/hexafluoro-2-propanol (HFIP) scaffold and observed that they formed soft dental pulp (71). Huang et al. created a poly-D, L-lactide, and glycolide (PLG) substance that formed a porous scaffold in which they seeded 1 × 107 DPSCs, which resulted in the development of odontoblast cells that produced dentin type material and also had the ability to regenerate pulp tissue type (72).

1.3.2.8. DPSCs and tissue repair

It is known that MSCs are involved in growth, wound healing, and cell replacement under both physiological and pathological conditions. These cells have been shown to be effective in regenerating periodontal tissue, diabetic critical limb ischemic tissue, bone damage caused by osteonecrosis, skin lesions caused by burns, liver, neuronal and skeletal muscle tissue, and blood vessels among other tissues. Regarding DPSCs, their ability to differentiate into odontoblasts was a major boon for their use in tooth-tissue engineering, but growing evidence that these stem cells were also capable of repairing extraoral tissues, for example, tissues of the musculoskeletal system, because of their similarities to bone marrow-derived MSCs, has resulted in their currently being recognized as one of the most accessible and attractive multipotent MSCs, with high rates of growth, for use in engineering tissue and in regenerative medicine. In light of the above reported evidences pertaining to MSCs, and the information available from literature about the differentiation ability of DPSCs, it would be interesting to evaluate the role of DPSCs in tissue engineering and compare them to that of MSCs.

2. HYPOTHESIS AND OBJECTIVES

2.1. HYPOTHESIS

Our working hypothesis is that the application of mesenchymal stem cells obtained from dental pulp, in an area to be regenerated, transported in a medium that facilitates their implantation, proliferation and differentiation, could increase the speed of bone regeneration process and the amount of regenerated tissue, in comparison with the standard procedures currently used.

2.2. OBJECTIVES

In order to corroborate the aforementioned hypothesis, our primary objective was to develop an experimental model of bone regeneration which facilitates implantation of mesenchymal stem cells derived from dental pulp along with different three-dimensional matrices and to understand the possible biological markers expressed during different phases of inflammation, resolution and bone regeneration. This model was designed in such a way that it could be clinically extrapolated.

In order to achieve this objective, the following secondary objectives were outlined:

- To isolate and characterize mesenchymal stem cells from dental pulp.
- To know the biological behavior of these stem cells in culture, their ability to proliferate and capacity to differentiate.
- To establish the morphological and phenotypic profile of the stem cells in culture.
- To establish the validity of an experimental model of critical size bone defect.
- To demonstrate superior bone regeneration with stem cells, in comparison to methods which do not employ stem cells.

- To understand intercellular communication through identification of expressed biomarkers, during phases of inflammation, resolution and bone regeneration.
- To lay the groundwork for a human clinical trial, by extrapolating the findings of the present research.

3. MATERIALS AND METHODS

3.1. INSTALLATIONS

- Service of Animal Experimentation at the University of Salamanca (PAE SA-001, Salamanca, Spain), which received the animals from Charles River España and housed them until their use.
- Cell Therapy and Regenerative Medicine Unit at the University Hospital of Salamanca which provided the DPSCs for experimentation.
- External research support services of the Cancer Research Center at University of Salamanca, where histological studies were performed.
- Department of Surgery, University of Salamanca:
  - "Laboratory 1" for conducting surgical procedures on experimental animals. This lab was equipped with temperature control, humidity monitoring and air renewal, and the furniture and equipment necessary for performing experimental surgical models using small and medium-sized animals.
  - "Laboratory 2" for conducting the experimental techniques of quantitative and qualitative determination, on all types of samples. This lab was equipped with temperature control, humidity monitoring and air renewal, and the furniture and equipment necessary for performing quantitative and qualitative determination, as described in this project.
  - "Laboratory 3", room type C, equipped with fixed installations and all the elements of a clean room. This lab was equipped with the furniture and infrastructure necessary, in a clean setting, for the development and conduct of experimental analysis proposed in this project.

- Seminar room for holding business meetings, equipped with a computer system, digital projection equipment and furniture suitable for such purposes.
- Warehouse for consumables.
- All the aforementioned facilities were complied with the regulations and legislation in force for the tasks that have been developed in each one of them.

3.2. EQUIPMENT USED

- ***Cleaning and sterilization:*** Autoclave bag sealer: Selecta Sealcom 600; Amprolene AN74i gas sterilizer; Raypa Steam Sterilizer autoclave; Heraeus E42 hot air oven; P-selecta oven; Branson 2510 ultrasonic bath
- ***Anesthesia:*** Matrix gas anesthesia system; Volumetric air respirators – 2; Volumetric ventilators for oxygen and anesthetic gases – 2; Ventilators for small animals (SRI) – 2; Braun infusion pumps – 4
- ***Surgery***: LEICA surgical microscopes with built-in video system and cold light sources; Cole-Parmer 74900 multichannel pump; Masterflex pump + Medingen thermostatized bath; Individual cold light sources
- ***Storage of samples and reagents***: Freezers (Capable of maintaining up to -80˚C) – 3; Freezers (Capable of maintaining up to -20˚C) – 3; Refrigerators (Capable of maintaining up to 4˚C) – 3
- ***Animal housing:*** Isolator, with HEPA system, for small laboratory animals.
- ***General equipment:*** "Cruma" fume hood. Miele thermo-disinfector. Automatic ice machine 85 AS-E. Safety cabinet for flammable and corrosive products. Precision balance:

Precisa 205ª. Balance Sartorius T2101. Sartorius T6101 balance. Millipore Elix 3 water purification system. 2 orbital shakers : Cole Parmer Rocker Platform. Magnetic stirrer : Raypa AG-2. 2 heated stirrers : Eppendorf Mixmate. pH meter: Oaktlon ph 510 series. Water bath: Lauda Ecoline Re 120 from -30 to 150ºC. Laminar flow hood TELSTAR CV-30/70. TELSTAR laminar flow hood. Liquid nitrogen container with THERMO delivery system. THERMO 110 1 liquid nitrogen container for freezing samples. Eppendorf 5417R refrigerated centrifuge (volume 1.5-2 mi). Eppendorf 5810 refrigerated centrifuge (volume 15-50 mi). Eppendorf miniSpin Centrifuge. Sanies Vibra Cell Tm Sonicator. Homogenizer: Glas Col GKH. Computer equipment in use for all specified systems. Eppendorf opMotion 5057 automated pipetting equipment.

- ***Specific equipment:*** Unicam HeAios a spectrophotometer. Thermo Electro Corporation Multiskan ascent plate reader (photometric measurement). Thermo Electro Corporation Varioskan-flashl plate reader (multimode scanning reader, including fluorescence intensity, with temporal resolution of fluorescence (TRF), photometric, and luminometric. Western Blot equipment: BIO-RAD Miniprotean. Western Blot equipment: BIO-RAD Protean-xi cell. Trans-Blot Semi-Dry transfer cell BIO-RAD. 2 Power-Pac HC feeders BIO-RAD/ Thermo-electron corporation. Nanodrop, Nanophotometer, Eppendorf PCR equipment. Image Quant RT ECL image development and analysis equipment from General Electrics.
- ***Computer equipment:*** Computers, printers, peripherals and software adapted to the proposed needs.

3.3. BIOLOGICAL MATERIAL

3.3.1. PROCUREMENT OF PULP TISSUE

Adult male rats, WISTAR Han™ (RccHan™:WIST), 350 g, from Harlan Laboratories Models, S.L., are used. All experiments are performed according to the guidelines established by RD53/013. (Favorable evaluation by the Ethics Committee of the University of Salamanca, with registration number 361).

For the extraction of DPSC, the molars of 6 rats were used (n=2 pulps in each extraction). Under general anesthesia, by intraperitoneal injection with 75 mg/kg of ketamine chloride (Ketolar® 50mg/mL Parke-Davis Pfizer Group) + 50 mg/kg of diazepam (Valium® 10mg/2mL Roche Farma S.A.) and 20 mg/kg of atropine (B/BRAUN 1 mg), the molars were aseptically removed from the mandibular bones of the rat. Subsequently, they were fractured by means of gouge forceps, accessing the pulp chamber and using a Hemingway® mini curettage spoon (Model 1145/0), the dental pulp fragments were obtained **(Figure 6)**.

After extraction, the animals were sacrificed by intraperitoneal anesthetic overdose with ketamine (Ketolar®).

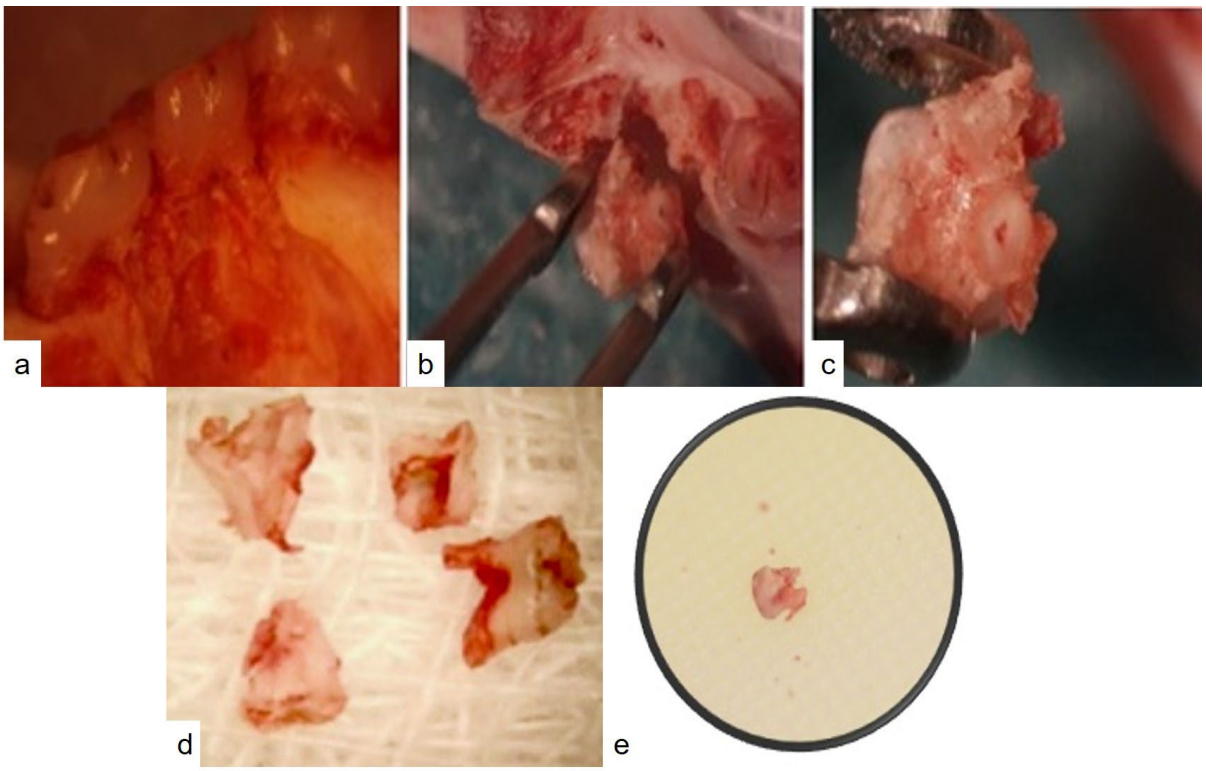

Figure 6. (a) Exposure of rat mandibuar molar teeth for extraction; (b) Extraction of the rat mandibular molar; (c) & (d) Extracted molar teeth; (e) Dental pulp fragments from the molar teeth.

The samples were deposited in a 50 ml falcon tube with 30 ml of Dulbecco's Modified Eagle Medium (DMEM) (Gibco®, Invitrogen), containing 7 mineral salts, 14 amino acids, 9 vitamins, 1 g/l glucose, 0.5 g/l L-glutamine, 0,0150 g/l phenol red and 0.11 g/l pyruvate, supplemented with penicillin, 100 U/ml and streptomycin, 100 µg/ml, and 10% fetal bovine serum (SBF) (Invitrogen), and kept refrigerated for a maximum of 6 hours until the sample was processed.

The time from the moment the molar was exodonated, the pulp tissue was exposed and the sample was prepared for culture did not exceed thirty minutes, since from that moment on the pulp loses its vitality.

After extraction, the animals were sacrificed by intraperitoneal anesthetic overdose with ketamine (Ketolar®).

3.3.2. CELL COLLECTION

3.3.2.1. Isolation and expansion of MSCs

The obtained tissue fragments were incubated with 0.2% collagenase type I (Worthington Biochemicals, Lakewood, NJ) and 0.4% disase II (Sanko Junyaku, Tokyo, Japan) for 70 min at 37 °C under agitation and then centrifuged at 1200rpm 10 min. The pellet was seeded into 9 cm tissue culture dishes[2] and incubated at 37 °C to allow cell adhesion. Cells were incubated in DMEM (Dulbecco's Modified Eagle Medium) supplemented with 10% fetal bovine serum (FBS; Equitech-Bio, Kerrville, TX), and penicillin/streptomycin (100 U/mL penicillin and 100 g/mL streptomycin; Nacalai Tesque) at 37 °C a humidified atmosphere and 5% CO_2. Twice a week the medium was replaced and the unattached cells were discarded. This culture was maintained until adherent cells reached 80-90% confluence.

At this time, the cells adhered to the culture flasks were lifted by the trypsinization method. For this, the culture medium was removed, washed with 10 ml of phosphate buffered saline, also known by its acronym in English, PBS (Phosphate Buffered Saline) and then 3 ml of 0.05% trypsin + EDTA was added, leaving it to act for 6 minutes. Contact with trypsin during this period of time causes the cells to detach from the bottom of the culture flask.

Subsequently, the MSCs are checked under the light microscope to ensure that they have lifted from the surface of the culture. Under the microscope, a morphological change in the cells can be observed, going from an elongated or fibroblastoid shape to a round morphology when they are floating in the medium.

Next, 4 ml of DMEM culture medium and 10% PBS were added to neutralize the toxic action of trypsin, the cell suspension obtained was collected and centrifuged for 10 min at 1,200 rpm, discarding the supernatant. The sediment obtained was diluted in culture medium and the cells were reseeded at a lower concentration to continue their growth and expansion. MSCs in the present study were subcultured to passage six.

MSCs were expanded until the third pass before proceeding to immunophenotypic and multilineage differentiation studies, as at this point the purity of the mesenchymal cell culture exceeded 98%, since residual hematopoietic cells have been removed with successive replacements of the expansion medium.

3.3.2.2. Characterization and differentiation

Characterization: For the characterization of MSCs, the assays indicated by the International Society for Cell Therapy were performed.

After the third pass, for immunophenotypic characterization in the flow cytometer of the samples obtained from dental pulp, the cells were washed with PBS and subsequently treated with trypsin. The trypsin reaction was stopped by the addition of DMEM medium and the cell suspension was transferred to a test tube. The suspension was centrifuged at 1,200 rpm for 5 min. The supernatant was discarded and labeled with the fluorochrome-conjugated monoclonal antibodies according to the following quadruple color combinations (FITC/PE/PerCPCy5.5/APC), as described in **Table 1.**

Table 1. Color combinations of flourochrome conjugated monoclonal antibodies

CD49e PE	**CD11b PE Cy7**	**CD90.1 APCH7**	**CD29 APC**	**CD45 Pacific Blue**	**7AAD PerCP**
1.5µl	1µl	0.5µl	5µl	0.5µl	2.5µl

Samples were incubated for 15 minutes at room temperature and in the dark. Sample acquisition were performed on a FACS Canto model flow cytometer (Becton Dickinson Biosciences, San Jose, CA, USA), and analyzed with the Infinicyt program (Cytognos, Salamanca).

Differentiation: The basis of the technique is to demonstrate the differentiation capacity of mesenchymal cells into three cell lines: osteoblast (bone), adipocyte (fat) and chondrocyte (cartilage).

The DPSCs of each sample were cultured in plates at low density and with bone and adipose differentiation induction media. This was done in duplicate and the control plate was maintained with culture medium. Through staining techniques with solutions such as NBT/BCIP and OilRed, the capacity of differentiation to bone and fat, respectively, were evaluated.

3.3.2.2.1. Osteoblast

To test the osteogenic capacity of rat DPSCs, they were cultured in osteogenic differentiation medium for 25 days. We started from MSCs in pass 3. 30,000 MSCs diluted in 2.5 - 3 ml of DMEM were planted in duplicate in 9 cm^2 plates, one for the control and one for the sample. When the culture reached 30% confluence (approximately 24 hours), the osteoblast differentiation medium (Osteodiff) was added.

Early osteogenic differentiation in osteoblasts was characterized by the activity of the enzyme alkaline phosphatase (ALP), which began to be expressed on the fifth day of culture. The medium was changed twice a week until the tenth day, when alkaline phosphatase staining was performed. ALP expression was examined on day 10 of differentiation using the diazonium salt staining cytochemical assay.

3.3.2.2.2. Adipocyte

200,000 MSCs in pass 3 diluted in 2.5 - 3 ml of DMEM were plated in duplicate in 9 cm^2 plates (Nunc), one for the control and one for the sample. When the culture reached 100% confluence, the adipocyte differentiation medium (Lonza) was added: it consisted of a kit of two media: induction and maintenance. We started adding the induction medium and alternate with the maintenance medium, so that the medium was changed twice a week, until day 21, when the Oil Red staining was performed.

Adipogenic differentiation was tested by intracytoplasmic distribution of lipid vacuoles, finding that they stain with oil red O and express adipophilin, an early marker of adipogenic differentiation.

3.3.2.3. Administration of MSCs in the murine model

Between $1x10^6$ MSC suspended in 200µl of saline were administered and placed in direct contact with the material.

3.4. THREE-DIMENSIONAL ARRAYS OR SCAFFOLDS

The matrix is OsteoBiol Gen-Os®, a 250-1000 micron grain bone substitute. It is a biomaterial of biological origin (porcine) formed by hydroxyapatite (HA) and type I collagen. Its composition is 80% cancellous bone and 20% cortical bone.

It is a natural replica of autologous bone, which preserves the same intimate structure (matrix and porous form) and is characterized by a high osteoconductivity. It is gradually resorbed and ensures a supporting action for bone formation, contributing to preserve the shape and volume of the original graft (osteoconductive property). Moreover, thanks to its collagen-rich content, the product facilitates the formation of the hematic clot and the consequent invasion of reparative and regenerative cells, favoring the complete "restitutio ad integrum" of the bone deficit. The bone tissue responses to prehydrated and collagenated cortico-cancellous porcine bone grafts. a study in rabbit maxillary defects. (101).

3.5. BONE MEMBRANE

Guided bone regeneration (GBR) is based on the use of barrier methods using membranes that isolate a specific bone defect, with the purpose of preventing the growth of tissues with rapid repair capacity, such as connective tissue, thus compromising the osteogenic potential of the bone defect. Evaluation of bone-regeneration effects and ectopic osteogenesis of collagen membrane chemically conjugated with stromal cell-derived factor-1 in vivo (73).

OsteoBiol Evolution® membranes, obtained from mesenchymal tissues, are completely resorbable. Its structure, consisting of dense collagen fibers, has a high consistency and

extraordinary strength, offering maximum adaptability to bone tissue and soft tissues. It is easy and safe to suture with surrounding tissues and provides stability and prolonged protection of the eventual covered graft. Experimental studies have shown histological evidence of the prolonged barrier effect of this membrane, which lasts at least eight weeks.

3.6. EXPERIMENTAL ANIMALS

Adult male rats, WISTAR Han™ (RccHan™:WIST), weighing between 225 and 250 g., from Harlan Laboratories Models, S.L., were used. All experiments were performed according to the guidelines established by RD53/013. (Favorable Evaluation of the Ethics Committee of the University of Salamanca, with registration number 361).

They were stabled in suitable conditions, according to current legislation, and fed, *ad libitum*, with water and standard diet (AØ4, Panlab, Madrid, Spain), with the following composition: crude protein (17.62% of the total), crude fats (2.50%), crude cellulose (4.05%), crude ash (4.38%), starch (43.30%), calcium (0.66%), phosphorus (0.49%), sodium (0.14%), moisture (10.54%), lysine (0.85%), methionine (0.29%), vitamin A (7500 IU), vitamin D (1500 IU) and vitamin E (tocopherol) (15 mg).

The animals were subjected to absolute diet, with water *ad libitum,* 12 hours before the corresponding experiment.

The project complied at all times with current regulations and legislation on the handling of experimental animals.

3.7. METHODS

3.7.1. GENERAL CONDITIONS OF THE STUDY

Bibliographic searches were performed in different Databases (WOS, MEDLINE, MLA Bibliography, PsycLIT Journal Articles, CC Search (R) All 7 CC Editions, U.S. National Library of Medicine) in the period from 2017 to 2021, using some older references.

The approach of the work was carried out following a randomized blinded study: after random assignment, both at the time of drug administration and in the determination and statistical evaluation of the results, we did not know which product was being administered, to which group the sample we were studying belonged, or the identity of the groups being statistically analyzed.

All anesthetic and surgical techniques, sample collection and the determination of the different variables studied were performed under strict aseptic conditions using all the means described in the previous sections.

3.7.1.1. Anesthetic technique used

- Inhalation with isofluorane gas (Forane , Abbott Laboratories, IL, USA).
- Intraperitoneal with 75 mg/kg ketamine chloride (Ketolar® 50mg/mL Parke-Davis Pfizer Group) + 50 mg/kg diazepam (Valium® 10mg/2mL Roche Farma S.A.) and 20 mg/kg atropine (B/BRAUN 1 mg).

3.7.1.2. Surgical techniques used

During the procedures, the experimental animal was placed on a heated microsurgical table, designed to minimize heat loss from the experimental animal, in supine decubitus position with restraint of all four extremities, thus providing complete exposure of the abdominal surgical field. As we have already mentioned, all surgical techniques were performed under strict aseptic conditions, using sterile material. After preparing the surgical field: shaving the skin and administering antiseptic solution of povidone iodine (Betadine, Asta medica), the surgical procedures were performed.

A submandibular approach was performed, accessing the angle and right mandibular ascending branch of the animal, where a circular bone defect of 4.8 mm in diameter (defect of critical size) was performed. The ostectomies were performed with an electric micromotor, using a 4.8 mm trephine drill, under continuous irrigation with physiological saline solution **(Figure 7)**.

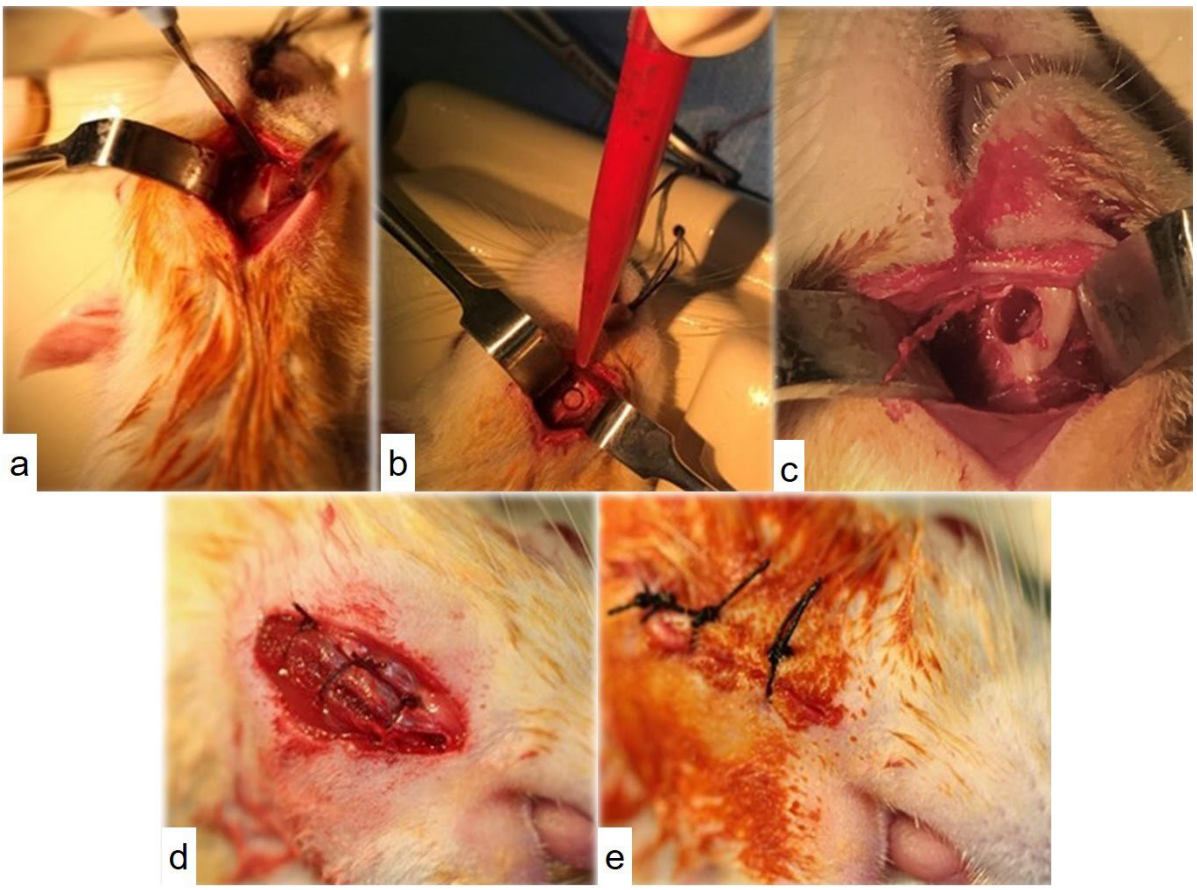

Figure 7. Surgical procedure: (a) Surgical approach to the right angle of mandible in the rat; (b) Circular bone defect (4.8 mm in diameter) marked in the angle of the mandible; (c) Completed circular bone defect ready for placement of biomaterials; (d) & (e) Closure of the surgical wound in layers (muscle and skin) with resorbable suture materials.

The different experimental groups were administered the different substances tested, which are summarized in **Table 2.**

Table 2. Biomaterials used and tested in the different study groups

	Group C	**G+M Group**	**G+M+S Group**
Biomaterial used to fill the defect	None	Filling with OsteoBiol® Gen-Os® (bone substitute in 250-1000 microns grain size).	Filling with OsteoBiol® Gen-Os® (bone substitute in 250-1000 microns grain size).
Biomaterial used to cover the defect	None	OsteoBiol® Evolution® membrane, 5 mm on each side. Modeled with sterile scissors; it was subsequently hydrated with warm, sterile physiological solution.	OsteoBiol® Evolution® membrane, 5 mm on each side. Modeled with sterile scissors; it was subsequently hydrated with warm, sterile physiological solution.
Biological material	No	No	1x10 ^{6}DPSC obtained from rat molars.

Once the surgeries were completed, the wounds were sutured in planes, the muscular plane by means of resorbable suture and the skin by means of non-resorbable suture.

A post-surgical clinical follow-up was carried out, assessing a series of parameters: general condition of the animals, appearance of the wound and the operated area, bleeding or exudate in

the surgical wound, rejection of the biomaterials or membranes and degenerative changes due to dental lesions.

3.8. EXPERIMENTAL MODELS

To carry out this study, the animals were randomly distributed (simple randomization) in four groups of evolution. A sham group, a control group with the defect untreated and two under treatment. For this purpose, 36 surgical interventions were carried out, obtaining a mandibular defect suitable for the study in 36 of the animals. We have used a total of 42 animals that have been distributed in the following groups described below and shown in **Table 3.**

Table 3. Distribution of the study animals in different groups along with characteristics biomaterials used in the defect

GROUPS	SUBGROUP	BONE DEFECT	OSTEOBIOL® EVOLUTION® MEMBRANE	OSTEOBIOL® BONE SUBSTITUTE GEN-OS®	DPSC	SACRIFICE
SHAM	N=6	No	No	No	No	3 months
GROUP C	A (n=6) B (n=6)	Yes Yes	No No	No No	No No	3 months 6 months

G+M GROUP	A (n=6) B (n=6)	Yes Yes	Yes Yes	Yes Yes	No No	3 months 6 months
G+M+S GROUP	A (n=6) B (n=6)	Yes Yes	Yes Yes	Yes Yes	Yes Yes	3 months 6 months

All the animals used in the study survived until the time of sacrifice, and no local or systemic complications related to surgery were observed in the postoperative period that could be a reason for their exclusion from the study.

3.8.1. SIMULATED GROUP

After the experimental animals were anesthetized, blood and tissue samples were extracted. (N=6).

3.8.2. CONTROL GROUP

According to the literature, the critical size of the defects is around 5 mm in diameter, presenting difficulty for their spontaneous closure, thus demonstrating the regenerative potential of the biomaterial under study.We used 12 male Wistar rats weighing between 225 and 250 g.

After the experimental animal was anesthetized, the surgical field was prepared by shaving the hair from the skin and administering an antiseptic solution of povidone iodine (Betadine, Asta Medica®). The bone surface was approached through a skin incision, then a submandibular approach was performed, accessing the angle and right mandibular ascending branch of the

animal, followed by a careful desperiostization until the area was exposed, where a circular bone defect of 4.8 mm in diameter (defect of critical size) was performed. In this way, blood loss and significant drops in blood volume that could lead to the formation of large hematomas were avoided, with the possibility of local infection and, in the worst case, the death of the animal. The ostectomies were performed with an electric micromotor, using a 4.8 mm trephine drill, under continuous irrigation with physiological saline solution, thus creating a contained bone defect that facilitated the stability of the implanted material in the receptor bed. The cortical bone was crossed avoiding one of the major complications of this type of surgery, which is the fracture of the mandible, which can result in the death of the animal due to a deficit in the intake **(Figure 2)**.

Once the appropriate bed was achieved, abundant washing with physiological saline was performed, trying to eliminate the bone particles produced during bone perforation. Subsequently, in the Control group, the defect was left empty and uncovered. Then, the operated area was washed repeatedly with saline solution and the wound was carefully closed following the anatomical planes, starting with the muscular plane with resorbable suture, with loose stitches, and eventually the skin plane with continuous and non-absorbable suture. Finally, after washing the wound, the antiseptic povidone iodine was reapplied.

With these animals the study of the validity of the experimental model is carried out, that is, to achieve this threshold of non-regeneration. Therefore, it is the optimal experimental model, used in our study, to investigate the efficacy of DPSCs in osteogenesis. Furthermore, we consider it to be reproducible, high throughout and cost-effective.

A post-surgical clinical follow-up was performed, assessing a series of parameters: general condition of the animals, appearance of the wound and the surgical site, bleeding, exudate or

seropurulent collections in the surgical wound, extrusion of the biomaterials or membranes and degenerative changes due to dental lesions.

At the end of the experimental period (3 and 6 months), the animals were sacrificed and samples were obtained: whole blood was extracted by aortic puncture, each of the hemimandibles was removed en bloc and tissue was collected.

In the pieces of this control group, the areas where the lesions were caused are visually identified. Half of the animals in each group, prior to slaughter, undergo radiological assessment by computed tomography (CT). Once the tissue is obtained, it is placed in liquid nitrogen, preserved in cryo-freezing tubes at -80ºC. The hemimandibles were immersed in 3.7-4.0% w/v buffered formaldehyde at pH=7. The blood samples, obtained by aortic puncture, were immediately centrifuged for 20 minutes at 4500 rpm and 4ºC, extracting the serum and after dividing them into aliquots, they were frozen at -80ºC in cryo-freezing tubes.

3.8.3. G+M GROUP

To evaluate the effect of OsteoBiol® Evolution® Membrane and OsteoBiol® Gen-Os® bone substitute on bone regeneration, 12 male Wistar rats (225-250 g) were operated on, causing 12 mandibular lesions.

After anesthetizing the experimental animals, the surgical field was prepared by shaving the hair from the skin and administering an antiseptic solution of povidone iodine (Betadine, Asta Medica®). A submandibular approach was performed, accessing the angle and right mandibular ascending branch of the animal, where a circular bone defect of 4.8 mm in diameter (defect of

critical size) was performed. The ostectomies were performed with an electric micromotor, using a 4.8 mm trephine drill, under continuous irrigation with physiological saline solution **(Figure 7)**.

In the G+M group, the defects were filled with a 250-1000 micron grained bone substitute (OsteoBiol® Gen-Os®) and covered with the membrane (OsteoBiol Evolution®). The membrane was modeled with the desired shape, (5 mm on each side), using sterile scissors; it was subsequently hydrated with warm, sterile physiological solution **(Figure 8)**.

A post-surgical clinical follow-up was performed, assessing a series of parameters: general condition of the animals, appearance of the wound and the surgical site, bleeding, exudate or seropurulent collections in the surgical wound, extrusion of the biomaterials or membranes and degenerative changes due to dental lesions.

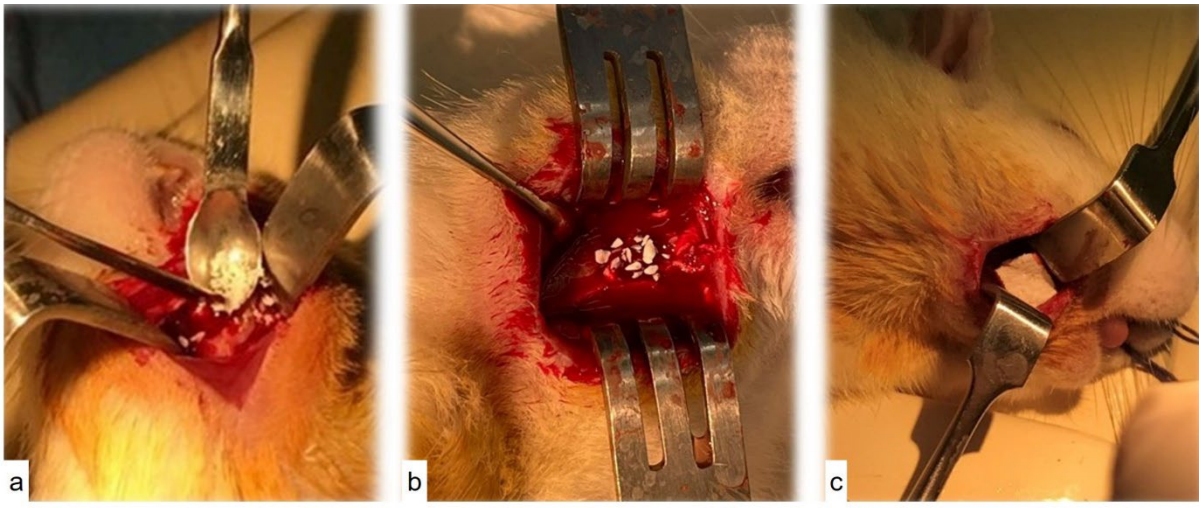

Figure 8. Biomaterial filling within the defect in G+M Group: (a) & (b) Filling the defect with bone substitute (OsteoBiol® Gen-Os®); (c) Covering the filled defect with membrane (OsteoBiol Evolution®).

At the end of the experimental period (3 and 6 months), the animals were sacrificed and samples were obtained: whole blood was extracted by aortic puncture, each of the hemimandibles was removed en bloc and tissue was collected.

Half of the animals in each group, prior to slaughter, underwent radiological assessment by computed tomography (CT). Once the tissue was obtained, it was placed in liquid nitrogen, preserved in cryo-freezing tubes at -80ºC. The hemimandibles were immersed in 3.7-4.0% w/v buffered formaldehyde at pH=7. The blood samples, obtained by aortic puncture, were immediately centrifuged for 20 minutes at 4500 rpm and 4ºC, extracting the serum and after dividing them into aliquots, they were frozen at -80ºC in cryo-freezing tubes.

3.8.4. G+M+S GROUP

To evaluate the effect of DPSCs on bone regeneration we used 12 male Wistar rats (225-250 g). After anesthetizing the experimental animal, the surgical field was prepared by shaving the hair from the skin and administering an antiseptic solution of povidone iodine (Betadine, Asta Medica®). A submandibular approach was performed, accessing the angle and right mandibular ascending branch of the animal, where a circular bone defect of 4.8 mm in diameter (defect of critical size) was performed. The ostectomies were performed with an electric micromotor, using a 4.8 mm trephine drill, under continuous irrigation with physiological saline solution **(Figure 2)**.

In the G+M+S group, the defects were filled with a 250-1000 micron grained bone substitute (OsteoBiol® Gen-Os®) containing the DPSCs and protected with the membrane (OsteoBiol Evolution®). The membrane was modeled with the desired shape (5 mm on each side) using sterile scissors; it was then hydrated with warm, sterile physiological solution. **(Figure 9)**.

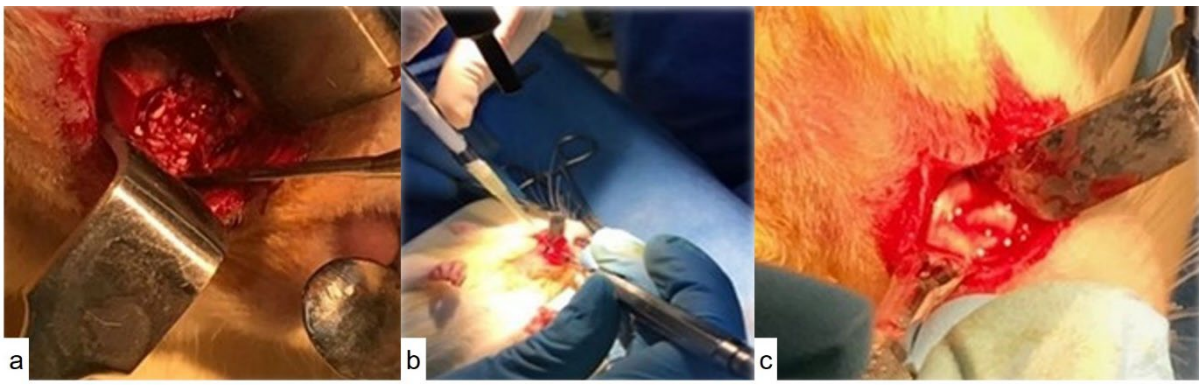

Figure 9. Biomaterial filling witin the defect in G+M+S Group: (a) Filling the defect with bone substitute (OsteoBiol® Gen-Os®); (b) Administration of dental pulp stem cells to the bone substitute in the defect; (c) Covering the filled defect with membrane (OsteoBiol Evolution®).

A post-surgical clinical follow-up was performed, assessing a series of parameters: general condition of the animals, appearance of the wound and the surgical site, bleeding, exudate or seropurulent collections in the surgical wound, extrusion of the biomaterials or membranes and degenerative changes due to dental lesions.

At the end of the experimental period (3 and 6 months), the animals were sacrificed and samples were obtained, extracting whole blood by aortic puncture, extirpation in block of each of the hemimandibles and collection of tissue. Half of the animals in each group, prior to slaughter, underwent radiological assessment by computed tomography (CT). Once the tissue was obtained, it was placed in liquid nitrogen, preserved in cryo-freezing tubes at -80ºC. The hemimandibles were immersed in 3.7-4.0% w/v buffered formaldehyde at pH=7.

The blood samples, obtained by aortic puncture, were immediately centrifuged for 20 minutes at 4500 rpm and 4ºC, extracting the serum and after dividing them into aliquots, they were frozen at -80ºC in cryo-freezing tubes.

3.9. REVERSION OR AWAKENING

At the end of the surgery, the animals were placed in their respective cages, avoiding manipulations in the first hours after the intervention. This phase was performed spontaneously, without requiring additional medication. No complications or toxic effects were observed, achieving a gentle and progressive awakening of the animals.

3.10. POSTOPERATIVE ANALGESIA

Postoperative pain control was performed by administration of buprenorphine hydrochloride: 0.3 mg/kg intramuscularly before surgery and for three days thereafter.

3.11. VARIABLES TO BE STUDIED

The following variables were studied: survival, cellular viability, macroscopic assessment, radiological study by Computerized Tomography (CT), histological damage with MO (H&E), immunohistochemistry (Runx2, ALP and osteocalcin), biochemical markers of bone formation: Calcitonin, parathyroid hormone (PTH), endoglin, transforming growth factor (TGFβ1) and Procollagen Type 1 and for analytical determinations of phosphocalcic and bone metabolism we studied Hepatic Metabolite (Calcidiol), Vit. D, Calcium, Phosphorus, Magnesium.

3.11.1. CELL VIABILITY TESTING

We checked that the implanted cells were viable. To do this, a small volume of implanted cells were preserved after surgery, transferred back to the laboratory and reseeded to check for live cells.

3.11.2. RADIOLOGICAL STUDY

Regarding the radiological evaluation (CT): a densitometric study of the bone repair of the mandibular defect was performed.

The anesthetized animals were placed in prone position and then the same protocolized study of radiological technique for CT was performed and the bone repairs of the mandibular defect were analyzed by means of a multimodal SPECT/CT Albira II ARS scanner belonging to the University of Salamanca. **(Figure 10)**.

Figure 10. Radiological evaluation of the bone defect: (a) Multimodal SPECT/CT Albira II ARS scanner; (b) The study animals placed in prone position during scanning.

The radiological images were transferred to a computer and digitized according to 16-bit gray levels. The program used was FIJI, an open source, "image processing package" that is a "distribution of IMAGE-J with added add-ons for image analysis" in its Windows version.

3.11.3. HISTOLOGICAL STUDY

The hemimandibles were fixed in formaldehyde 3.7-4% buffered at pH 7 and stabilized with methanol. Once the specimens were fixed after remaining in this solution for 24 hours, they were accordingly processed, sectioned and stained with H&E for the histological investigations.

3.11.3.1 Sample processing materials

i. Nitric Acid
ii. Distilled water
iii. Absolute ethanol
iv. Xylol
v. Kerosene
vi. Rotation microtome. (Micron HM 350 S. Thermo Scientific. Germany)
vii. Slides
viii. Cover slip

a. Solution preparation

To prepare a 5% solution of Nitric Acid. 5 ml of nitric acid were diluted in 95 ml distilled water. 50%, 70%, 80% and 95% ethanol solutions. 50, 70, 80 and 95 ml of absolute ethanol were taken and mixed with 50, 30, 20 and 5 ml, respectively, of distilled water.

b. Bone decalcification

The samples were introduced in 5% nitric acid solution, in a volumetric relation of at least 1/20, at 25ºC for 24 hours. After decalcification, the acid was rinsed with distilled water.

c. Dehydration of the sample

Water was removed from the samples by immersing it in ethanol solutions of increasing concentrations, 50%, 70%, 80%, 95% and absolute. The samples were kept for one hour in each solution so that dehydration occurs slowly, thus avoiding deformation of the sample.

d. Clarification

Once the samples have been dehydrated, the ethanol was replaced by immersing them in a miscible substance in both ethanol and kerosene, xylol or xylene was used. The bath was kept for one hour at room temperature.

e. Inclusion and formation of blocks in kerosene.

The samples were placed in a beaker and melted kerosene was added at 60ºC, the samples were placed in the oven at 60ºC for up to 6 hours, depending on the thickness of the samples. The samples were then placed, oriented, in a mold with melted kerosene and allowed to solidify at room temperature to form blocks.

f. Obtaining the cuts

Using a rotating microtome, 4 to 6 micron slices were obtained, left floating in a thermostatized bath with warm water, the slices were carefully spread out to avoid wrinkling and collected on a degreased slide covered with a layer of Mayer's adhesive.

g. Staining of sections

Prior to staining, the sections were deparaffinized by means of a bath in xylol at 58ºC for 15 minutes. Then they were rehydrated in alcoholic solutions of decreasing concentrations, starting with absolute ethanol followed by 95%, 80%, 70% and 50%, the samples were bathed 30" in each one, then they were rinsed 30" in distilled water and proceeded with the Hematoxylin and Eosin staining procedure .

Once the specimens were stained, they were dehydrated with ascending alcohols of increasing gradation, rinsed with xylol and coverslipped with a drop of Canada balsam adhesive, which has a refractive index similar to that of glass. It is left to dry for a few hours and then observed under the optical microscope.

The sections were eventually analyzed under an optical microscope (Leica DMLB) with an Olympus DP70 digital camera.

Comparative histological study was performed by observing the characteristics of each sample under the optical microscope.

3.11.4. IMMUNOHISTOCHEMISTRY TECHNIQUE

3.11.4.1. Basis

This technique is based on the specific localization of proteins in tissue samples. It consists of the conjugation of a primary antibody with the protein to be identified and its subsequent detection by means of secondary antibodies linked to substrate molecules that allow microscopic visualization after the addition of a chromogen.

3.11.4.2. Sample preparation

The histological sections, once rehydrated, were prepared for the optical microscopic studies. Initially, an antigen retrieval treatment was applied, maintained for 4 minutes in a pressure cooker and the samples were left to stand for 20 minutes. They were then washed under running water for three minutes.

In order to block the possible endogenous peroxidase signals, the specimens were kept for 10 minutes in hydrogen peroxide with 3% methanol.

After removing the endogenous signal from the sections, the sections were washed for 5 minutes with PBS,then incubated for one hour with blocking serum diluted 67-fold to prevent nonspecific labeling. The excess liquid remaining in the preparations was removed and they were incubated for one hour with the primary antibody, at the appropriate dilution for each molecule.

3.11.4.3. Antibodies

Primary antibodies:

i. Anti-Runx2 (ab192256, 1:100, Abcam).
ii. Anti-ALP (ab108337 1:100, Abcam).
iii. Anti-Osteocalcin (M65178420, 1:100 Mybiosource).

Then, followed by a 5 minute wash with PBS and incubated with a multilink secondary antibody for 30 minutes. After washing with PBS for 5 minutes again, the samples were incubated with a multilink HPR tertiary antibody for 30 minutes and washed once again with PBS. Immediately thereafter, DAB chromogen was added for 10 minutes. DAB generates a brown color at the site where the target antigen recognized by the primary antibody was present. The preparations were washed with plenty of running water and lightly counterstained by immersing them in Mayer’s Hematoxylin for a few seconds and rinsing under running water till the nuclei appear blue.

Finally, the sections were dehydrated using alcohols of increasing concentration, 70º, 80º, 90º and 100º, coverslipped using a mounting medium (Tissue-Tek) and subsequently observed under an optical microscope.

3.11.5. ELISA TECHNIQUE

For the study of the biochemical markers of bone formation: calcitonin, parathyroid hormone (PTH), endoglin, transforming growth factor (TGFβ1) and Procollagen Type 1, the Elisa Technique was used.

3.11.5.1. Sample collection

We used non-hemolyzed blood samples (N=6 per group). Immediately after extraction, they were centrifuged, serum was extracted, divided into aliquots and frozen at -80ºC.

3.11.5.2. Principles of testing

An ELISA kit was employed with multiple antibodies with the "sandwich" principle. First, a 96-well plate was used with a monoclonal anti- (Endoglin, Procollagen I, Calcitonin, TGF-, PTH) antibody attached to each well to capture the antibody present in the samples and standards were added in duplicate to each well along with the corresponding blanks. After washing the dish to remove unattached material, an anti-cytokine polyclonal peroxidase conjugate was added. The plate was then washed again to remove the unattached material and the substrate solution that initiated peroxidase catalysis was added. The color change was stopped by acidification.

3.11.5.3. Plate preparation and test procedure

The Capture Antibody was diluted in PBS to the required concentration. Immediately a 96-well plate was covered with 100 µl per well of diluted Capture Antibody. The plate was covered and incubated overnight at room temperature, each well was aspirated and washed with wash buffer, repeating the process 2 times for a total of three washes, the wells were thoroughly washed with 400 µl of wash buffer using a multiplex dispenser. Removing the liquid well at each step was essential for a good result. After the last wash, the wash buffer residues were removed by suction or by turning the plate upside down on blotting paper. Added 300 µl of Reagent Diluent to each well. Incubated at room temperature for at least one hour. Repeated the aspiration/washing step as in step 2, and the plates were ready for sample addition. Added 100 µl of sample or Standards in Reagent Diluent or an appropriate diluent per well. Covered with an adhesive strip and incubated for 2 hours at room temperature. Repeated the aspiration/washing as in step 2 of plate preparation. Added 100 µl of Detection Antibody, diluted in Reagent Diluent, per well. Covered with a new adhesive strip and incubated for 2 hours at room temperature. Repeated the aspiration/washing as in step 2 of the plate preparation. Added 100 µl of Streptavidin-HRP working dilution to each well. Covered the plate and incubated for 20 minutes at room temperature. The plate was protected from direct light. Repeated aspiration/washing as in step 2 of plate preparation. Added 100 µl of substrate solution to each well. Incubated for 20 minutes at room temperature. Protected the plate from direct light. Added 50 µl of Stop Solution to each well, gently moved the plate very carefully to mix well. Determined the optical density. The absorbance was measured at 450 nm and the results obtained were proportional to the amounts of cytokine in the samples, which were calculated by interpolation with the standard curve.

The following ELISA kits were used for identification of the cytokines

i. Transforming Growth Factor Beta 1 (TGFβ1): Enzyme-linked Immunosorbent Assay kit ABK1-E1239.
ii. Rat Procollagen Type 1: Enzyme-linked Immunosorbent Assay kit LSBio LifeSpan BioSciences.
iii. Endoglin (ENG): Enzyme-linked Immunosorbent Assay kit ABK1-E2467.
iv. Calcitonin: Enzyme-linked Immunosorbent Assay kit ABK1-E1354.
v. Parathyroid Hormone (PTH): Enzyme-linked Immunosorbent Assay kit ABK1-E1599.

3.11.6. DETERMINATION OF MINERALS.

Calcium (Ca), Phosphorus (P) and Magnesium (Mg) determinations were performed by colorimetric/spectrophotometric techniques using Wiener lab® kits.

3.11.6.1. Determination of Calcium

Rationale: Ca reacts with cresolphthalein complexone (cfx) at pH 11 to form a purple color that is measured photocolorimetrically at 575 nm wavelength. The intensity of the purple color is proportional to the Ca concentration in the sample (74).

Reagents:

i. Cfx reagent: cresolphthalein complexone solution 3.7 mmol/L.

ii. Buffer: 0.2 mol/L aminomethyl propanol (AMP) solution. In methanol 35% v/v for final pH 11.

iii. Standard: Ca solution 10 mg/dL

Procedure: In two tubes labeled S (Standard) and M (Sample) 25 µL of cfk reagent and 1.7 mL buffer were placed in each tube. It was mixed immediately and the reading of the absorbance of both tubes was made in the spectrophotometer at 570 nm wavelength, taken to zero the spectrophotometer with distilled water. Then 10 µL of standard solution was added to tube S and 10 µL of sample (acid solution) to tube M, mixing them immediately. After 10 minutes a second reading was taken at 570 nm.

Calculation of results: The following formula was used to calculate the results:

$[\text{Calcium}] = F_c \times A_m$

Where:

F_c = Calibration Factor

$$Fc = \frac{[\text{Standard}]}{As} = \frac{10}{0.392} = 25.51 \text{ mg/dL}$$

Standard = 10 mg/dL

A_s = Absorbance of the standard = 0.392

A_m = Absorbance of the sample material

Results are expressed in milligrams of Ca per 100 mL of plasma (mg/dL).

3.11.6.2. Determination of Phosphorus

Rationale: Inorganic P reacts in acid medium with molybdate to give a phosphomolybdic complex which is measured spectrophotometrically at 340 nm wavelength.

Reagents:

i. Working reagent: 2 mmol/L ammonium molybdate solution in 1% sulfuric acid.
ii. Standard: stabilized phosphate solution equivalent to 4 mg/dL of inorganic phosphorus.

Procedure: Three tubes labeled B (blank), S (standard), and M (sample) were prepared. To tube S 10 µL of standard solution was added and to tube M 10 µL of sample (acid solution). Then 1 mL of the working reagent was added to the 3 tubes. They were mixed and incubated for 10 minutes at room temperature. Finally the reading was made in UV spectrophotometer at 340 nm wavelength, previously calibrated the spectrophotometer with distilled water.

Calculation of results: The following formula was used to calculate the results:

$[\text{Phosphorus}] = F_c \times A_m$

Where:

F_c = Calibration Factor

$$Fc = \frac{[\text{Standard}]}{As} = \frac{4}{0.206} = 19.42 \text{ mg/dL}$$

Standard = 4 mg/dL

A_s = Absorbance of the standard = 0.206

A_m = Absorbance of the sample material

Results are expressed in milligrams of P per 100 mL of plasma (mg/dL).

3.11.6.3. Determination of Magnesium

Rationale: Mg forms a colored complex by reacting with calcagite in alkaline solution. EGTA eliminates Ca interference. The colored complex is measured at 520 nm wavelength (100)

Reagents:

2 Methyl-2 Amino-1-propanol 10 ml/L.

EGTA 210 µmol/L

Calmagite 170 µmol/L

Standard: Mg 3 mg/dL or 0.82 mmol/L

Procedure: Three tubes labeled B (blank), S (standard), and M (sample) were prepared. To tube S 10 µL of standard solution was added and to tube M 10 µL of sample (acid solution). Then 1 mL of the working reagent was added to the 3 tubes. It was incubated for 5 minutes at room temperature and then read at 520 nm wavelength in the spectrophotometer.

Calculation of results: The following formula was used to calculate the results:

$[\text{Magnesium}] = F_c \times A_m$

Where:

F_c = Calibration Factor

$$Fc = \frac{[Standard]}{As} = \frac{3}{0.055} = 54.54 \text{ mg/dL}$$

Standard = 3 mg/dL

A_s = Absorbance of the standard = 0.055

A_m = Absorbance of the sample material

Results are expressed in milligrams of Mg per 100 mL of plasma (mg/dL).

3.11.6.4. Estimation of Vitamin D

Vitamin D and its hepatic metabolite (calcidiol) were determined using a Hitachi 747-200 automatic analyzer (Boehringer Mannheim, Indianapolis, IN).

Results are expressed in milligrams of Vitamin D per 100 mL of plasma (mg/dL).

3.12. STATISTICAL ANALYSIS

The statistical program used for the present study was NCSS 2007. (Dr. Jerry L. Hintze, Utah USA). All values in this work have been represented as X ±SD (mean ± standard deviation). For all the above studies a value of $p<0.05$ was considered statistically significant.

Statistical inference of the results presented (numerical values from independent random samples obtained from the populations studied) was performed with one-way analysis of variance

(ANOVA) applying the following statistical tests depending on the type of distribution and variances:

i. For Normal variables with equal variances, we applied the Scheffe test.
ii. In the case of Normal variables with different variances, we applied variance stabilizing transformations and then the Scheffe test.
iii. For variables of any other distribution with equal or different variances, we used non-parametric methods: the Kruskal Wallis test.

4. RESULTS

4.1. ISOLATION OF DENTAL PULP MESENCHYMAL STEM CELLS (DPSCS)

Dental pulp from rat molar teeth was extracted as a source of DPSC cells, in order to develop the first objective, which is to isolate and characterize mesenchymal cells from rat dental pulp. In addition to testing the expansion and differentiation capacity of dental pulp MSCs.

4.1.1. ISOLATION OF PULP TISSUE

Pulp tissue samples were successfully obtained from the molars of six rats (n=2 pulps from each extraction).

4.1.1.1. Cell culture and expansion

The results obtained show that it is possible to isolate MSCs from dental pulp tissue using enzymatic digestion methods. The cells obtained after culture show a fibroblastoid type morphology, elongated and flattened, which were adhered to the plastic surface of the culture, essential characteristics of MSCs **(Figure 11)**.

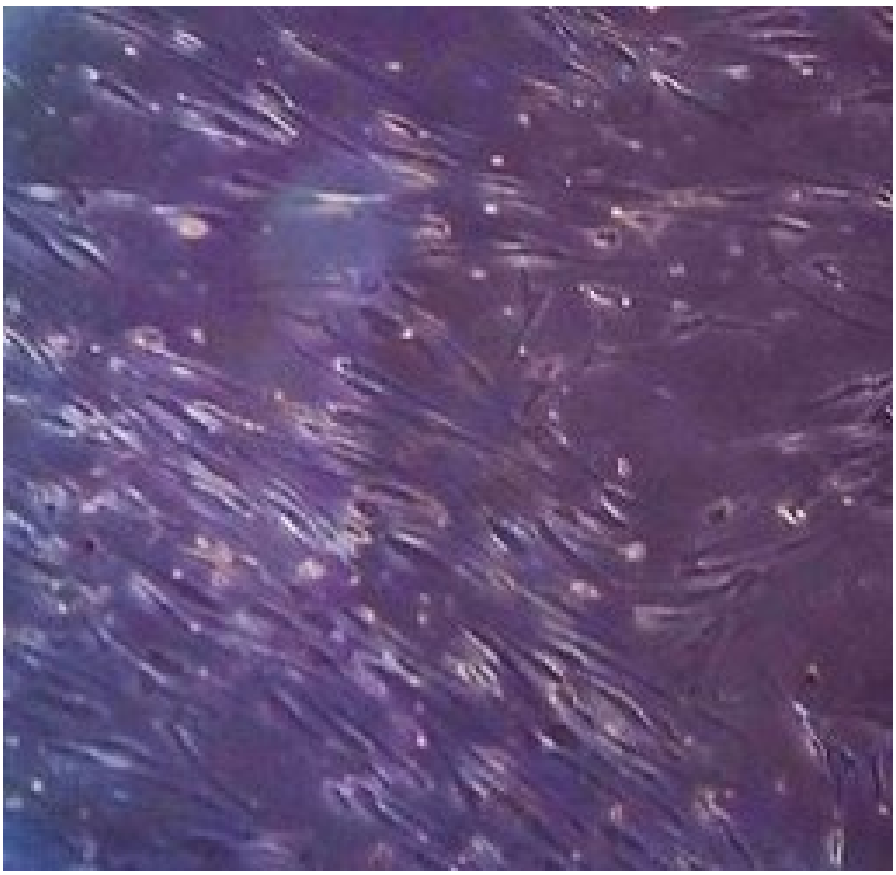

Figure 11. Confluence of mesenchymal stem cells derived from dental pulp.

4.1.1.2. Characterization and flow cytometry

Marking with fluorochrome-conjugated monoclonal antibodies according to the following combinations:

Unchecked (control)

CD90-FITC/CD166-PE/CD73-PE-Cy7/7AAD-PerCp

CD90-FITC/CD95-PE/HLA-APC/7AAD-PerCP

CD90-FITC/CD104-PE/CD117-APC/7AAD-PerCP

CD44-FITC/CD146-PE/CD29-Pacific Blue/7AAD-PerCP

(CD45, CD14, CD19)-FITC/CD106-PE/7AAD-PerCP/CD90-PE- Cy7/CD105-APC/CD34-APC-Cy7

According to the ISCT (International Society of Cellular Therapy), the expression of CD90 and CD105 antigens should be positive in the presence of mesenchymal cells and the expression of CD45, CD34, CD3, CD117 and CD11b antigens should be negative because they are markers of hematopoietic cells.

In the "Dot Plot" illustrations, FSC is expressed on the "X" Axis and SSC on the "Y" Axis, which gives us cell size and viability as well as complexity.

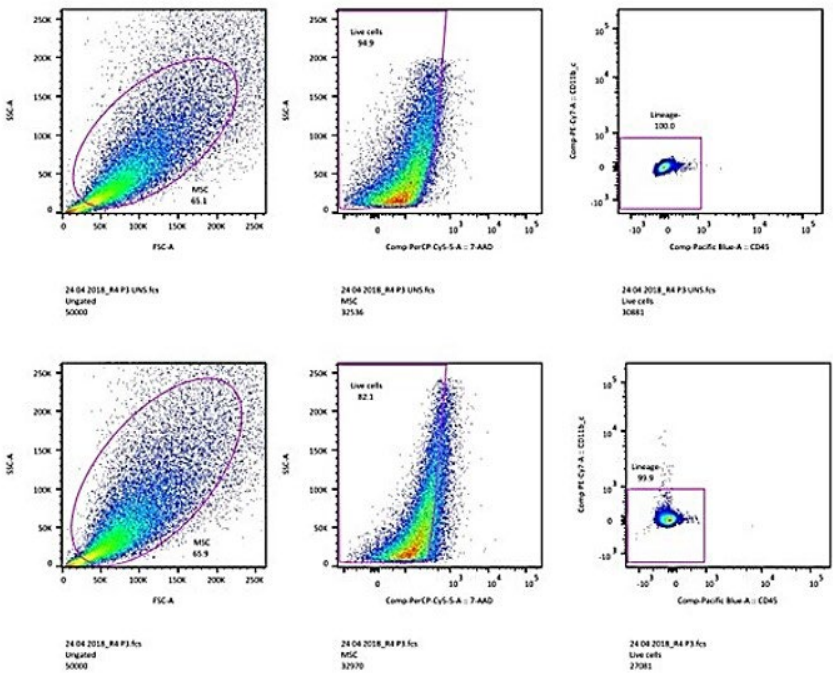

Figure 12. Dot plots of mesenchymal stem cells derived from dental pulp.

Figure 12 shows the mono-parametric histograms with the cell population of the rat dental pulp. The "X" axis and "Y" axis corresponding to the fluorescence intensity and the number of cells is related, respectively. They are in logarithmic decimal scale. The logarithmic scales are of great importance because they group high signals and distinguish the negative control. The cell population is represented by the CD90 and CD29 markers and for the negative control the expression of the CD49e marker was used. Thus, it was demonstrated that no lymphocytes were found within the cell population.

The ranges obtained for the positive markers for mesenchymal stem cells were for CD90 (99.7%), for CD29 (86.5%) and negative (0%) for CD49e **(Figure 13)**.

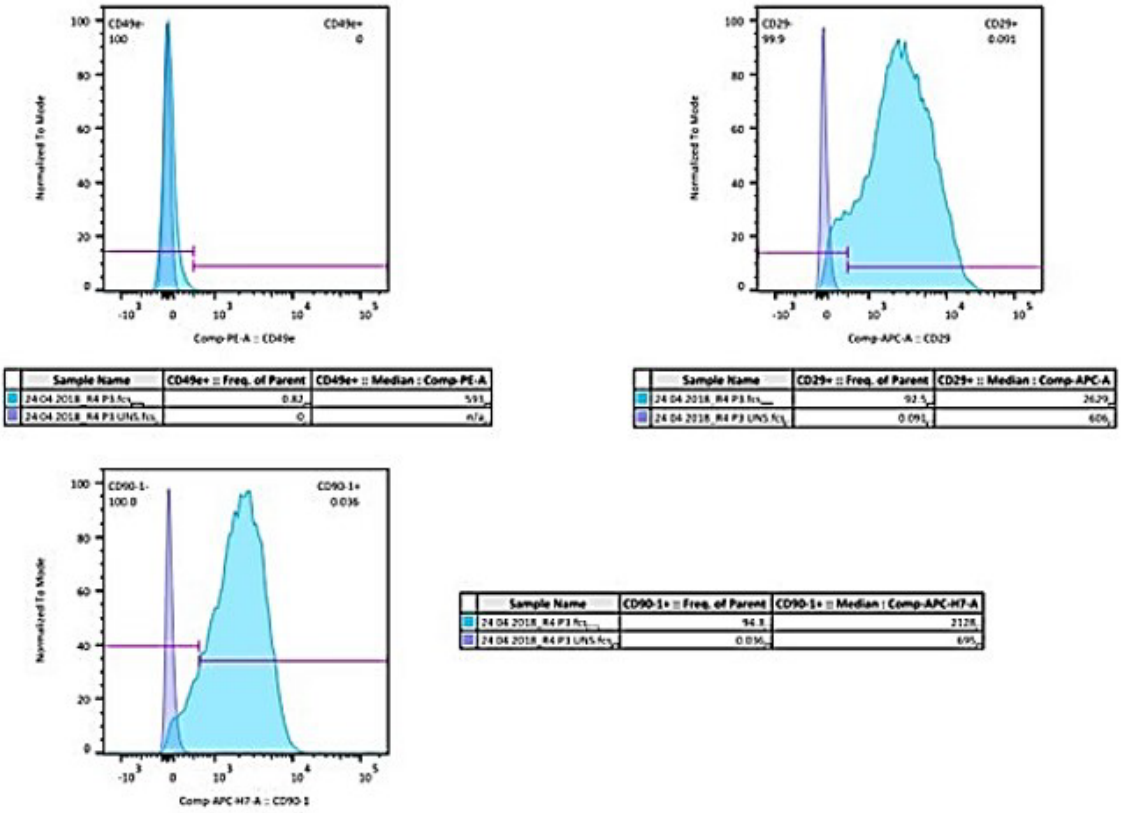

Figure 13. Mono-parametric histograms of mesenchymal stem cells derived from dental pulp.

4.1.1.3. Differentiation

The rationale of the technique was to demonstrate the differentiation capacity of MSCs to two lines, using a control group with undifferentiated DPSC cells.

MSCs obtained from dental pulp tissue were able to differentiate into osteogenic and adipogenic lineages. Thus, demonstrating the capacity for plasticity towards other cell lineages **(Figure 14)**.

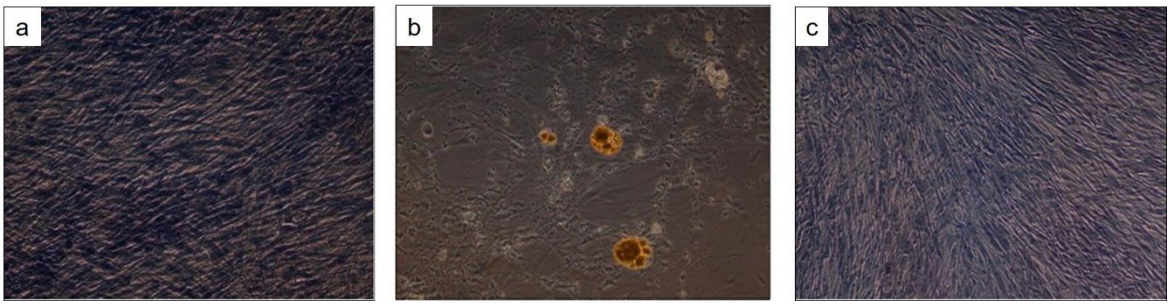

Figure 14. Cell morphology of the differentiated dental pulp stem cells: (a) Osteogenic differentiation with Osteodiff medium (Miltenyi Biotec) showing alkaline phosphatase staining; (b) Adipogenic differentiation, showing the presence of intracellular lipid vacuoles stained with Oil Red; (c) Control sample.

To test the osteogenic capacity of rat DPSCs, ALP expression was examined at day 10 of differentiation using the diazonium salt staining cytochemical assay, finding high ALP expression in differentiated cells and no expression in undifferentiated DPSCs used as controls.

Adipogenic differentiation was tested by intracytoplasmic distribution of lipid vacuoles, finding that they stain with oil red O and express adipophilin, an early marker of adipogenic differentiation. At 14 days of differentiation, they found 50% differentiated cells, which had 70% of their cytoplasm occupied by lipid droplets, if the culture was prolonged to 28 days of differentiation the cells did not detach and 100% of the cells differentiated, with lipids occupying 80% of the cytoplasm.

Therefore, it is possible to isolate mesenchymal cells from dental pulp, demonstrating that the criteria established by ISCT are met as shown in **Table 4.**

Table 4. Summary of ISCT criteria to identify mesenchymal stem cells (75).

Summary of the criteria ISCT to identify MSC		
Adherence to plastic under standard culture conditions		
Phenotype	Positive (≥95%) CD105 CD73	Negative (≤ 2%) CD45 CD39 CD14 o CD11B CD79α o CD 19
in vitro differentiation: osteoblasts, adipocytes, chondroblasts		

4.1.1.4. Conclusion

We have observed that access to the dental pulp is easy and the extraction of DPSC is highly efficient. Demonstrating that the criteria established by ISCT are met.

4.2. *IN VIVO* RESULTS IN ANIMAL EXPERIMENTAL MODEL

4.2.1. GROUP C

An essential step in our trial was to create an experimental bone defect in the mandible large enough to prevent spontaneous regeneration. A critical defect is defined as one that will regenerate less than 10% of bone during the lifetime of the animal and in the rat, mandible will be an area greater than 4 mm in diameter.

To achieve this non-regeneration threshold, the experimental model used in our study is optimal for investigating the efficacy of DPSCs in osteogenesis. In addition, we consider it to be reproducible, high-throughput, and cost-effective.

Twelve animals were operated on, causing six mandibular lesions. No animal died postoperatively, nor suffered fractures. The general condition of the animals was favorable; some soft tissue swelling was observed due to the ostectomy, which disappeared spontaneously. Twelve lesions suitable for the study were obtained.

4.2.1.1. Radiological analysis

The study area was defined as a circular area of 4.8 mm in diameter. **Figures 15 and 16** shows the results of performing a simple radiological study of the highest resolution on two animals of each group. In the figures the defects in the jaws of the anesthetized rats are observed, before being sectioned and taking as reference the study periods of 3 and 6 months. In the radiological

tests in the Control Group, no signs of healing were observed at 3 months. As a consequence of the continued hypoxia in the osteocytes that border the lesion (no capillaries arrive), they die and necrotize, producing a dental degeneration that can be seen very well in the **Figure 16**.

Table 5. Radiological evidence in Group C at 3 and 6 months

	3 months	**6 months**
Group C **(No treatment)**	there are no signs of healing	there are no signs of healing degeneration or dental transformation

Figure 15. Radiological image of a group C defect at 3 months.

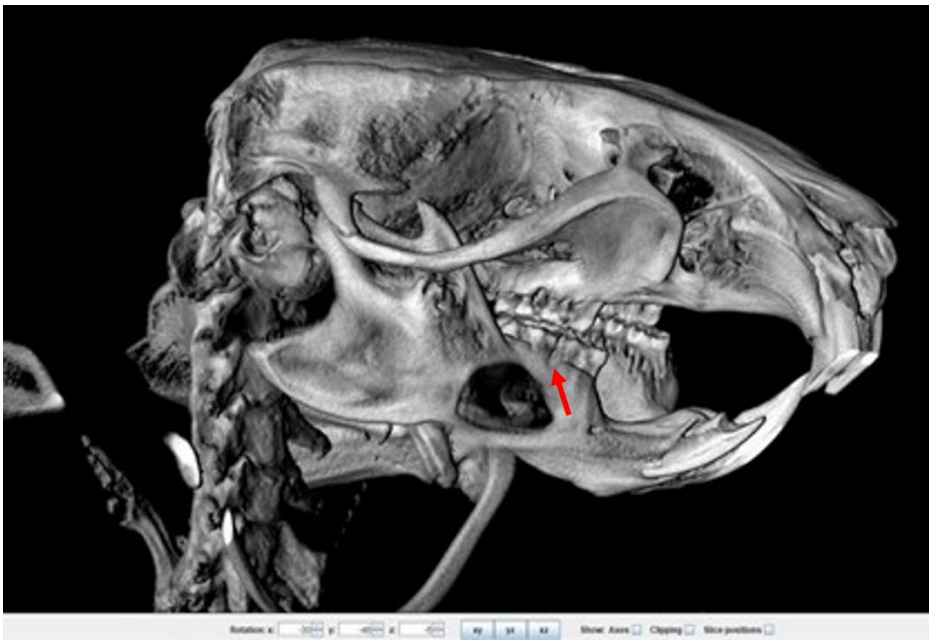

Figure 16. Radiological image of a group C defect at 6 months, with a red arrow indicating dental degeneration.

4.2.1.2. Conclusion

The experimental model used in our study is optimal for investigating the efficacy of DPSCs in osteogenesis. In addition, we consider it to be reproducible, high-yielding and cost-effective.

4.2.2. G+M GROUP

The results obtained with the two types of biomaterials used were analyzed: OsteoBiol® Evolution® membrane (based on dense collagen fibers) and OsteoBiol® Gen-Os® (bone substitute with high osteoconductivity).

Twelve animals were operated on, causing 12 mandibular lesions. No animal died postoperatively, nor suffered fractures. The general condition of the animals was favorable; some soft tissue swelling was observed due to the ostectomy, which disappeared spontaneously. Twelve lesions suitable for the study were obtained.

In the post-surgical clinical follow-up, there was no rejection or degenerative changes due to the dental lesion. As for the membrane, it showed bio-resorption, low immunogenicity, stability and prolonged protection of the eventual covered graft.

4.2.2.1. Radiological analysis

Before sacrifice, two animals from each group underwent radiological evaluation by computed tomography (CT) at 3 and 6 months. A densitometric study of the bone repair of the mandibular defect was performed.

The application of a collagen membrane + scaffold at three months, both soft tissue collapse, and poor restitution of the defect are prominent, the biomaterial has not experienced a decrease in volume. The radiopacity of the lesion is very heterogeneous in the center of the defect **(Figure 17)**.

At six months there is a change in the geometric morphology of the defect, it has experienced a decrease, acquiring a denser appearance with accentuated irregularity of its contour and a radiological density significantly higher than the previous stage and more homogeneous, although the granular appearance persisted There is an attempt to form trabeculae between the biomaterial and the cortex, the appearance of dense bone tracts in the defect treated with the membrane + scaffold, compared to the three months **(Figure 18)**.

Table 6. Radiological evidence in Group G+M at 3 and 6 months

Group	3 months	6 months
G+M	The soft tissue has collapsed	An area of regenerated bone and soft tissue have been observed as well as poor defect restoration

Figure 17. Radiological image of a group G+M defect at 3 months.

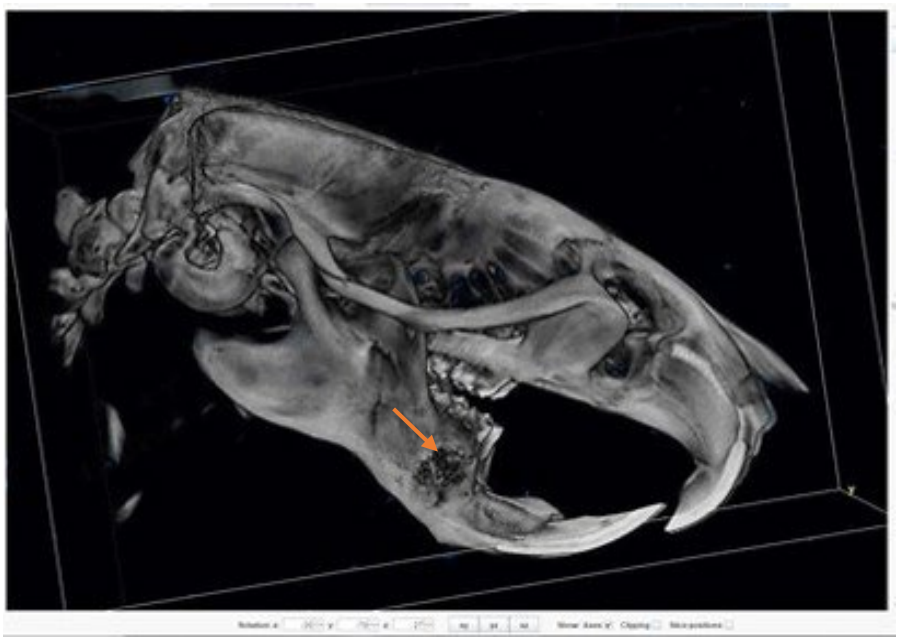

Figure 18. Radiological image of a group G+M defect at 6 months, with a red arrow indicating dental degeneration.

4.2.2.2. Conclusion

The results obtained with this technique are merely descriptive, but we can observe that the application of a collagen membrane + scaffold for bone regeneration in a bone defect promotes partial restitution of the defect with newly regenerated bone compared to the untreated control defect.

4.2.3. G+M+S GROUP

The results obtained with OsteoBiol® Gen-Os® (bone substitute with high osteoconductivity) containing the DPSCs and protected by OsteoBiol® Evolution® membrane (based on dense collagen fibers) were analyzed.

Twelve animals were operated on, causing 12 mandibular lesions. No animal died postoperatively, nor suffered fractures. The general condition of the animals was favorable; some soft tissue swelling was observed due to the ostectomy, which disappeared spontaneously. Twelve lesions suitable for the study were obtained.

In the post-surgical clinical follow-up, there was no rejection or degenerative changes due to the dental lesion. As for the membrane, it showed bio-resorption, low immunogenicity, stability and prolonged protection of the eventual covered graft.

4.2.3.1. Radiological analysis

Before sacrifice, two animals from each group underwent radiological evaluation by computed tomography (CT) at 3 and 6 months. A densitometric study of the bone repair of the mandibular defect was performed.

The application of a collagen membrane + scaffold + DPSC at three months shows homogeneous levels of radiopacity in the defect, and the continuity in the flange was very relevant **(Figure 19)**. At 6 months, the radiological repair of the defects was practically complete in all of them (80-100%), showing a high continuity with the bone flanges, and with a very homogeneous distribution of the radiological density **(Figure 20)**.

Table 7. Radiological evidence in Group G+M+S at 3 and 6 months

Group	Months	6 months
G+M+S	Partial restoration of the total structural defect with the new bone	total structural restoration of the defect with new bone

Figure 19. Radiological image of a group G+M+S defect at 3 months.

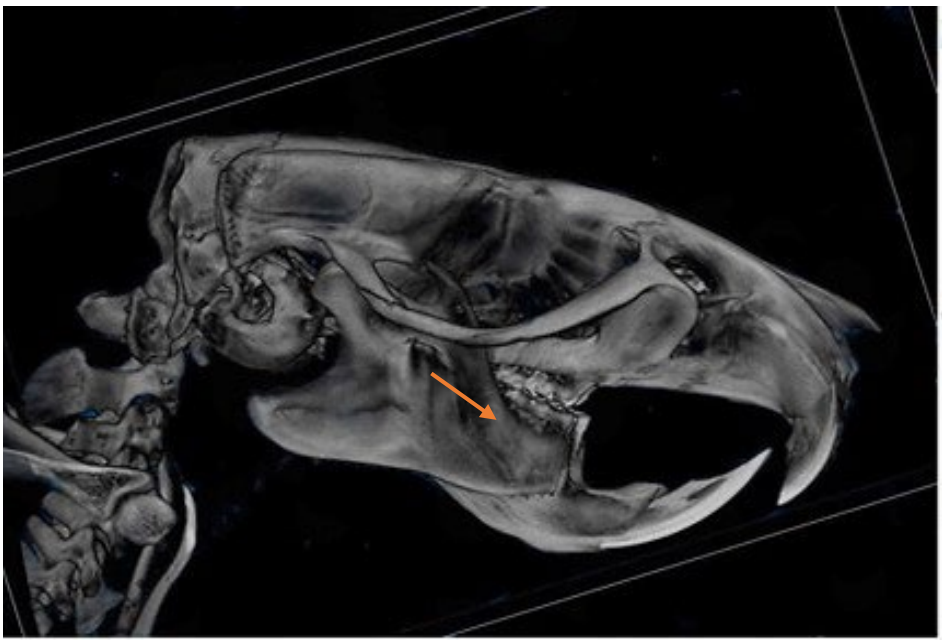

Figure 20. Radiological image of a group G+M+S defect at 6 months, with a red arrow indicating dental degeneration.

4.2.3.2. Conclusion

The results obtained with this technique are merely descriptive, but we can observe that the application of a collagen membrane + scaffold + DPSCs for bone regeneration in a trabecular bone defect promotes the structural restitution of the defect with newly regenerated bone compared to the untreated control defect.

4.3. TESTING OF CELL VIABILITY IN IMPLANTS

After surgery, the remains of the vials were seeded on plates. After a few days , cells appeared attached to the plate, thus viable and proliferating cells.

4.4. HISTOLOGICAL STUDY

The histological study of the samples obtained from the blocks containing the different types of treatments performed on the lesions was carried out. The blocks were obtained by direct visual observation of the hemi-mandibles after removal of the soft tissues. A thin white membrane covering the lesioned areas was frequently observed; this was stained with India ink to orient the histological sections.

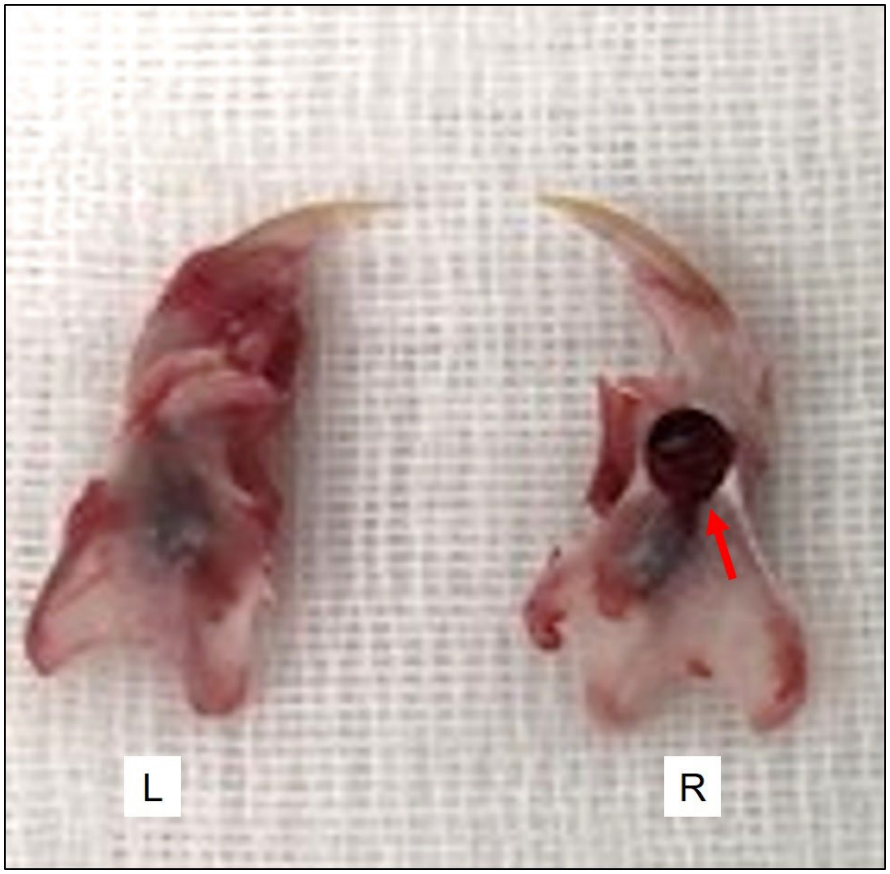

Figure 21. Representative specimens of the dissected right (R) and left (L) mandibles after removal of soft tissue parts. Red arrow shows the bony defect, which can be seen through naked eyes.

In all cases, following fixation and processing, the specimens were stained with hematoxylin and eosinand were observed under an optical microscope.

4.4.1. DESCRIPTIVE HISTOLOGICAL ANALYSIS

Histomorphological analysis was performed on three of the six lesions in each group.

In the group of lesions that were left untreated, a fibrous scar reaction was found, sometimes overflowing the wound margins, and no signs of bone regeneration were observed **(Figure 22)**.

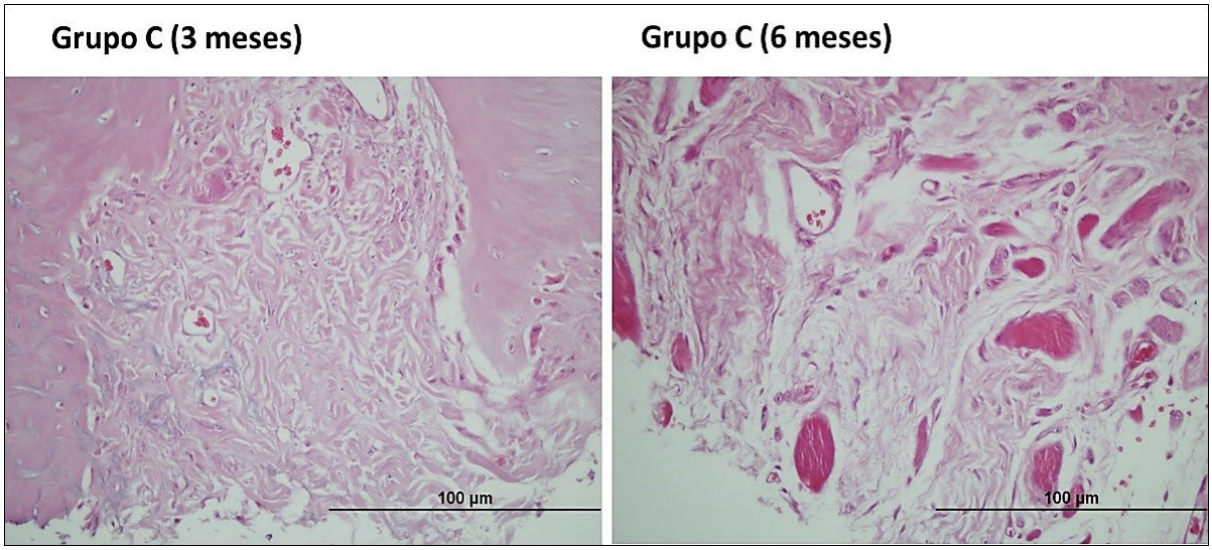

Figure 22. Descriptive histological analysis of the bone defect in Group C, after 3 months and 6 months. Hematoxylin and Eosin stained histological photomicrographs show, fibrous reaction of an untreated lesion. The fibrous scar reaction extends beyond the limits of the lesion. No sign of reactive bone regeneration is detected.

In the two experimental groups (G+M and G+M+S groups), microscopic evaluation of the histological images revealed regenerative changes within the defect in both groups **(Figure 23)**. In Group G+M there were hardly any signs of bone regeneration, with a chronic inflammatory

infiltrate with the presence of multinucleated giant cells. In Group G+M+S at 3 months, signs of bone regeneration and a considerable decrease in the inflammatory reaction were observed. Increased cellularity was found, evidencing active osteoblasts, with cuboid morphology, which were readily included in the osteoid matrix. In some areas, a considerable amount of immature reticular bone was found, and in others the formation of several lines of ossification was observed.

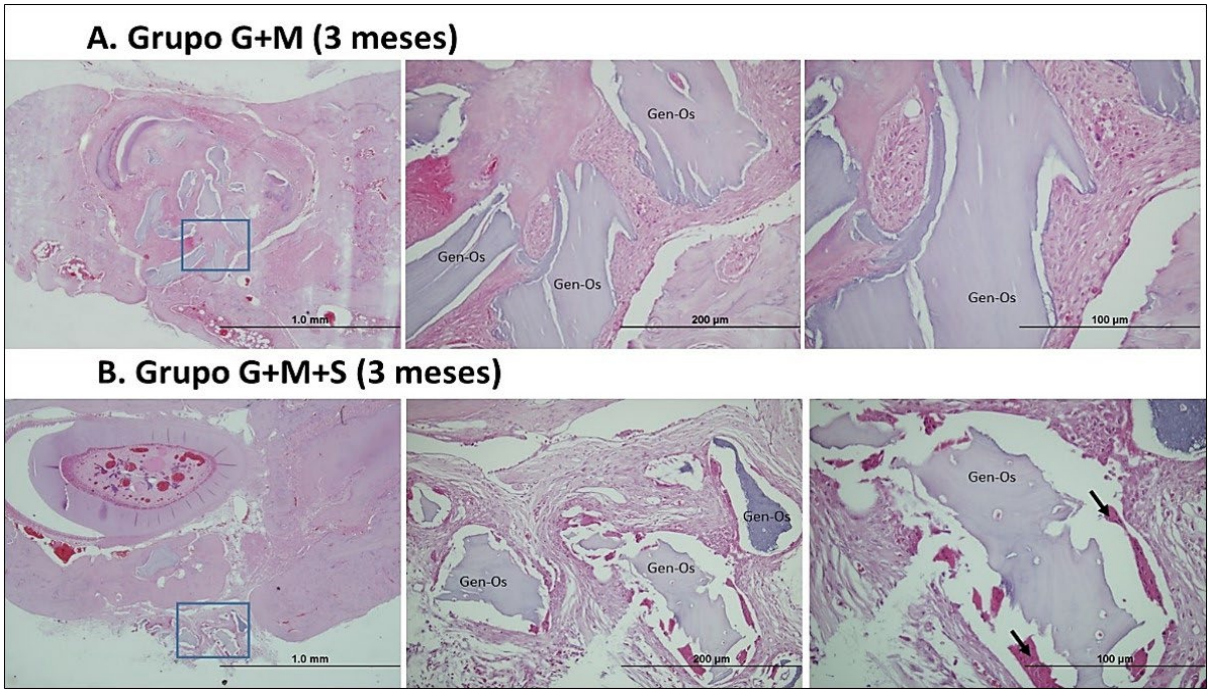

Figure 23. Descriptive histological analysis after 3 months - Hematoxylin and Eosin stained histological photomicrographs of the bone defect in: (A) Group G+M, showing several biomaterial particles and chronic inflammatory component; (B) Group G+M+S, showing osteogenesis, evidenced by osteoblasts included in the osteoid (black arrows).

Histological analysis of the specimens in groups G+M and G+M+S at 6 months **(Figure 24)**, showed greater bone regeneration in the group treated with DPSC, wherein the edges of the lesion are not distinguished. However, in Group G+M, without DPSC, we continue to observe particles

of biomaterials. While these particles are not surrounded by bone, we do observe new bone at the edges of the lesion.

All the results of descriptive histological analysis in the different experimental groups (Group C, Group G+M and Group G+M+S), and at different time periods (3 months and 6 months) are summarized in **Table 8.**

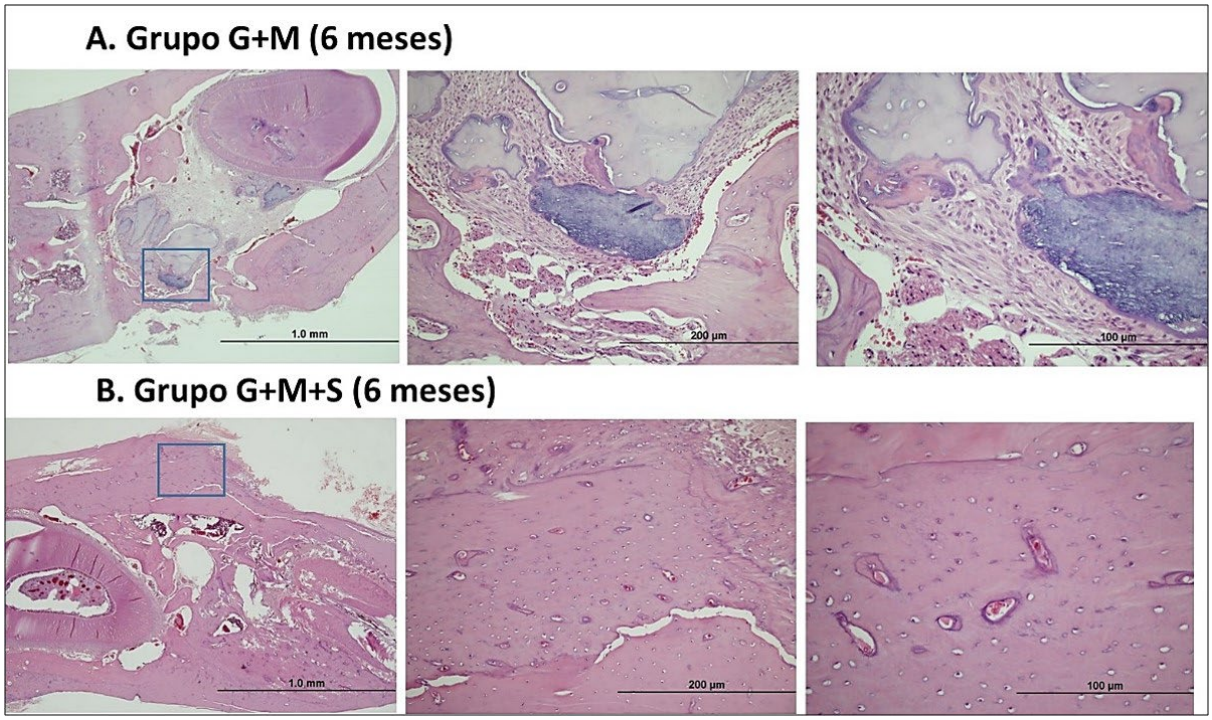

Figure 24. Descriptive histological analysis after 6 months - Hematoxylin and Eosin-stained histological photomicrographs of the bone defect in: (A) Group G+M, showing biomaterial particles and chronic inflammation with new bone in the edges of the defect; (B) Group G+M+S, showing clear signs of osteogenesis throughout the defect.

Table 8. Summary of descriptive histological analysis in the different experimental groups (Group C, G+M and G+M+S), after 3 months and 6 months

	Group C	**Group G+M**	**Group G+M+S**
Treatment	No empty defect, covered with osteobiol® and evolution ® membrane.	yes, defect filled with osteobiol® and Gen-os® (the bone was substituted with grain) and covered with osteobiol® and Gen-os® as a membrane	yes, defect filled with osteobiol® and Gen-os® (the bone was substituted with grain) and DPS (biological material) and covered with osteobiol® and evolution ® as a membrane
Results at 3 months	There is evidence of fibrous reaction but there are no signs of regeneration **(Figure 7a).**	We distinguish the borders of the lesions, observe biomaterial particles and components, signs of chronic inflammatory without signs of regeneration **(Figure 8a).**	great cellularity, active osteoblasts are evident and, in some areas, newly formed bone trabeculae surrounding the biomaterial. Ossification lines show osteocytes and areas with

			osteoblastic precursor cells. osteoblasts, partially included in the osteoid, which are calcifying, there is osteoclastogenesis, great osteoforming activity on the biomaterial is evident as well **(Figure 24b).**
Results at 6 months	fibrous reaction that spills over the margins of the defect without signs of bone regeneration was detected **(Figure 7)**.	We continue to observe biomaterial particles that are encapsulated in a fibrotic matrix. There are no signs of bone formation, chronic inflammatory component is present with no signs of regeneration **(Figure 9a)**.	We observed complete bone regeneration in the area treated with DPSC with a well-organized, well-vascularized bone and with a lamellar structure surrounded by Haversian canals **(Figure 9b).**

4.4. MOLECULAR STUDIES

At different times (3 and 6 months after surgery), concentrations of calciotropic hormones such as calcitonin (CT) and parathormone (PTH), TGF-β growth factor, procollagen type 1 levels and endoglin expression were evaluated in the serum of rats.

Calcium-tropic hormone markers: calcitonin (CT), parathormone (PTH) and Procollagen-I.

In relation to calciotropic hormones (parathormone and calcitonin) our results show a significant increase in the DPSC group, stimulating osteogenesis and collagen type I constitutive protein of the bone matrix. In this study, serum TC concentration decreased and PTH concentration increased. The results are shown in graphs below.

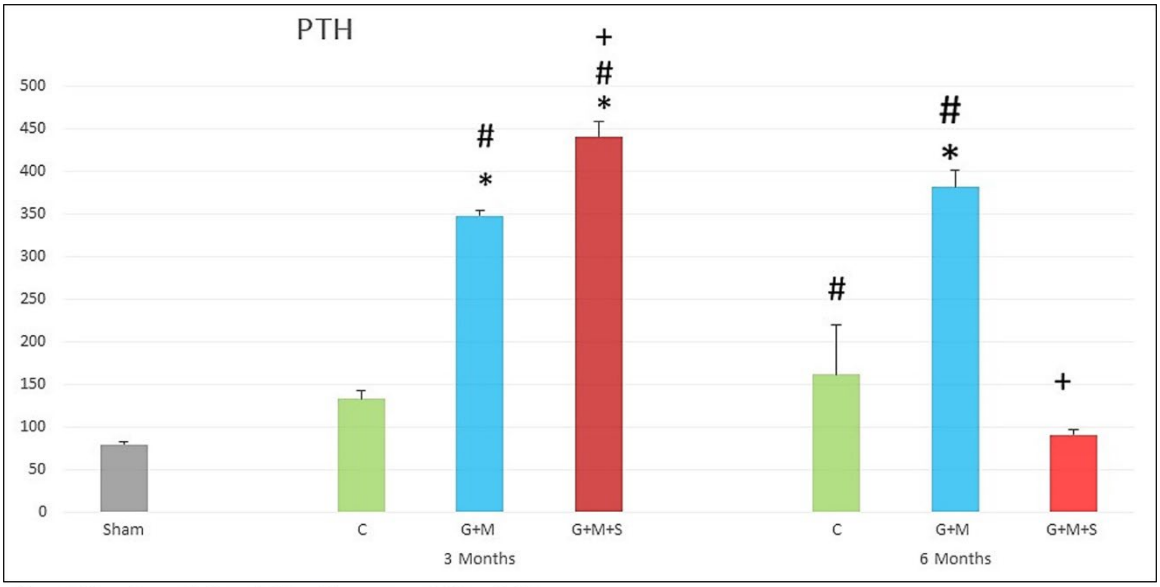

Figure 25: Graphic analysis of Parathormone Serum Level in the 3- and 6-months Groups

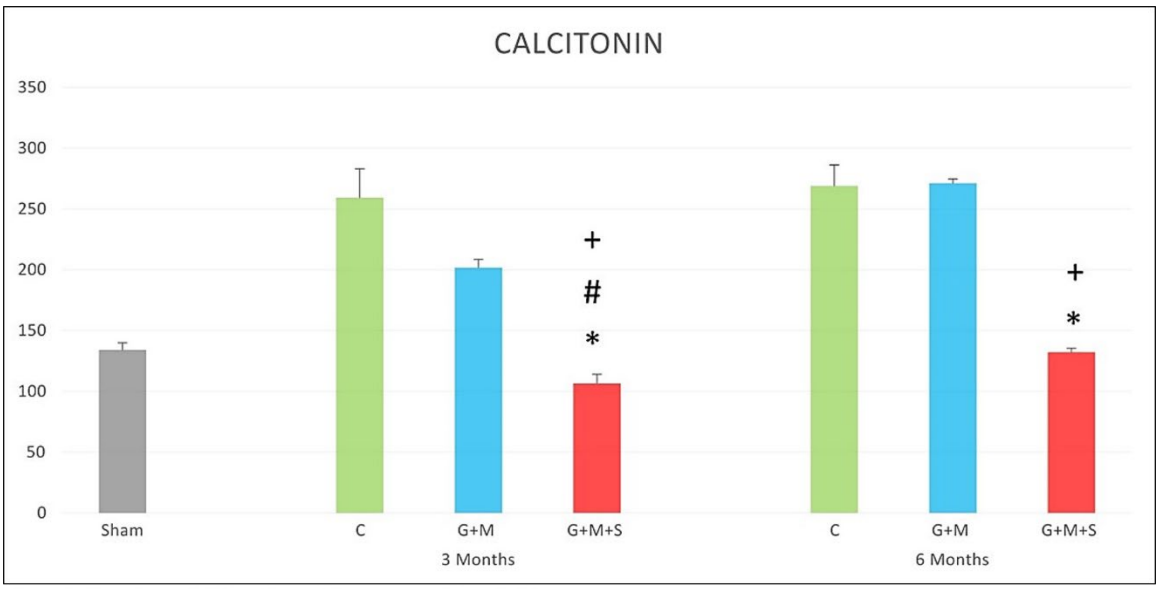

Figure 26: Graphic analysis of Calcitonin Serum Level in the 3- and 6-months Groups

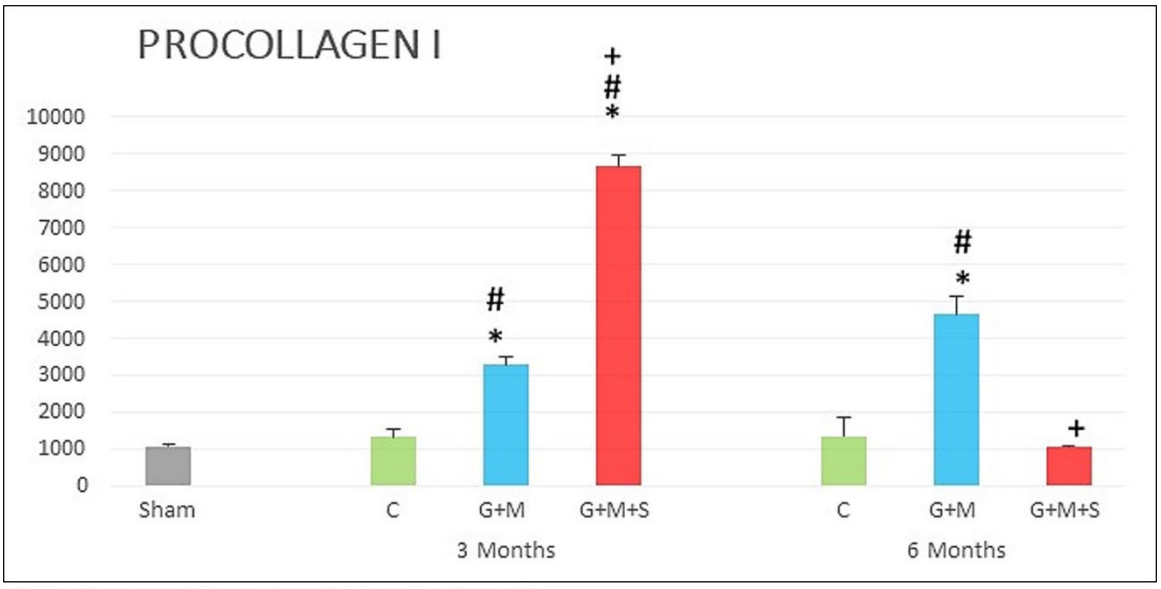

Figure 27: Graphic analysis of Procollagen I Serum Level in the 3 and 6 months Groups

As a marker of neovascularization, we studied endoglin essential for TGF-β signaling in endothelial cells and our results show, in the DPSC group a significant increase in both endoglin expression and in the production of growth factors such as TGFβ1, a potent stimulator of bone formation, enhancing osteoblastic differentiation and osteoid matrix synthesis. The results are shown in the underlying graphs.

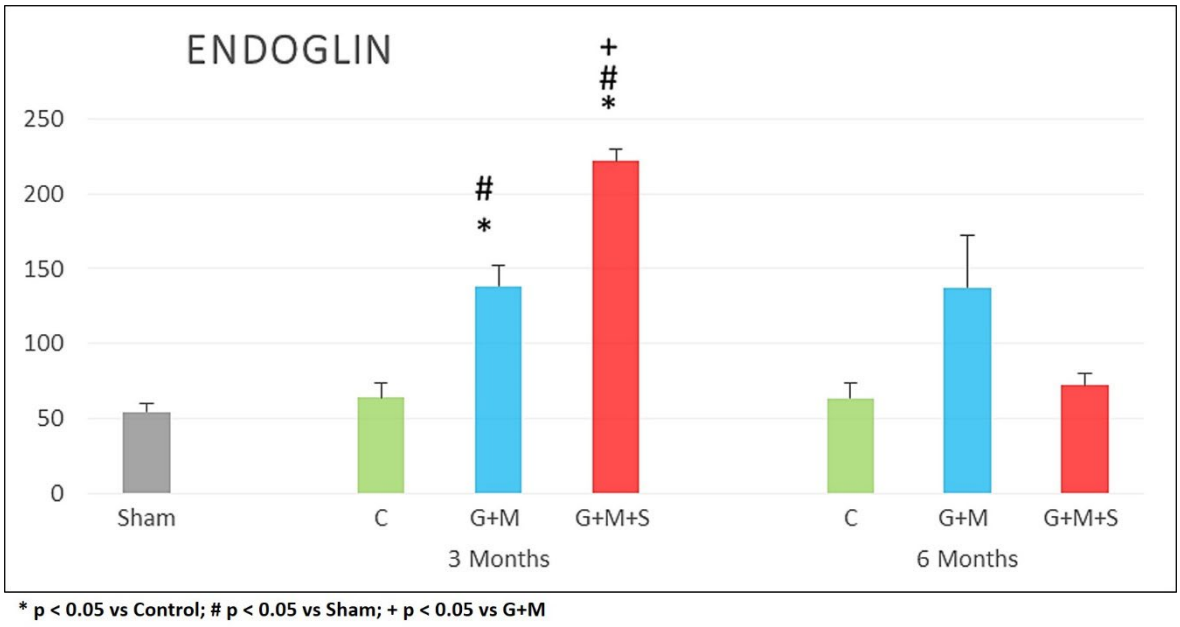

Figure 28: Graphic analysis of Endoglin Serum Level in the 3- and 6-months Groups

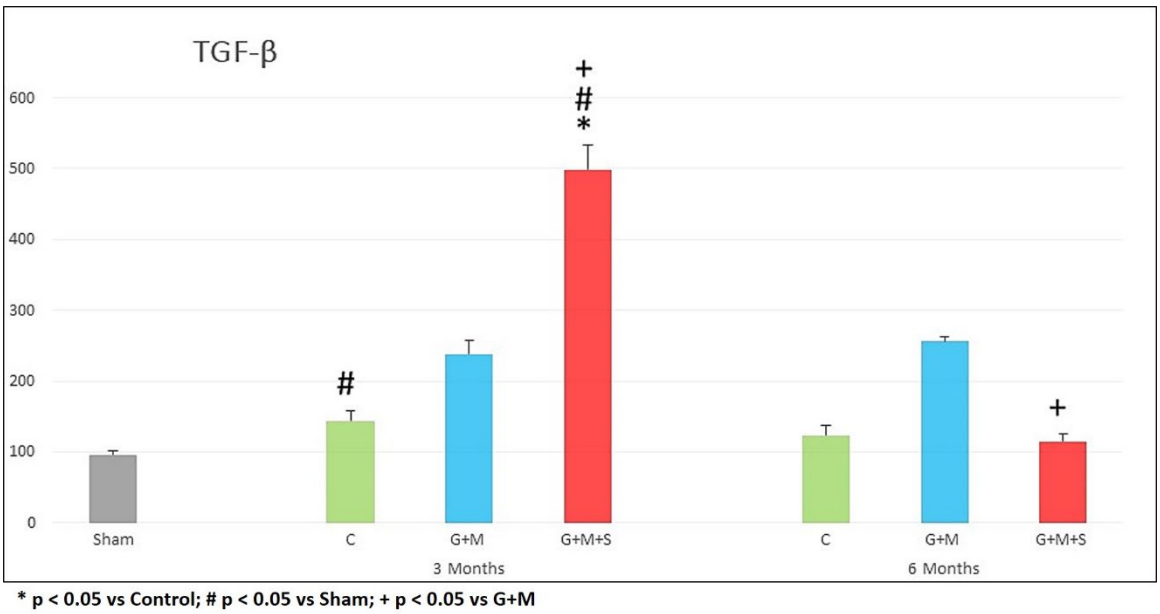

Figure 29: Graphic analysis of TGF-β Serum Level in the 3- and 6-months Groups

At different times (3 and 6 months after surgery), the concentrations of phosphocalcic and bone metabolism markers were evaluated through the study of hepatic metabolite (calcidiol), vitamin D, calcium, phosphorus and magnesium. The results are shown in the graphs here below.

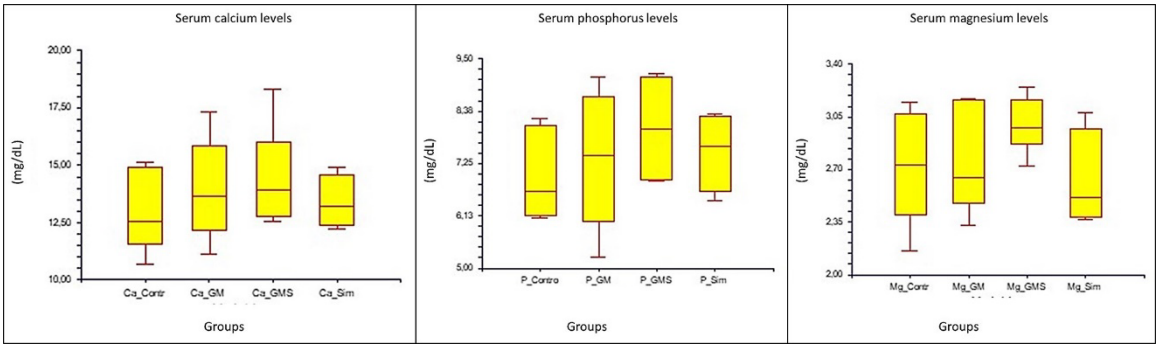

Figure 30: Graphic analysis of Serum level of Calcium, Phosphorus, and Magnesium in the 3- and 6-months groups

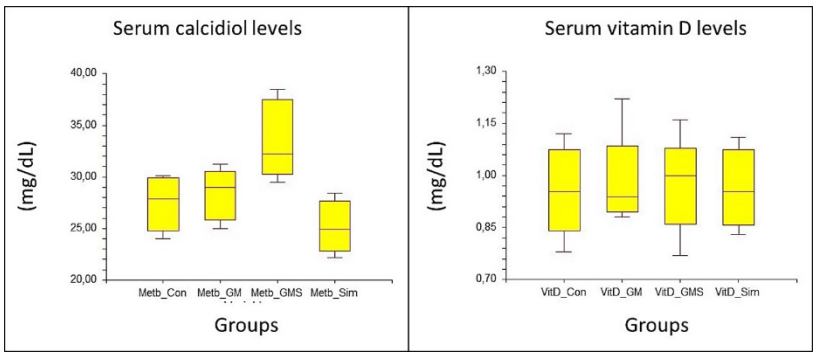

Figure 31: Graphic analysis of Serum level of Calcidiol and Vit D in the 3 and 6 groups

5. DISCUSSION

In this study, we investigated the ability of the human Dental Pulp Stem Cells (DPSCs) to increase new bone formation when added to an OsteoBiol Gen-Os® scaffold. The study shows that DPSCs can play a significant role in enhancing the regeneration of bone in rat mandibular defects. It became apparent from the increased levels of osteogenic differentiation and formed bone matrix in the defects treated with DPSCs compared to controls. The goal was to explore the implications of this conversation further. We aimed to corroborate our findings with existing research, describe the mechanisms on which the DPSCs contribute to bone regeneration, and analyse the effectiveness of OsteoBiol Gen-Os® as a scaffold. Furthermore, we evaluated the possible use of the method in dental and orthopaedic clinics, assuming the limitations of this study and making recommendations for future research. This study provided us with insights into the consequences of applying DPSCs in the regenerative medicine area.

5.1. CONTEXTUALISATION OF FINDINGS

This study demonstrated that the use of DPSCs in combination with OsteoBiol Gen-Os® improved bone regeneration to a significant extent. This result corresponds to previous studies which have mentioned the osteogenic potency of DPSCs. For example, similar studies by Ariano et al. that previously demonstrated that DPSCs can differentiate into osteoblast-like cells and aid bone tissue engineering (76). On the contrary, they also bring new ideas. Unlike other studies which used DPSCs with distinct scaffold materials, we mainly applied an OsteoBiol Gen-Os® scaffold (77). These results proved remarkably effective, suggesting that the OsteoBiol Gen-Os® properties are compatible with DPSCs, leading to better bone integration and healing. This varies from the other research where alternative scaffolds like synthetic polymers were used, and in several cases, bone regeneration outcomes were

ineffective (78). Additionally, the study backs DPSCs application in bone regeneration and also contributes further understanding of the proper conditions and materials that give the best outcomes (76). This commitment is of great importance since it provides a roadmap to researchers working on different kinds of scaffolds with DPSCs, i.e., research will be directed towards finding more effective methods that can be widely applied in regenerative medicine.

5.2. RADIOLOGICAL AND HISTOLOGICAL FINDINGS ACROSS DIFFERENT STUDY GROUPS

5.2.1. GROUP C, G+M AND G+M+S ANALYSIS:

5.2.1.1. Radiological Analysis

Computed Tomography (CT): We performed CT scans to evaluate bone repair at 3- and 6-months post-operation. The scans provided detailed insights into the bone density and structure at the defect's site.

- **Group C:** Bone regrowth and healing response signs were not observed at 3 or 6 months. According to Blázquez-Carmona et al., this lack of healing means that the size of a defect is becoming critical, and regeneration cannot be performed without intervention (79).
- **Group G+M:** After three months, there was soft tissue trapped and inferior bone deposition with inhomogeneous radiopacity within the defect. According to Sparks et al., the anomaly at six months consisted of the higher density combined with more uniform borders; thus, this could be a sign of bone regeneration (80).

- **Group G+M+S:** The first radiographic evaluation revealed uniform radiopacity, signifying good integration of these scaffolds with DPSCs. After six months, a notably complete structural restoration of the bone defect can be seen with high continuity and homogeneity in radiological density.

5.2.1.2. Histological Analysis:

Staining Techniques: We used specific staining methods to highlight the different stages of bone healing and integration of biomaterials.

- **Group C:** At 3 Months, the formation of fibrous cells at the injury site could be seen; nevertheless, there was no evidence of bone regeneration. At six months, similar findings were noticed as the fibrous reaction was observed to have spread over the margins of the defect. No signs of bone regeneration were detected. The lack of bone regeneration observed in Group C at 3 and 6 months suggests a failure of the natural healing process, possibly due to a critical-sized defect that exceeds the body's intrinsic regenerative capacity (81).
- **Group G+M:** The histology of the chronically inflamed biomaterial particles at three months was visible, but no bones were formed significantly. At six months, the biomaterial was still progressively encapsulated within a fibrotic matrix, with very little bone growth.
- **Group G+M+S:** At three months, active osteoblasts and fresh bone trabeculae increased around the biomaterial, a positive indication for osteointegration. Trinh et al. found that in the sixth month, complete bone regeneration was observed, with a well-

structured, well-vascularized new bone confirmed by the combination of DPSCs and the scaffold (82).

5.3. SIGNIFICANCE OF DPSCS IN BONE REGENERATION

This study reveals the strong connection of DPSCs with bone regeneration, particularly when placed in the OsteoBiol Gen-Os® scaffold. DPSCs have the advantage that they can differentiate into many other cell types, such as osteoblasts, which are very important in bone formation and development (83). In these experiments, we demonstrated that DPSCs facilitated the healing of mandibular defects in rats. Many aspects of DPSCs are the functions that make bone regeneration possible. Besides, the work of Fujii et al. also showed that DPSCs produce BMP (Bone Morphogenetic Protein) and VEGF (Vascular Endothelial Growth Factor), which are already known to be factors determining bone formation and blood vessel development. These conditions expedite bone regeneration via the cycle of resting and growing states. They exhibited that these growth factors were precious for osteogenic differentiation and ossification rate amplification in bony deficits. Based on their review, Mortada and Mortada reported the role of several growth factors such as BMP, TGF-β, VEGF, EGF, FGF, IGF-1 and TNF-α, through different cytokine mediated pathways, in osteogenic differentiation of DPSCs (83). They further highlighted the osteogenic lineage progression of DPSCs upon exposure to chemical mediators such as dexamethasone and ascorbate-2-phosphate and the presence of mineral trioxide aggregates and calcium (Ca^{2+}) ions. In the present study, osteogenic differentiation of harvested and isolated DPSCs was achieved through culturing in

commercially procured OsteoDiff medium. These differences were clearly illustrated in DPSCs plus OsteoBiol Gen-Os®, part of DPSCs (84). Moreover, this couple of DPSCs and OsteoBiol Gen-Os® scaffold has an additional osteoconductive effect. The scaffolding material functions as the organic skeleton, enabling osteogenesis from DPSCs (85). It illustrates that the relationship between deprived periosteal-derived cells (DPSCs) and particular scaffolds leads to more efficient bone formation, which may be why this practice will increase bone reconstruction in the clinic (84).

5.4. COMPARISON OF ISOLATION AND CHARACTERIZATION METHODS

Mesenchymal stem cells (MSC) derived from a variety of sources including bone marrow, adipose tissue, blood and dental pulp have shown promising preclinical results in terms of bone tissue engineering and regeneration (19). The present study was based on the premise that DPSCs comprise an easily harvestable source of pluripotent mesenchymal stem cells which can be used for bone defect regeneration (86). Allogeneic DPSCs were harvested from the molar teeth pulpal tissues of 6 rats and were isolated using enzymatic digestion method aided by collagenase type 1. Comparing the two popular methods of stem cell isolation from dental pulp tissue, namely the enzymatic digestion and explantation methods, Hilkens et al. observed no significant differences between the two methods (87). However, they noted that the enzymatic digestion technique enable faster isolation of MSCs (87).

The Mesenchymal and Tissue Stem Cell Committee of the International Society for Cellular Therapy (ISCT) has defined the characterization criteria for MSCs employed in regenerative

applications (88). Accordingly, isolated MSCs should be plastic-adherent under standard culture environment, express CD73, CD90 and CD105 cell surface markers, while lacking expression of CD11b, CD14, CD19, CD34, CD45, CD79α and HLA-DR. Furthermore, the MSCs should be capable of differentiation into osteogenic, adipogenic and chondrogenic lineages. Based on flow cytometry, CD90 expression in the isolated and cultured DPSCs was as high as 99.7%, in addition to CD29 expression of 89.5%. Moreover, the absence of any lymphocytic or hematopoietic differentiation was further evidence by non-expression of CD49e.

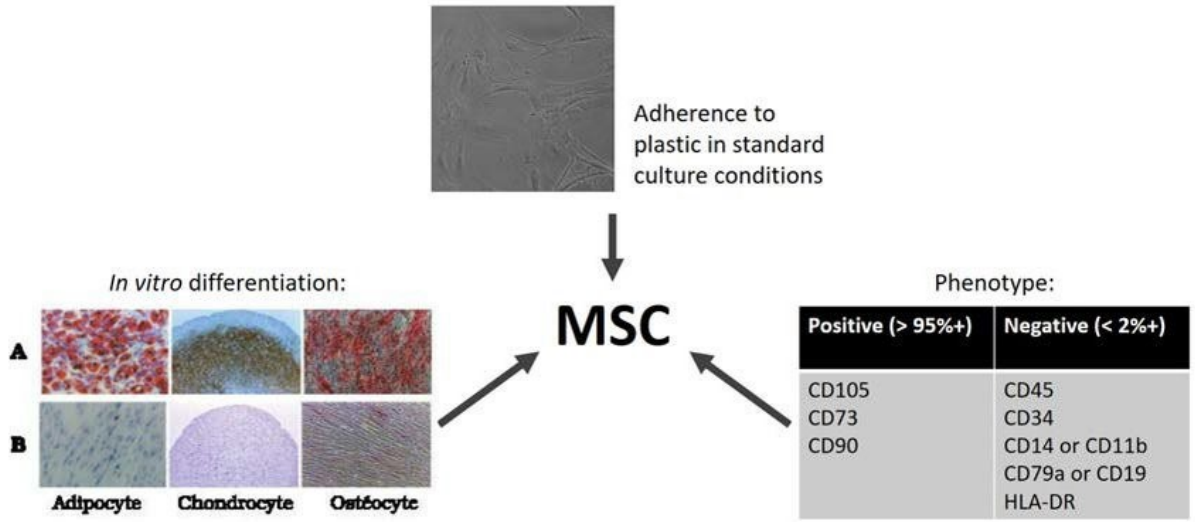

Figure 32. Characterization criteria for MSCs employed in regenerative applications according to The Mesenchymal and Tissue Stem Cell Committee of the International Society for Cellular Therapy (ISCT). Source- Loubière, Céline. (2018). Characterization and impact of hydrodynamics on the performance of umbilical-cord derived stem cells culture in stirred tank bioreactors.

The study used such an enzymatic extraction technique to isolate DPSC from the dental pulp. The DPSCs were extracted from the pulp of rats' molars, which serve as a constant, reliable source for such studies due to their accessibility and the satisfactory proliferative ability of rat

DPSCs, which has been extensively investigated in regenerative medicine research (89). This decision enables a uniform and efficient cell collection for scientific experiments. This procedure will break down the tissue with some enzymes, such as collagenase, and the cells will be dissociated into single cells. This method often contrasts with the explanatory approach, where cells can naturally move outwards by necessitating tissue pieces. The enzymatic digestion technique offers multiple advantages; the predominant advantage is efficiency (90). It generates quick mobilisation and non-specific activation of many cells within the first few hours. This effect is especially vital for fast-paced surgeries (90). The study's results showed that DPSCs were adherent and confluent early, which allowed us to begin the experimental protocol earlier. This is also because cells are the primary site of stable results. To start with, it does as well have some inconveniences. This will likely interfere with correct cell differentiation, resulting in cell surface receptor destruction. This problem is mentioned in the literature that uses Shi et al.'s work (91). Despite that, the outcomes of our study impugned no significant detriment for DPSC viability and differentiation. Due to the nature of enzymatic digestion being the key to DPSCs extraction, care must be exercised to prevent cell damage. Furthermore, the other way out is to change the enzyme level and the duration of the exposure to prevent the harmful nature of enzymes on the whole cell fitness.

5.5. EFFICACY OF OSTEOBIOL GEN-OS®

In this study, the scaffold was OsteoBiol Gen-Os®, which helped grow dental pulp stem cells (DPSCs) for bone regeneration. The OsteoBiol Gen-Os® is obtained from pig bone, from which the natural ingredients are removed, leaving a mineral structure almost identical to the human competitor’s texture and density. Primarily, such a scaffold is considered to be

osteoconductive (92). Osteoconductive is the property of material that allows it to act as a scaffold to facilitate attachment, growth, and, in the end, the formation of new bone by the native bone cells (93). In the in vivo model, the scaffold was designed as the structural scaffold for the bone healing process. It induced the development and multiplication of DPSC cells into osteo-forming cells. We learnt that a mixture of DPSCs with OsteoBiol Gen-Os® promoted repair processes of defects to a greater extent than the control group. The scaffold allows the newly developed bone tissue integration by providing a hospitable environment for DPSCs crucial for bone regeneration (93). The success of the treated OsteoBiol Gen-Os®, in our case, essentially supports its use as a highly efficacious scaffold in regenerative dentistry. It closely interacts with the DPSCs, providing it as a future allograft substitute. It provides enhanced effects in bone regeneration.

5.6. IMPLICATIONS FOR CLINICAL APPLICATION

The findings from the study emphasise the potential translational use of the DPSCs with the OsteoBiol Gen-Os® in the clinical applications of bone regeneration. These findings confirm that the DPSC have potential regenerative dental and bone healing capabilities for clinical management. Besides intrabony defects, animal studies have assessed the efficacy of autologous or allogeneic DPSCs in reconstructing bone defects in other aspects of oral and facial surgery, including maxillo-mandibular defect and cleft craniofacial reconstruction. This integration could be a game changer in dentistry and orthopaedics, particularly in patients who undergo bone grafting surgeries at reconstructive ends. The primary clinical significance of the study lies in the possible development of a better and more minimally invasive substitute for conventional bone grafting techniques (94). When DPSCs are employed with an OsteoBiol

Gen-Os®, faster bone healing and recovery time is achieved, which will be highly beneficial for patient outcomes. However, the issues with this procedure must be addressed before it can be implemented in regular clinical practice. Safety concerns are foremost, particularly concerning the risk of immune rejection and potential transmission of diseases from the OsteoBiol Gen-Os® (95). While the study failed to demonstrate serious side effects, long-term studies and clinical trials are still needed to determine the immunogenicity and safety of these devices in human bodies. Ethical considerations are as important as others, especially in topics involving human and animal tissues. Definite rules and regulations should be enforced to protect the ethics of exploitation and application of DPSCs and OsteoBiol Gen-Os® materials. Moreover, one should consider the standardisation of technique for separating and applying DPSC and preparing OsteoBiol Gen-Os® to guarantee consistent safety of clinical outcomes. However, when implementing such a scaffold in the clinical application of DPSCs, deep attention must be paid to the safety, ethical and technical factors to realise their full potential in regenerative bone repair.

5.7. LIMITATIONS OF THE STUDY

In this study on the performance of DPSCs in combination with OsteoBiol Gen-Os® used in bone regeneration, we have experienced some limitations that could influence the interpretation of our findings. The most important limitation of the experiment was that it was conducted on a representative animal (rat). However, the data from rat models can only be considered necessary for initial biological research to be applied to treat humans. Bone density, rate of healing, and immune response among rats and humans are different, and these can ultimately affect the translation of our findings to human treatment (96). Besides scale, it is worth

improving the study's size. We can only cover the resources and constraints of a few samples, and the observation period gets reduced. This restriction may get in the way of the strength and broad applicability of the conclusions that we draw. A larger sample size, more extended duration and monitoring will result in a complete picture of the long-term impacts and the stability of bone regrowth using DPSCs and OsteoBiol Gen-Os®. Finally, the study was mainly concerned with OsteoBiol Gen-Os® as the scaffold material. While the scaffold exhibited impressive outcomes, the chances are that it can be better if it turns out to be compared with other biomaterials on this matter. The final thing to be noted is that the isolation and the preparation of DPSCs specifically require delicate techniques that probably limit the clinical use of our findings outside of the specialised settings without equipment and trained personnel. These shortcomings, among others, indicate that though the findings are positive, they should be treated with restraint. Additional investigation involving clinical trials on humans is essential to verify the implementation ability and safety of using DPSCs and in bone OsteoBiol Gen-Os® regeneration.

5.8. FUTURE RESEARCH DIRECTIONS

The study's investigation of using DPSCs with OsteoBiol Gen-Os® for bone regeneration provides multiple fields of future research to broaden our knowledge and employment of the findings. The first, but not the least important step would be running human clinical trials. These trials are crucial to check the security, functionality, and immune response of the DPSCs and the OsteoBiol Gen-Os® in human patients, allowing testing of their clinical applicability. Furthermore, according to Amin et al., assessing the efficacy of DPSCs with a range of other scaffolds, including synthetic biomaterials and other animal-origin OsteoBiol Gen-Os®, will

reveal the best material for bone regeneration (97). Along with long-term studies, information about the stability and durability of regenerated bones, which is a significant factor, would be gained. Thus, worries about the durability of these methods in the long run would be eliminated. A larger sample size is also essential to strengthen the robustness of our findings. A different population should also test the results for validity and generalizability. Besides that, investigating cutting-edge approaches aimed at the purification and culture of DPSCs may help overcome some drawbacks, thus making these procedures more broadly applicable in actual clinical practice. In this way, future research could ensure that DPSCs should be applied in regenerative medicine, especially when considering bone deformities.

6. CONCLUSION

In summary, the role of dental pulp stem cells (DPSCs) in combination with an OsteoBiol Gen-Os® scaffolds is suspicious in the reconstruction of the bone. This study substantiates the importance of DPSCs in dental and orthopaedic applications and focuses on bone defect repair. The study discloses that DPSCs, which facilitate bone formation, blend efficiently with the OsteoBiol Gen-Os® structure to complement and boost the healing process. With OsteoBiol Gen-Os® as the scaffold, the permeability in nurturing bone regeneration, demonstrating osteoconductive properties, increases.

The clinical consequence of this study is enormous, suggesting that DPSCs with mineralised scaffold could be an effective and fast method against bone grafting and bring forth shorter recovery times and better results. On the one hand, these are optimistic outcomes, but on the other, they call for additional study. Subsequently, more research, specifically human clinical trials, should be undertaken to confirm the validity and applicability of these outcomes.

Through further research and subsequent development of this technique, it will be possible to increase the use of regenerative medicine and dentistry in therapy for people with bone defects and improve the efficiency of the recovery process.

7. REFERENCES

1. Tortora, G. and B. Derrickson, Vol. 1: Organization, support and movement, and control systems of the human body. 2009: Hoboken, NJ: Wiley.

2. Mancini, L., et al., Biomaterials for Periodontal and Peri-Implant Regeneration. Materials (Basel), 2021. 14(12).

3. Ramalingam, S., et al., Chapter 1 - Alveolar bone science: Structural characteristics and pathological changes, in Dental Implants and Bone Grafts, H. Alghamdi and J. Jansen, Editors. 2020, Woodhead Publishing. p. 1-22.

4. Salamanca, E., et al., Bone regeneration using a porcine bone substitute collagen composite in vitro and in vivo. Sci Rep, 2018. 8(1): p. 984.

5. Ramalingam, S., N. Nooh, and K. Al-Hezaimi, Beta-tricalcium phosphate with adjuvant bone-marrow stem cells for bone regeneration in calvarial defects: an in vivo microcomputed tomographic and histologic experiment in rats. International Journal of Oral and Maxillofacial Surgery, 2017. 46: p. 213.

6. Binsalah, M.A., et al., Guided Bone Regeneration of Femoral Segmental Defects using Equine Bone Graft: An In-Vivo Micro-Computed Tomographic Study in Rats. J Invest Surg, 2019. 32(5): p. 456-466.

7. Al-Ahmari, F., et al., Efficacy of Mesenchymal Stem Cells as Adjunct to Guided Bone Regeneration in Standardized Calvarial Defects in Rats: An In Vivo Microcomputed Tomographic and Histologic Analysis. Int J Periodontics Restorative Dent, 2016. 36 Suppl: p. s23-37.

8. Al-Hezaimi, K., et al., Real-time-guided bone regeneration around standardized critical size calvarial defects using bone marrow-derived mesenchymal stem cells and collagen membrane with and without using tricalcium phosphate: an in vivo micro-computed tomographic and histologic experiment in rats. Int J Oral Sci, 2016. 8(1): p. 7-15.

9. Al-Omar, N.A., et al., Bone Regeneration Using Bone Morphogenetic Protein-2 and Biphasic Calcium Phosphate With and Without Collagen Membrane in Calvarial Standardized Defects: An In Vivo Microcomputed Tomographic Experiment in Rats. Int J Periodontics Restorative Dent, 2016. 36 Suppl: p. s161-70.

10. Ramalingam, S., et al., Guided bone regeneration in standardized calvarial defects using beta-tricalcium phosphate and collagen membrane: a real-time in vivo micro-computed tomographic experiment in rats. Odontology, 2016. 104(2): p. 199-210.

11. Alkindi, M., et al., Guided bone regeneration with osteoconductive grafts and PDGF: A tissue engineering option for segmental bone defect reconstruction. J Appl Biomater Funct Mater, 2021. 19: p. 2280800020987405.

12. Al-Qutub, M.N., et al., Guided Bone Regeneration Using Biphasic Calcium Phosphate With Adjunct Recombinant Human Bone Morphogenetic Protein-2 With and Without

Collagen Membrane in Standardized Calvarial Defects in Rats: A Histologic and Biomechanical Analysis. Int J Periodontics Restorative Dent, 2016. 36 Suppl: p. s11-20.

13. Ramalingam, S., et al., Lateral Periodontal Cyst Treated with Enucleation and Guided Bone Regeneration: A Report of a Case and a Review of Pertinent Literature. Case Rep Dent, 2019. 2019: p. 4591019.

14. Govoni, M., et al., Commercial Bone Grafts Claimed as an Alternative to Autografts: Current Trends for Clinical Applications in Orthopaedics. Materials (Basel), 2021. 14(12).

15. Annibali, S., et al., A comparative morphometric analysis of biodegradable scaffolds as carriers for dental pulp and periosteal stem cells in a model of bone regeneration. J Craniofac Surg, 2013. 24(3): p. 866-71.

16. Pagliani, L., et al., A collagenated porcine bone substitute for augmentation at Neoss implant sites: a prospective 1-year multicenter case series study with histology. Clin Implant Dent Relat Res, 2012. 14(5): p. 746-58.

17. Falacho, R.I., et al., Collagenated Porcine Heterologous Bone Grafts: Histomorphometric Evaluation of Bone Formation Using Different Physical Forms in a Rabbit Cancellous Bone Model. Molecules, 2021. 26(5).

18. Husch, J.F.A. and J.J.J.P. van den Beucken, Chapter 9 - Cell-based therapies in bone regeneration, in Dental Implants and Bone Grafts, H. Alghamdi and J. Jansen, Editors. 2020, Woodhead Publishing. p. 217-250.

19. Asatrian, G., et al., Stem cell technology for bone regeneration: current status and potential applications. Stem Cells Cloning, 2015. 8: p. 39-48.

20. Villarroel, V., P. Fagalde, and D. Reininger, Potential therapeutic uses of intraoral mesenchymal stem cells in other tissues of the body: A review. J Clin Exp Dent, 2021. 13(3): p. e259-e267.

21. Gaubys, A., V. Papeckys, and M. Pranskunas, Use of Autologous Stem Cells for the Regeneration of Periodontal Defects in Animal Studies: a Systematic Review and Meta-Analysis. J Oral Maxillofac Res, 2018. 9(2): p. e3.

22. Gu, Y., et al., Osteogenic stimulation of human dental pulp stem cells with self-setting biphasic calcium phosphate cement. J Biomed Mater Res B Appl Biomater, 2020. 108(4): p. 1669-1678.

23. Trivedi, S., et al., Hydroxyapatite-collagen augments osteogenic differentiation of dental pulp stem cells. Odontology, 2020. 108(2): p. 251-259.

24. Badwelan, M., et al., The Efficacy of Recombinant Platelet-Derived Growth Factor on Beta-Tricalcium Phosphate to Regenerate Femoral Critical Sized Segmental Defects: Longitudinal In Vivo Micro-CT Study in a Rat Model. J Invest Surg, 2020. 33(5): p. 476-488.

25. Johnson, E.O., T. Troupis, and P.N. Soucacos, Tissue-engineered vascularized bone grafts: basic science and clinical relevance to trauma and reconstructive microsurgery. Microsurgery, 2011. 31(3): p. 176-82.

26. Spicer, P.P., et al., Evaluation of bone regeneration using the rat critical size calvarial defect. Nat Protoc, 2012. 7(10): p. 1918-29.

27. Smith, R. and J.J.Q.A.I.J.o.M. Triffitt, Bones in muscles: the problems of soft tissue ossification. 1986. 61(2): p. 985-990.

28. Ahrlund-Richter, A.O.A.B.J.N.B., L. Amit M. Andrews PW. Beighton G. Bello PA. Benvenisty N. Berry LS, et al. Characterization of human embryonic stem cell lines by the international stem cell initiative. 2007. 25: p. 803-816.

29. Pispa, J. and I.J.D.b. Thesleff, Mechanisms of ectodermal organogenesis. 2003. 262(2): p. 195-205.

30. Jernvall, J. and I.J.M.o.d. Thesleff, Reiterative signaling and patterning during mammalian tooth morphogenesis. 2000. 92(1): p. 19-29.

31. Tummers, M., I.J.E. Thesleff, and development, Observations on continuously growing roots of the sloth and the K14-Eda transgenic mice indicate that epithelial stem cells can give rise to both the ameloblast and root epithelium cell lineage creating distinct tooth patterns. 2008. 10(2): p. 187-195.

32. Tummers, M. and I. Thesleff, Root or crown: a developmental choice orchestrated by the differential regulation of the epithelial stem cell niche in the tooth of two rodent species. 2003.

33. Thesleff, I. and M. Tummers, Tooth organogenesis and regeneration. 2010.

34. Martini, F., et al., Martini's atlas of the human body. 2006.

35. Tortora, G.J. and B.H. Derrickson, Principles of anatomy and physiology. 2018: John Wiley & Sons.

36. Canalis, E., A.N. Economides, and E.J.E.r. Gazzerro, Bone morphogenetic proteins, their antagonists, and the skeleton. 2003. 24(2): p. 218-235.

37. Ito, Y., K.J.C.o.i.g. Miyazono, and development, RUNX transcription factors as key targets of TGF-β superfamily signaling. 2003. 13(1): p. 43-47.

38. Chen, D., M. Zhao, and G.R.J.G.f. Mundy, Bone morphogenetic proteins. 2004. 22(4): p. 233-241.

39. Farhadieh, R.D., et al., The role of bone morphogenetic proteins BMP-2 and BMP-4 and their related postreceptor signaling system (Smads) in distraction osteogenesis of the mandible. 2004. 15(5): p. 714-718.

40. Ducy, P., et al., Osf2/Cbfa1: a transcriptional activator of osteoblast differentiation. 1997. 89(5): p. 747-754.

41. Komori, T., et al., Targeted disruption of Cbfa1 results in a complete lack of bone formation owing to maturational arrest of osteoblasts. 1997. 89(5): p. 755-764.

42. Otto, F., et al., Cbfa1, a candidate gene for cleidocranial dysplasia syndrome, is essential for osteoblast differentiation and bone development. 1997. 89(5): p. 765-771.

43. Jonason, J., et al., Post-translational regulation of Runx2 in bone and cartilage. 2009. 88(8): p. 693-703.

44. Golub, E.E. and K.J.C.o.i.O. Boesze-Battaglia, The role of alkaline phosphatase in mineralization. 2007. 18(5): p. 444-448.

45. Chen, J., et al., Developmental expression of bone sialoprotein mRNA in rat mineralized connective tissues. 1992. 7(8): p. 987-997.

46. Ogata, Y.J.J.o.p.r., Bone sialoprotein and its transcriptional regulatory mechanism. 2008. 43(2): p. 127-135.

47. Arnett, T. and B. Henderson, Methods in bone biology. 2007: springer science & Business Media.

48. Gilbert, D.J.J.o.c.n., Treatment of children and adolescents with tics and Tourette syndrome. 2006. 21(8): p. 690-700.

49. Hall, B.K.J.A.S., The embryonic development of bone. 1988. 76(2): p. 174-181.

50. Bruder, S.P. and A.I.J.C.t.r. Caplan, Cellular and molecular events during embryonic bone development. 1989. 20(1-4): p. 65-71.

51. Hatori, M., et al., End labeling studies of fragmented DNA in the avian growth plate: evidence of apoptosis in terminally differentiated chondrocytes. 1995. 10(12): p. 1960-1968.

52. Alison, M.R., et al., An introduction to stem cells. 2002. 197(4): p. 419-423.

53. Blau, H.M., T. Brazelton, and J.J.C. Weimann, The evolving concept of a stem cell: entity or function? 2001. 105(7): p. 829-841.

54. Lavker, R.M. and T.-T.J.P.o.t.n.a.o.s. Sun, Epidermal stem cells: properties, markers, and location. 2000. 97(25): p. 13473-13475.

55. Vessey, C.J. and P.d.l.M.J.P. Hall, Hepatic stem cells: a review. 2001. 33(2): p. 130-141.

56. Fernandes, K.J., et al., A dermal niche for multipotent adult skin-derived precursor cells. 2004. 6(11): p. 1082-1093.

57. Grimm, W.D., et al., Translational research: palatal-derived ecto-mesenchymal stem cells from human palate: a new hope for alveolar bone and cranio-facial bone reconstruction. 2014. 7(1): p. 23.

58. Brar, G.S. and R.S.S.J.I.J.o.D.R. Toor, Dental stem cells: dentinogenic, osteogenic, and neurogenic differentiation and its clinical cell based therapies. 2012. 23(3): p. 393-397.

59. Gronthos, S., et al., Postnatal human dental pulp stem cells (DPSCs) in vitro and in vivo. 2000. 97(25): p. 13625-13630.

60. Vogel, G., Nobel laureates lobby for stem cells. 2001, American Association for the Advancement of Science.

61. Caplan, A.I.J.J.o.o.r., Mesenchymal stem cells. 1991. 9(5): p. 641-650.

62. Baddoo, M., et al., Characterization of mesenchymal stem cells isolated from murine bone marrow by negative selection. 2003. 89(6): p. 1235-1249.

63. Alhadlaq, A., J.J.J.S.c. Mao, and development, Mesenchymal stem cells: isolation and therapeutics. 2004. 13(4): p. 436-448.

64. Strauer, B.E. and R.J.C. Kornowski, Stem cell therapy in perspective. 2003. 107(7): p. 929-934.

65. Krebsbach, P.H. and P.G.J.J.o.d.e. Robey, Dental and skeletal stem cells: potential cellular therapeutics for craniofacial regeneration. 2002. 66(6): p. 766-773.

66. Khetan, S. and J. Burdick, Cellular encapsulation in 3D hydrogels for tissue engineering. JoVE (Journal of Visualized Experiments), 2009(32): p. e1590.

67. Khetan, S. and J. Burdick, Cellular Encapsulation in 3D Hydrogels for Tissue Engineering. JoVE. 32. 2009, Citeseer.

68. Schneider, R.K., et al., The osteogenic differentiation of adult bone marrow and perinatal umbilical mesenchymal stem cells and matrix remodelling in three-dimensional collagen scaffolds. Biomaterials, 2010. 31(3): p. 467-480.

69. Ledesma-Martínez, E., V.M. Mendoza-Núñez, and E.J.S.c.i. Santiago-Osorio, Mesenchymal stem cells derived from dental pulp: a review. 2016. 2016.

70 Ravindran, S., C.-C. Huang, and A.J.F.i.p. George, Extracellular matrix of dental pulp stem cells: applications in pulp tissue engineering using somatic MSCs. 2014. 4: p. 72925.

71. Zhang, L., et al., Pluripotent stem cell-derived CAR-macrophage cells with antigen-dependent anti-cancer cell functions. 2020. 13: p. 1-5.

72. Huang, S., et al., Process development and scale-up of pluripotent stem cell manufacturing. 2020.

73. Yu, X., et al., Evaluation of bone-regeneration effects and ectopic osteogenesis of collagen membrane chemically conjugated with stromal cell-derived factor-1 in vivo. 2019. 15(1): p. 015009.

74. Morin, L.G.J.A.j.o.c.p., Direct colorimetric determination of serum calcium with o-cresolphthalein complexon. 1974. 61(1): p. 114-117.

75. Dominici, M., et al., Minimal criteria for defining multipotent mesenchymal stromal cells. The International Society for Cellular Therapy position statement. 2006. 8(4): p. 315-317.

76. Ariano, A., et al., Molecules inducing dental stem cells differentiation and bone regeneration: state of the art. International Journal of Molecular Sciences, 2023. 24(12): p. 9897.

77. Jeanneau, C., et al., The Added Value of a Collagenated Thermosensitive Bone Substitute as a Scaffold for Bone Regeneration. Materials, 2024. 17(3): p. 625.

78. Filippi, M., et al., Natural polymeric scaffolds in bone regeneration. Frontiers in bioengineering and biotechnology, 2020. 8: p. 474.

79. Blázquez-Carmona, P., et al., Mechanics predicts effective critical-size bone regeneration using 3d-printed bioceramic scaffolds. Tissue Engineering and Regenerative Medicine, 2023. 20(6): p. 893-904.

80. Sparks, D.S., et al., Convergence of scaffold-guided bone regeneration principles and microvascular tissue transfer surgery. Science advances, 2023. 9(18): p. eadd6071.

81. Arvidson, K., et al., Bone regeneration and stem cells. Journal of cellular and molecular medicine, 2011. 15(4): p. 718-746.

82. Trinh, H.A., et al., Acemannan induced bone regeneration in lateral sinus augmentation based on cone beam computed tomographic and histopathological evaluation. Case Reports in Dentistry, 2020. 2020.

83. Mortada, I. and R. Mortada, Dental pulp stem cells and osteogenesis: an update. Cytotechnology, 2018. 70(5): p. 1479-1486.

84. Fujii, Y., et al., Application of dental pulp stem cells for bone and neural tissue regeneration in oral and maxillofacial region. Stem Cells International, 2023. 2023.

85. Kirankumar, S., et al., Modern approaches on stem cells and scaffolding technology for osteogenic differentiation and regeneration. Experimental Biology and Medicine, 2022. 247(5): p. 433-445.

86. Yamada, Y., et al., Promising advances in clinical trials of dental tissue-derived cell-based regenerative medicine. Stem Cell Res Ther, 2020. 11(1): p. 175.

87. Hilkens, P., et al., Effect of isolation methodology on stem cell properties and multilineage differentiation potential of human dental pulp stem cells. Cell Tissue Res, 2013. 353(1): p. 65-78.

88. Dominici, M., et al., Minimal criteria for defining multipotent mesenchymal stromal cells. The International Society for Cellular Therapy position statement. Cytotherapy, 2006. 8(4): p. 315-7.

89. Yuan, S.-M., et al., Therapeutic potential of dental pulp stem cells and their derivatives: Insights from basic research toward clinical applications. World Journal of Stem Cells, 2022. 14(7): p. 435.

90. Gittel, C., et al., Isolation of equine multipotent mesenchymal stromal cells by enzymatic tissue digestion or explant technique: comparison of cellular properties. BMC veterinary research, 2013. 9: p. 1-14.

91. Shi, X., J. Mao, and Y. Liu, Pulp stem cells derived from human permanent and deciduous teeth: Biological characteristics and therapeutic applications. Stem cells translational medicine, 2020. 9(4): p. 445-464.

92. Bow, A., Novel Osteobiologics for Bone Tissue Engineering. 2019.

93. Bracey, D.N., et al., A decellularized porcine xenograft-derived bone scaffold for clinical use as a bone graft substitute: a critical evaluation of processing and structure. Journal of functional biomaterials, 2018. 9(3): p. 45.

94. Kim, N.-h., et al., Customized three-dimensional printed ceramic bone grafts for osseous defects: a prospective randomized study. Scientific Reports, 2024. 14(1): p. 3397.

95. Zhou, Y., et al., Mitigating Cross-Species Viral Infections in Xenotransplantation: Progress, Strategies, and Clinical Outlook. Cell Transplantation, 2024. 33: p. 09636897241226849.

96. Peric, M., et al., The rational use of animal models in the evaluation of novel bone regenerative therapies. Bone, 2015. 70: p. 73-86.

97. Namjoynik, A., M.A. Islam, and M. Islam, Evaluating the efficacy of human dental pulp stem cells and scaffold combination for bone regeneration in animal models: A systematic review and meta-analysis. Stem cell research & therapy, 2023. 14(1): p. 132.

98 U.P.S. Chauhan, B.C. Ray Sarkar Use of calmagite for the determination of traces of magnesium in biological materials. Analytical Biochemistry 1969. 32 (1): p. 70

99 R J Liedtke, G Kroon.Automated calmagite complexiметric measurement of magnesium in serum, with sequential addition of EDTA to eliminate endogenous interference.1984. 30(11): p.1801

100 Edgar Ledesma-Martínez et al. Mesenchymal Stem Cells Derived from Dental Pulp: A Review. Stem Cells Int. 2016. 2016. p 1-12

101 The Ulf Nannmark [1], Lars Sennerby. Bone Tissue Responses to Prehydrated and Collagenated Cortico-Cancellous Porcine Bone Grafts: A Study in Rabbit Maxillary Defects. Clin Implant Dent Relat Res. 2008 Dec;10(4).p264

102 Suchánek J, et al. Human dental pulp stem cells--isolation and long term cultivation. Acta Medica (Hradec Kralove). 2007;50(3).p195-201.

103. Yamada Y., Ito K., Nakamura S., Ueda M., Nagasaka T. Promising cell-based therapy for bone regeneration using stem cells from deciduous teeth, dental pulp, and bone marrow. *Cell Transplantation.* 2011;20(7) p:1003–1013.

104 Takeda-Kawaguchi T, Sugiyama K, Chikusa S, Iida K, Aoki H, Tamaoki N, et al. (2014) Derivation of iPSCs after Culture of Human Dental Pulp Cells under Defined Conditions. PLoS ONE 9(12): e115392. doi: 10.1371/journal.pone.0115392

105 El Alami M et al. Activation of p38, p21, and NRF-2 mediates decreased proliferation of human dental pulp stem cells cultured under 21% O_2 . Stem Cell Reports. 2014;3(4):566–573.

106 von Bahr L., Sundberg B., Lönnies L., et al. Long-term complications, immunologic effects, and role of passage for outcome in mesenchymal stromal cell therapy. Biology of Blood and Marrow Transplantation. 2012;18(4):557–564

107 Choi M. R., Kim H. Y., Park J.-Y., et al. Selection of optimal passage of bone marrow-derived mesenchymal stem cells for stem cell therapy in

patients with amyotrophic lateral sclerosis. *Neuroscience Letters*. 2010;472(2):94–98